University of Liège
Faculty of Applied Science
Urban and Environmental Engineering Dept.

Spatiotemporal modeling of interactions between urbanization and flood risk: a multi-level approach

Thesis submitted in partial fulfillment of the requirements for the degree of Doctor of Philosophy in Engineering and Technology Sciences

Ahmed MUSTAFA

February 2018

D/2018/13.315/2
ISBN 978-2-9307-7225-7
DOI: https://doi.org/10.13140/RG.2.2.21270.86082/1

Promoter: Prof. Jacques TELLER (University of Liège).

Co-promoter: Prof. Mario COOLS (University of Liège).

Jury

Prof. Benjamin DEWALS – president (University of Liège).

Prof. Alison HEPPENSTALL (University of Leeds).

Prof. Anton VAN ROMPAEY (Katholieke Universiteit Leuven-KU Leuven).

Prof. Daniel G. ALIAGA (Purdue University).

Thesis submitted in partial fulfillment of the requirements for the degree of Doctor of Philosophy in Engineering and Technology Sciences by
Ahmed Mohamed Elsaeid Mustafa

February 2018

Acknowledgments

It's time to look back and relive the experience. I would like first to express my deepest appreciation to my promoter, Prof. Jacques Teller. I owe a lot to him for making my PhD journey significantly easier and for all the feedback and assistance during the PhD journey. I would also like to thank the PhD committee members, Prof. Anton Van Rompaey, Prof. Mario Cools, and Prof. Benjamin Dewals for the help and support they have offered me. My sincere thanks to Prof. Daniel G. Aliaga for hosting me at Purdue University, and for always being available to discuss ideas.

Thanks for the support from my colleagues and friends. I would like to thank Ismaïl Saadi, Martin Bruwier, Mohamed Amer, Xiaowei Zhang, Gen Nishida, Amr Ebaid, Ayman Lotfi, and Shady Attia. Your friendship had a great contribution to my success and I cannot be grateful enough. I also extend my thanks to Prof. Alison Heppenstall, Dr. Andreas Rienow, and Dr. Hichem Omrani for sharing their knowledge and for taking the time to help me with my research.

A special thanks must go to my family, and above all to my parents for their constant support and reassurance. I hope this makes you proud. I would like to thank my siblings Mohamed, Abdelrahim, and Omnia for always being so supportive and beside me.

Finally, no words could express my gratitude to my wife Sara. I wouldn't have done it with your continuous support and unconditional love. Thank you, my baby, Adam for being a breath of fresh air away from the research work.

Funding: This research was funded through the ARC grant for Concerted Research Actions for project number 13/17-01 entitled "Land-use change and future flood risk: influence of micro-scale spatial patterns (FloodLand)" financed by the French Community of Belgium (Wallonia-Brussels Federation).

Abstract

Flood in urban areas is an increasing problem and it causes over one-third of overall economic losses due to natural hazards across the globe. For many river basins, studies show that flood risk will further increase during the 21st century as a result of a combination of climate change and urban development. It is important in this respect to evaluating flood risks at different time horizons by coupling urban development models with hydrological models. Although often focused on flood hazard only, the existing studies suggest (i) an overwhelming contribution of urbanization to the future increase in flood risk in some river basins, and (ii) a likely high influence of small-scale spatial patterns in future urbanization, requiring analyses at a finer scale than performed so far. The main goal of this PhD thesis is to investigate the expected flood damage for possible future built-up patterns at different scales. Wallonia (Belgium) is selected as a case study for this thesis. Four main steps are followed to accomplish the thesis' goal. First, this thesis takes a retrospective analysis of the evolution of the urban development in Wallonia through the use of a multinomial logistic regression model (MNL). Second, in order to estimate the future flood damage for urban areas, there is a need for urbanization scenarios that are based on a realistic land-use change model. In this context, this research proposes and compares two land-use change models: (i) a coupled MNL and cellular automata model (MNL-CA), and (ii) a coupled CA and agent-based model (CA-AB). Based on the comparison of both modeling approaches, the CA-AB model is employed to simulate several future urbanization scenarios. These scenarios are typically considering long-term time horizons, i.e. 2050-2100, as this is the appropriate time frame for analyzing such effects. In this thesis, Belgian cadastral datasets for 1990, 2000 and 2010 are used to calibrate and validate the land-use change models. A remarkable feature of this research is that it considers multiple densities of built-up which enables us to study both expansion and densification processes. As the model simulates urbanization up to 2100, forecasting land-use change over such time frames entails very significant uncertainties. In this regard, one of the main themes of this thesis is attributed to the modeling of uncertainty in the land-use change models. Third, 24 urbanization scenarios for the entire Wallonia for 2030, 2050, 2070 and 2100 that differed in terms of the rate of development and spatial policies are generated. The simulated scenarios will then be integrated with a hydrological model for the same time horizon. The inundation extents and water depths for each scenario are determined by a hydraulic model for

steady flows corresponding to return periods of 25, 50 and 100 years. The results suggest that urban development will continue within flood hazard zones in many of the simulated scenarios. Therefore, fourth, a procedural urban generation system is developed to analyze the respective influence of various urban layout characteristics on inundation flow which assists in designing flood-resistant urban layouts within the flood hazard zones. The results pointed out that the assumption of a binary approach of urbanization modeling, urban vs non-urban, may lead to inaccurate conclusions as the relative importance of the development controlling factors typically varies with density. Our results show that the densification strategy, without spatial policy interventions, may lead to an increase in the flood absolute damage by a 100% at the end of the century. Another important finding of this thesis is that the geometric factors of urban layouts, such as road width, orientation or curvature, have a role in water flow properties during floods. Thus, the thesis provides some guidelines for designing flood-sensitive urban layouts.

Table of Contents

General Introduction

Background

Floods claim many lives and cause major economic losses. A recent report by the UN, "Human Cost of Weather Related Disasters", shows that 157,000 people have died as a result of floods between 1995 and 2015. Additionally, floods damages cost US$104 billion/year globally according to the UN report "Global Assessment Report on Disaster Risk Reduction". The magnitude and occurrence of floods in many areas are currently increasing (Moel and Aerts, 2010; Pfister et al., 2004) as a result of climate change. However, not only climate will change; but also economic development and land-use (mainly urbanization). Poelmans et al. (2011) investigated the relative impact of both climate change and urban expansion on the peak flows and flood extent for a small-scale catchment situated in the center of Belgium. This study concluded that the potential damage related to a flood is largely influenced by land use changes that occur in the floodplain. Land use change influences flood risk through multiple pathways, including climate (e.g., modified evapotranspiration), run-off in the catchment (reduced infiltration), inundation flows (obstruction by buildings) and flood exposure (higher value of elements-at-risk in the floodplains).

For several decades hard flood protection measures such as levees, dams, and dikes have been widely used to control floods. These measures have been criticized because they often interrupt natural flooding processes by removing the natural land cover, reduce natural water storage capacity and disrupt water flow paths (Lennon et al., 2014; O'Neill, 2013). In the recent years, there is a shift in focus from hard flood controls towards a more strategic approach characterized by mitigating flood risk and increasing resilience during the urban design process (Lennon et al., 2014; White, 2008). Several soft solutions have been introduced at different spatial scales ranging from regional scale to building scale. For example, storing water in farmland, where the land remains property of the farmer and is used for temporary water storage in extreme flooding (e.g. Fokkens, 2006). Other case-studies relocate the most sensitive land-use types; e.g. suggest moving residential areas to zones with a lower flood risk (e.g. Satterthwaite, 2007). Within this context, it is crucial for planners and policymakers to consider flood damage for possible future urban patterns. It is also important to concern the possibility of accommodating unavoidable floods by pre-emptive modifications to the urban design. This thesis studies the impacts of urban development on future flood in Wallonia (Belgium) as a case study. Urbanization in Wallonia is

characterized by a mix of urban cores and several small settlements, together with a dense road network resulted in ribbon and fragmented development. Over the last decades, the main land-use change form was the conversion of agricultural lands to urban lands, Figure 1.

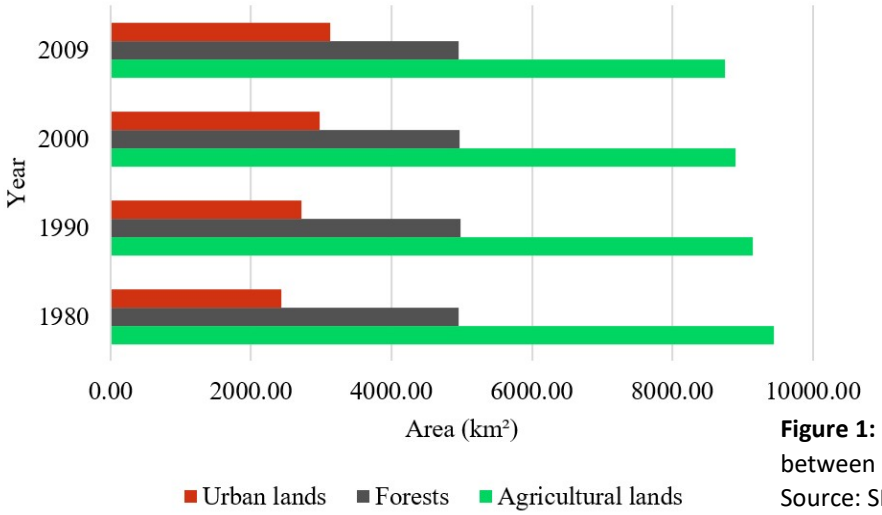

Figure 1: Land-use evolution between 1980 and 2009. Source: SPF Economie – DGSIE.

What should we consider as urban land-use?

The total urban area is provided by several sources. Figure 2 gives the variation in the calculated urban land-use in four data sources: Corine Land Cover (CLC), La Carte d'Occupation du Sol de Wallonie, Land-use Map of Wallonia, (COSW), Conférence Permanente du Développement Territorial, permanent conference of territorial development, (CPDT) and Cadastral Data (CAD).

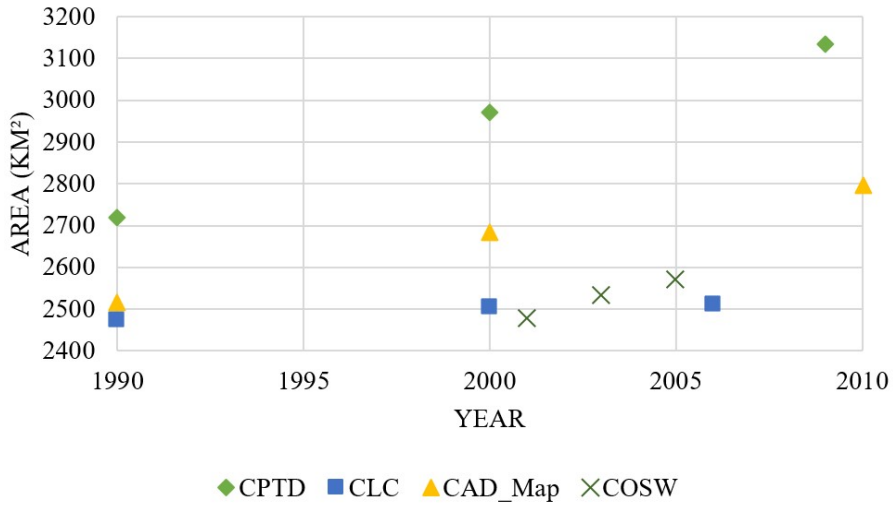

Figure 2: Urban area in Wallonia reported by different data sources.

CLC datasets provide a detailed inventory of the biophysical land cover in Europe. It is made available by the European Environment Agency (EEA, 1994) at resolutions of 100 m × 100 m and 250 m × 250 m grid cells. CLC datasets have been generated based on different sets of satellite images and topographic maps (EEA, 1994). COSW datasets are detailed land cover maps for

Wallonia developed by Wallonia Public Service (SPW). The method used to produce the maps is based on the use a base layer which is the PLI (Plan of Location Information). This is combined with the nature of the land register and crossed by geoprocessing with different layers describing certain types of land-uses including agricultural plot (from the SIGEC), water bodies, extraction areas, waste dumps, landfills, brownfield sites (SAR), port areas or airfields (SPW, 2008) . CPTD provides statistics about the total area of land uses in Wallonia based on Belgian statistics (SPF Economie - DGSIE). CAD is a vector dataset representing buildings in two dimensions as polygons, made available by the Land Registry Administration of Belgium. CAD provides numerous information on buildings from which the construction date is used to develop urban land-use maps for several time points.

Each data source is based on different nomenclatures that define urban land, a different methodology to develop the dataset, and/or a different generalization level. Therefore, different data sources are difficult to compare and the resulting areas of urban land show a relatively large variation. For example, the urban class in CLC configuration consists of land that is covered by buildings and other man-made elements such as residential areas and related functions services, industries, firms, and transport infrastructure. Whereas, CAD considers only lands that are completely or partially covered by buildings as urban lands. CLC is mainly based on the acquisition of satellite data. The remotely sensed data often underestimates dispersed classes such as urban lands, because of the coarse resolution of most satellite sensors (Poelmans, 2010) . On the other hand, data based on land registration and statistics such as CPTD tend to overestimate urban lands because they assume that an urban parcel in the land register is completely covered by buildings.

Land-use classification resulting from free satellite imagery is another source for land-use data. However, CAD data is used in this research for two main reasons:

(i) at the regional level, this study uses raster grids with spatial resolution of 100m to reduce computational resources and CAD allows to assign built-up density index for every 100 m × 100 m cell, and

(ii) this research investigates the relationship between urban layout design and flood damage by generating a large number of synthetic layouts using procedural system. The variance of the input parameters for the procedural system is obtained by inspecting CAD for 500 km² of Wallonia.

Considering the different existing definitions of urban land use, one of the main originality of our research consists in avoiding a dual urban/non-urban approach as the one adopted in most existing studies. We will hence consider different levels of urban land use, from low- to high-density levels, and measure exposure to floods for these different levels of urban land use. This multi-level approach is more in line with the reality, as there is no sharp break between urban and non-urban

in our daily landscapes. Further on such a multi-level approach is highly relevant from a policy-driven perspective, especially in those areas where there is a significant potential for a further urbanization of already urban areas.

It should be stressed at this regard that different approaches have been implemented throughout the research to assign urban density ranges to each urban class in the different chapters. This is related to the fact that the different chapters have been submitted as separate articles in scientific journals, which led to some differences in the approach adopted to set the number and limits of urban density classes over time. These minor changes do not affect the general conclusions that can be drawn from the results.

Research objectives and questions

The overall goal of this thesis lies in identifying the impact of urban development on the flood damage at multiple scales for Wallonia (as a case study) in which many built-up neighborhoods are characterized by low density and some discontinuity with historical urban cores (Marique et al., 2013). The thesis addresses the following research questions:

Q1. What is the potential of analyzing and modeling multiple urban densities in a highly fragmented urban landscape?

Q2. Which urban expansion model structure is the most appropriate?

Q3. What is the relative impact of future urbanization on the flood damage across Wallonia?

Q4. What is the relation between urban layout and flood damage?

These questions approach future flood risks from two angles: urbanization and inundation modeling, and at two different levels: mesoscale (Q1 to Q3), and microscale (Q4).

Thesis structure: methodological workflow

The structure of the thesis, which is graphically summarized in Figure 3, consists of three distinct parts. Part one (P1) answers Q1, part two (P2) answers Q2, and part three (P3) is dedicated to Q3 and Q4. The main aim of P1, which includes chapter 1, is to analyze the recent urbanization in Wallonia and its drivers and to figure out whether it is important to consider several urban densities or to follow a binary classification, i.e. urban vs non-urban, as in many existing studies.

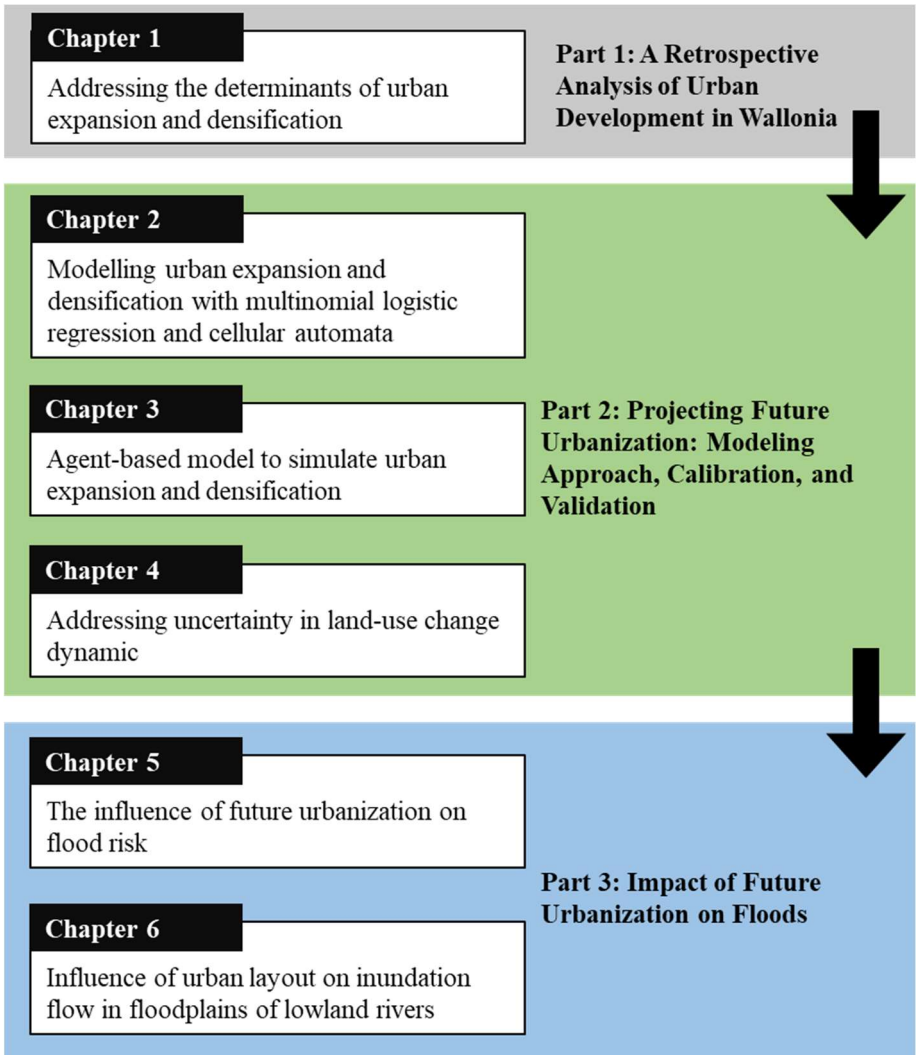

Figure 3: Overview of the thesis structure.

This part concludes that the relative influence of the development drivers typically varies with density. In addition, this part shows that it is crucial to study both expansion and densification (infill development) processes.

The second part (P2) aims at simulating future urban land use. The main contribution of this step is improving the understanding of calibration process through urban expansion models. Unlike most commonly used models which simulate expansion, our approach considers expansion and the potential for densification within already built-up areas. This thesis examines the most common urbanization modeling approaches including a coupled multinomial logistic regression and cellular automata (MNL-CA) approach, and a coupled CA and agent-based (CA-AB) approach. Chapter 2, introduces an MNL-CA model in which the transition potential of each cell to be converted into a specific urban density class are based on a set of static variables which is calibrated with MNL, and a dynamic neighborhood interaction which is calibrated with a genetic algorithm (GA). In chapter 3, a CA-AB model is proposed whereby new developments are simulated through land developers' decisions. The agents are categorized into three agent groups with different characteristics and goals: developers, existing residents and planning permission

authority. The model's parameters are also calibrated with GA. Further, this chapter presents a discussion and comparison of the allocation ability of the two models: MNL-CA (chapter 2), and CA-AB model (chapter 3). This comparison highlights that CA-AB model is the best performing model. Chapter 4 describes a novel approach for tuning land-use allocation uncertainty over time. Our approach is referred to as Time Monte-Carlo (TMC) technique. It uses a specific range of randomness to allocate new land uses. This range is associated with the transition probabilities from one land-use to another. The range of randomness is increased over time so that the magnitude of uncertainty increases over time.

One of the aims of P3 is to evaluate the flood damage related to every urbanization scenario by coupling the corresponding scenario with inundation maps and by using a stage-damage function for urban areas and specific prices. Based on P2, our CA-AB model is employed to simulate 24 different urbanization scenarios for 2030, 2050, 2070 and 2100 (chapter 4). These scenarios differ in terms of expansion and densification rates (low, medium, and high) and in allocation procedure (business-as-usual, ban on expansion, and ban on new constructions within flood-prone zones). The main contribution of chapter 5 is to acquire a better insight into the importance of simulating different levels of urban densities as well as considering different expansion and/or densification policies.

Although simulating future urban land-use at the mesoscale based on a relatively coarse spatial resolution is perfectly suitable for analyzing the influence of future urbanization on climate itself and on hydrology, it fails to capture the influence of small-scale urban layouts on inundation characteristics. Another aim of P3 is to clarify how flood is influenced by the characteristics of urban layout parameters such as road width, building setbacks, etc. Chapter 6 provides guidelines for designing flood-sensitive urban layouts in the future urban areas which were simulated within P2. In chapter 6, a large set of alternate urban layouts was generated randomly using an urban procedural model. This model provides the shape of roads, parcels, and buildings with their geometry, over a square area of 1 km². Steady 2-D hydraulic computations were performed for the generated layouts with identical hydraulic conditions. Based on the computed hydraulics, a regression analysis is performed to outline the most influential layout parameters.

Chapters 5 and 6 are based on a close collaboration with Martin Bruwier, a PhD student in the ARC FloodLand research project. The hydraulic models, used in this research, were developed and operated by Martin Bruwier. Finally, chapter 7 draws general conclusions and proposing future possible research lines.

The thesis is made up of a series of articles that have been published/submitted to peer-reviewed journals. For this reason some overlap may occur between the various chapters.

Key findings of the thesis

- In Wallonia, urban densification processes are mainly driven by local factors, whereas the expansion processes are strongly controlled by the zoning plan.
- Densification mainly occurs in already dense areas and is dominated by self-organization dynamics rather than deliberate land-use policies at the regional level.
- Without appropriate spatial policies, the increase in total flood risk by 2100 would increase by a factor of approximately two.
- The sensitivity of the flood risk to spatial policy (business-as-usual vs. densification) is shown to be high.
- General guidelines to design flood-resilient urban layouts is increasing the fragmentation of the urban layout.

List of publications

Peer-reviewed journal articles

Included in the thesis:

- Chapter 1 is based on:

1. Mustafa, A., Rompaey, A. V., Cools, M., Saadi, I., & Teller, J. (2018). Addressing the determinants of built-up expansion and densification processes at the regional scale. *Urban Studies,* 0(0), 1-20.

- Chapter 2 is based on:

2. Mustafa, A., Heppenstall, A., Omrani, H., Saadi, I., Cools, M., & Teller, J. (2018). Modelling built-up expansion and densification with multinomial logistic regression, cellular automata and genetic algorithm. *Computers, Environment and Urban Systems*, 67, 147–156.

- Chapter 3 is based on:

3. Mustafa, A., Bruwier, M., Archambeau, P., Erpicum, S., Pirotton, M., Dewals, B., & Teller, J. (under review). Effects of spatial planning on future flood risks in urban environments. *Journal of Environmental Management*.
4. Mustafa, A., Cools, M., Saadi, I., & Teller, J. (2017). Coupling agent-based, cellular automata and logistic regression into a hybrid urban expansion model (HUEM). *Land Use Policy*, 69C, 529–540.

- Chapter 4 is based on:

5. Mustafa, A., Cools, M., Saadi, I., & Teller, J. (under review). A Time Monte-Carlo method for addressing uncertainty in land-use change dynamic. *International Journal of Geographical Information Science.*

- Chapter 5 is based on:

3. Mustafa, A., Bruwier, M., Archambeau, P., Erpicum, S., Pirotton, M., Dewals, B., & Teller, J. (under review). Effects of spatial planning on future flood risks in urban environments. *Journal of Environmental Management*.

- Chapter 6 is based on:

6. Bruwier, M., Mustafa, A., Aliaga, D. G., Archambeau, P., Erpicum, S., Nishida, G., ... Dewals, B. (2018). Influence of urban pattern on inundation flow in floodplains of lowland rivers. *Science of the Total Environment*, 622-623, 446–458.
7. Mustafa, A., Wei Zhang, X., Aliaga, D. G., Bruwier, M., Nishida, G., Dewals, B., … Teller, J. (under review). Procedural generation of flood-sensitive urban layouts. *Environment and Planning B: Urban Analytics and City Science*.

Not included in the thesis:

8. Mustafa, A., Rienow, A., Saadi, I., Cools, M., & Teller, J. (2018). Comparing support vector machines with logistic regression for calibrating cellular automata land use change models. *European Journal of Remote Sensing,* 51 (1), 391-401.
9. Mustafa, A., Saadi, I., Cools, M., & Teller, J. (2018). Understanding urban development types and drivers in Wallonia. A multi-density approach. *International Journal of Business Intelligence and Data Mining*, 13(Nos. 1/2/3), 309–330.
10. Saadi, I., Mustafa, A., Teller, J., & Cools, M. (2017). Investigating the impact of river floods on travel demand based on an agent-based modeling approach: The case of Liège, Belgium. *Transport Policy,* 0(0), 1-9.
11. Amer, M., Mustafa, A., Teller, J., Attia, S., & Reiter, S. (2017). A methodology to determine the potential of urban densification through roof stacking. *Sustainable Cities and Society*, 35C, 677–691.
12. Saadi, I., Bruwier, M., Mustafa, A., Peltier, Y., Archambeau, P., Erpicum, S., … Cools, M. (2016). Development trajectory of an integrated framework for the mitigation of future flood risk: results from the FloodLand project. *Transportation Letters*, 0(0), 1–14.
13. Saadi, I., Liu, F., Mustafa, A., Teller, J., & Cools, M. (2016). A framework to identify housing location patterns using profile Hidden Markov Models. *Advanced Science Letters*, 22(9), 2117–2121.
14. Saadi, I., Mustafa, A., Teller, J., & Cools, M. (2016). Forecasting travel behavior using Markov Chains-based approaches. *Transportation Research Part C: Emerging Technologies*, 69, 402–417.

15. Saadi, I., Mustafa, A., Teller, J., Farooq, B., & Cools, M. (2016). Hidden Markov Model-based population synthesis. *Transportation Research Part B: Methodological*, 90, 1–21.

Refereed Conference Proceedings

16. Saadi, I., Mustafa, A., Teller, J., & Cools, M. (2017). A bi-level Random Forest based approach for estimating O-D matrices: Preliminary results from the Belgium National Household Travel Survey. *Transportation Research Procedia*, 25C, 2566–2573.
17. Mustafa, A., Nishida, G., Saadi, I., Cools, M., & Teller, J. (2017). A Markov Chain Monte Carlo Cellular Automata Model to Simulate Urban Growth. *E-proceedings of GEOProcessing 2017-the 9th International Conference on Advanced Geographic Information Systems, Applications, and Services*, 73–74. **(Best paper award)**.
18. Bruwier, M., Mustafa, A., Aliaga, D., Erpicum, S., Archambeau, P., Nishida, G., … Dewals, B. (2017). Influence of urban patterns on flooding. *E-proceedings of the 37th IAHR World Congress*.
19. Saadi, I., Mustafa, A., Teller, J., & Cools, M. (2017). Mitigating the Error Rate of an IPF-Based Population Synthesis Approach by Incorporating More Heterogeneity into the Initial Seed. *E-proceedings of the Transportation Research Board 96th Annual Meeting*.
20. Mustafa, A., Rienow, A., Saadi, I., Cools, M., & Teller, J. (2016). Cellular automata urban expansion model based on support vector machines. *E-proceedings of CAMUSS 2016-the 2nd International Symposium on Cellular Automata Modeling for Urban and Spatial Systems*, 100–104.
21. Mustafa, A., Saadi, I., Cools, M., & Teller, J. (2016). Modelling Urban Expansion: A Multiple Urban-Densities Approach. *E-proceedings of GEOProcessing 2016-the 8th International Conference on Advanced Geographic Information Systems, Applications, and Services*, 22–25. **(Best paper award)**.
22. Mustafa, A., Bruwier, M., Teller, J., Archambeau, P., Erpicum, S., Pirotton, M., & Dewals, B. (2016). Impacts of urban expansion on future flood damage: A case study in the River Meuse basin, Belgium. *Sustainable Hydraulics in the Era of Global Change (Proceedings of the 4th IAHR Europe Congress),* 856-862. Taylor & Francis Group.
23. Saadi, I., Mustafa, A., Teller, J., & Cools, M. (2016). Calibration of MATSim in the context of natural hazards in Liège (Belgium): Preliminary results. *Proceedings of the 12th Conference on Transport Engineering*.
24. Saadi, I., Mustafa, A., Teller, J., & Cools, M. (2016). An integrated framework for forecasting travel behavior using Markov Chain Monte-Carlo simulation and profile Hidden Markov Models. *E-proceedings of the Transportation Research Board 95th Annual Meeting*.
25. Mustafa, A., Cools, M., Saadi, I., & Teller, J. (2015). Urban Development as a Continuum: A Multinomial Logistic Regression Approach. *Proceedings of ICCSA 2015-Computational Science and its Applications*, 729–744.
26. Mustafa, A., Saadi, I., Cools, M., & Teller, J. (2015). Modelling Uncertainties in Long-Term Predictions of Urban Growth: A Coupled Cellular Automata and Agent-Based Approach. *E-proceedings of CUPUM 2015-the 14th International Conference on Computers in Urban Planning and Urban Management.*

27. Saadi, I., Mustafa, A., Teller, J., Limbourg, S., & Cools, M. (2015). Modelling Agents' Behavior in the Context of River Floods: An Ant Colony based Approach. *E-proceedings of EASTS 2015-the 11th International Conference of Eastern Asia Society for Transportation Studies*.
28. Dewals, B., Bruwier, M., Mustafa, A., Peltier, Y., Saadi, I., Archambeau, P., …, Michel, P. (2015). Landuse change and future flood risk: an integrated and multi-scale approach. *E-proceedings of the 36th IAHR World Congress*.
29. Mustafa, A., Saadi, I., Cools, M., & Teller, J. (2014). Measuring the Effect of Stochastic Perturbation Component in Cellular Automata Urban Growth Model. *Procedia Environmental Sciences*, 22, 156–168.
30. Saadi, I., Eftekhar, H., Mustafa, A., Teller, J., & Cools, M. (2014). An agent-based micro-simulation framework to assess the impact of river floods on transportation systems: implementation trajectory for an assessment in the Brussels metropolitan area. *E-proceedings of ICTTE 2014-the 2nd International Conference for Traffic and Transport Engineering*.

Posters and Briefs

31. Bruwier, M., Mustafa, A., Aliaga, D., Archambeau, P., Erpicum, S., Nishida, G., … Dewals, B. (2017). Systematic flood modelling to support flood-proof urban design (Vol. 19, p. 17077). Presented at the EGU General Assembly 2017.
32. Dewals, B., Bruwier, M., Mustafa, A., Archambeau, P., Erpicum, S., … Pirotton, M. (2017). Urbanization and changing flood risk: a multi-level analysis. Presented at the International Symposium on the effects of global change on floods, fluvial geomorphology and related hazards in mountainous rivers.
33. Bruwier, M., Mustafa, A., Archambeau, P., Erpicum, S., Pirotton, M., Teller, J., & Dewals, B. (2016). Contribution of future urbanisation expansion to flood risk changes (Vol. 18, p. 16532). Presented at the EGU General Assembly 2016.
34. Saadi, I., Liu, F., Mustafa, A., Teller, J., & Cools, M. (2016). Uncertainty quantification in profile Hidden Markov Models (pHMM)-based activity sequences characterization. Presented at the 6th European Transport Research Conference.
35. Mustafa, A., Saadi, I., Cools, M., & Teller, J. (2015). Spatial variations of urban development drivers: Comparing an administrative logit approach with a geographically weighted regression model. Presented at ILUS 2015-the 1st International Land Use Symposium.

Unrefereed Publications

36. Dewals, B., Bruwier, M., Mustafa, A., Yan, P., Saadi, I., … Teller, J. (2017). Landuse change and future flood risk: the influence of micro-scale spatial patterns (FloodLand) - 5th progress report.
37. Dewals, B., Bruwier, M., Mustafa, A., Yan, P., Saadi, I., … Teller, J. (2016). Landuse change and future flood risk: the influence of micro-scale spatial patterns (FloodLand) - 4th progress report.

38. Dewals, B., Bruwier, M., Mustafa, A., Yan, P., Saadi, I., … Teller, J. (2016). Landuse change and future flood risk: the influence of micro-scale spatial patterns (FloodLand) – 3rd progress report.
39. Mustafa, A., Dewals, B., Archambeau, P., Pirotton, M., & Teller, J. (2015). Sustainable integrated land-use plan and flood risk management: A review. Presented at the 2015 Doctoral Seminar on Sustainability Research in the Built Environment (DS²BE-2015).
40. Dewals, B., Bruwier, M., Mustafa, A., Yan, P., Saadi, I., … Teller, J. (2014). Landuse change and future flood risk: the influence of micro-scale spatial patterns (FloodLand) – 2nd progress report.
41. Dewals, B., Bruwier, M., Mustafa, A., Yan, P., Saadi, I., … Teller, J. (2014). Landuse change and future flood risk: the influence of micro-scale spatial patterns (FloodLand) – 1st progress report.

PART 1: A Retrospective Analysis of Urban Development in Wallonia

Chapter 1: Addressing the Determinants of Urban Expansion and Densification

1.1. Introduction[1]

Urban sprawl is increasingly acknowledged as a significant environmental, economic, and social challenge in both the USA (Nechyba and Walsh, 2004; Song and Zenou, 2006) and Europe (EEA, 2006; Hennig et al., 2015). Accordingly, policies have been developed to curb this phenomenon and foster a more efficient use of the land (Danielsen et al., 1999; Grant, 2009). Such policies are typically based on a combination of spatial planning with fiscal and economic measures, promoting infill development and land recycling. Infill development is expected to reduce the consumption of land and thereby lower the pressure on green and agricultural areas (Jehling et al., 2016; McConnell and Wiley, 2011). It contributes to fostering urban development through the regeneration of vacant land and/or brownfields within cities (Loo et al., 2017) and to promoting a more efficient use of available amenities, such as roads, schools, retail areas, and public spaces (Burchell et al., 2000; Downs, 2001; Ooi and Le, 2013). Infill development is further expected to reduce traffic congestion through a more intensive use of public transport, especially when designed in a transit-oriented development perspective (Litman, 2016).

It should be stressed that infill development is not restricted to the reconversion of brownfields, even though it certainly has a role to play in this regard. Infill development is now increasingly targeting low- and medium-density urban areas, with significant densification capacities in terms of both available land and services. This is especially the case in countries like Belgium, where a number of built-up neighborhoods are characterized by low density and some discontinuity with historical urban cores (Marique et al., 2013). Indeed, Belgium in general and more specifically Wallonia (the southern part of Belgium) are in a remarkable situation within the European context with regard to urban sprawl (Dujardin et al., 2012; EEA, 2011a; Thomas et al., 2008). Hennig et al. (2015) measured urban sprawl trends for 32 European countries and reported that Belgium is one of the countries most affected by sprawl. Belgium is characterized by a mixed spatial planning

[1]This chapter is based on: Mustafa, A., Rompaey, A. V., Cools, M., Saadi, I., & Teller, J. (2018). Addressing the determinants of built-up expansion and densification processes at the regional scale. *Urban Studies,* 0(0), 1-20.

style, which combines regulatory with comprehensive planning dimensions (European Union, 1997). Land allocation is highly controlled by the regional zoning plan (plan de secteur) that covers the entire territory of the country. Dating back to the 1970s and 1980s, the zoning plan has long contributed to creating urban sprawl, as it dedicates large scattered zones to built-up uses throughout the country (Poelmans and Van Rompaey, 2009). Furthermore, the spatial planning system in Belgium is characterized by weak vertical relationships between territorial levels (regions and municipalities) and weak horizontal relationships between actors at the same territorial level (ESPON, 2005).

The combination of these two elements—the role of an oversized zoning plan and the lack of coordination between stakeholders—may somehow hinder infill development, even when land recycling and controlling sprawl are explicitly pursued by the spatial development strategies adopted in all three regions of the country.

A better understanding of the mechanisms underlying urban development processes is essential to improve the efficiency of the spatial planning system. Spatial models that explore the factors that control urban development and/or simulate future expected scenarios may provide valuable information in this respect (Poelmans and Van Rompaey, 2009). The objective of this research is to compare the controlling factors of urban expansion with densification, which is an essential component of spatial policies that aim to tackle urban sprawl (Nabielek, 2012; Tachieva, 2010). Our key motivation is to identify potential spatial drivers of low-density development and densification. To this end, urban development in Wallonia was analyzed from 1990 to 2010 based on datasets derived from cadastral data. A multinomial logistic regression (MNL) model was employed to explore the relationship between expansion/densification and a set of socioeconomic, geographic, and spatial planning factors.

The research proceeds as follows. Section 1.2 presents previous work in the domain of land-use change models, stressing the need for greater consideration of urban densities within these models. Section 1.3 gives details about the study area (Wallonia), the MNL model, and data preparation. We report our results and discuss these in Section 1.4, with Section 1.5 presenting our conclusions.

1.2. Previous work on densification

Aguayo et al. (2007) identified three main elements for land-use change spatial models: (i) examining the factors that control the change (e.g. Liu and Ma, 2011; Shu et al., 2014); (ii) projecting future scenarios and their potential impacts (e.g. Mustafa et al., 2016; Robinson et al., 2012); and (iii) evaluating the impacts of different spatial policies on land-use patterns (e.g. Guzy

et al., 2008; Jantz et al., 2003). In line with the aims of this study, we focus on exploring the factors that control urban development considering both expansion and densification processes.

A number of studies have aimed at a better understanding of urbanization controlling factors. Oueslati et al. (2015) examine the relationship between urban sprawl and a set of controlling factors in several European cities. Their results show the significant role that socioeconomic, transportation, and environmental factors play in urban sprawl. Li et al. (2013), Nong and Du (2011), Shu et al. (2014), and Traore and Watanabe (2017) explore the historical effects of physical, socioeconomic, and neighborhood factors on urban expansion in relation to different geographical locations. Braimoh and Onishi (2007) identify the factors underlying residential and industrial/commercial development in Lagos (Nigeria) between 1984 and 2000. The findings of these studies provide important implications for spatial planning. In many studies, the relationship between controlling factors and urban development is analyzed with logistic regression (logit) models. These studies confirmed that logit models are empirically robust.

Typically, the identification of potential factors controlling urban expansion is based on expert knowledge of the specific study area as well as a literature review (Cammerer et al., 2013). The variety of controlling factors introduced in recent urban studies is summarized in Table 1.1. These factors can be grouped into five categories: (i) accessibility factors; (ii) topological factors; (iii) neighborhood factors; (iv) socioeconomic factors; and (v) planning policies.

Table 1.1. Controlling factors of urban expansion considered in some recent studies.

	Accessibility factors	Topological factors	Neighborhood factors	Socio-economic factors	Spatial planning policies
Mustafa et al. (2017)	●	●	●	●	●
Achmad et al. (2015)	●			●	
Chen et al. (2014)	●	●			
Mustafa et al. (2014)	●	●	●	●	●
Zhang et al. (2013)	●	●			
Li et al. (2013)	●	●	●		
Cammerer et al. (2013)	●	●	●	●	
Vermeiren et al. (2012)	●	●	●		
Dubovyk et al. (2011)	●	●	●	●	
Poelmans and Van Rompaey (2010)	●	●		●	●
Batisani and Yarnal (2009)	●	●		●	●
Verburg et al. (2004)	●	●	●	●	●

Accessibility factors, such as distance to roads, are often taken into consideration in land-use change modeling (Aguayo et al., 2007). Herbert and Thomas (1982) claim that sprawl is commonly controlled by accessibility factors. A high accessibility level plays a decisive role in decreasing travel costs and making far-out land more accessible, resulting in lower-density urban developments.

Topological factors, such as elevation, are correlated with the price of urban development. Liu et al. (2016) suggest that the construction cost is considerably high for rugged lands.

Neighborhood factors, such as the proportion of urban land in the neighborhood, are especially important because of the fact that urban development can be regarded as a self-organization dynamics in which neighboring interaction strongly influences new developments (Poelmans and Van Rompaey, 2010). Many developers tend to develop land near to existing built-up areas because of the lower development risk for their investment (Rui and Ban, 2010). Socioeconomic factors, such as population density and employment potential, are quite often considered as active drivers of urbanization (Liu and Ma, 2011). For instance, economic activities may lead to a concentration of populations, which increases pressure on housing and housing prices in the center. Thus, it could be cheaper to develop land outside urban centers in areas characterized by lower density (Christiansen and Loftsgarden, 2011).

The influence of these controlling factors on urban development is usually measured on regular grids composed of square cells of a dimension between 30×30 m and 300×300 m (e.g. Feng et al., 2011; Hao et al., 2013; Hu and Lo, 2007; Liu et al., 2008; Vermeiren et al., 2012). Most studies assume that urban expansion is a binary process, contrasting two classes of cells, i.e., urban vs non-urban cells (e.g., Mustafa et al., 2017; Vermeiren et al., 2012). Such a binary representation of urban environment somehow disregards the fuzzy nature of urban boundaries (Ban and Ahlqvist, 2009). More importantly, it tends to conceal the potential for further infill development within already built-up areas when their present density and level of services allow it. Some studies have specifically considered multiple urban densities (Mustafa et al., 2015a, 2016; Xian and Crane, 2005; Yang, 2010). Considering various levels of densities is necessary to measure the influence of controlling factors on densification processes and infill development (Loibl and Toetzer, 2003); this is especially important as the factors governing sprawl and infill development may not be identical in their nature or their relative importance. Eliciting these differences requires modeling both expansion and densification processes. Finally, measuring past densification processes and the factors behind these may help to reveal and activate available capacity in already urban areas, which is in line with current land recycling policies.

In sum, a major difference in our approach compared with previous work is that we examine the potential of the spatial models to explore the factors behind urban development, considering different levels of density and the drivers of infill development.

1.3. Material and methods

1.3.1 Study area

Wallonia (Figure 1.1) accounts for 55% of the territory of Belgium with a total area of 16,844 km^2 – to give an idea, this area is slightly larger than Northern Ireland in the UK or the US state of Connecticut. Its main urban cores are Charleroi, Liège, Mons, and Namur, which are all characterized by a historical city center, around which the urban development has expanded. The total population of Wallonia in 2010 was 3,498,384 inhabitants, corresponding to one-third of the Belgium population (Belgian Federal Government, 2013). The population is mainly concentrated in the northern areas, following the nineteenth-century industrial axis, running from east (Liège) to west (Mons) (Thomas et al., 2008). North of this axis, urban landscapes are highly influenced by the Brussels metropolitan area. Toward the far south of Wallonia, urban development is influenced by the presence of the city of Luxembourg (Thomas et al., 2008). Topographically, elevations in the region range from sea level to 693 m above sea level.

Wallonia is characterized by a strong sprawl and the resulting landscape fragmentation (Dujardin et al., 2014; EEA, 2011a). Densification strategies are especially important in such a context so as to limit the further consumption of land and to better structure existing peri-urban areas considering their specificities (De Smet and Teller, 2016).

1.3.2. Outline of the model

The built-up density index is calculated per 1 ha (100m $\times$100m) over Wallonia using Belgian cadastral data. The range of density values is then subdivided into four classes (non-urban, low-, medium-, and high-density urban areas) by means of the natural breaks technique (Jenks and Caspall, 1971). To understand the expansion and densification processes, the methodology is tailored to identify the controlling factors of (i) expansion of the three density classes vs the non-urban class, and (ii) transitions from low- and medium-density classes to medium- and high-density classes.

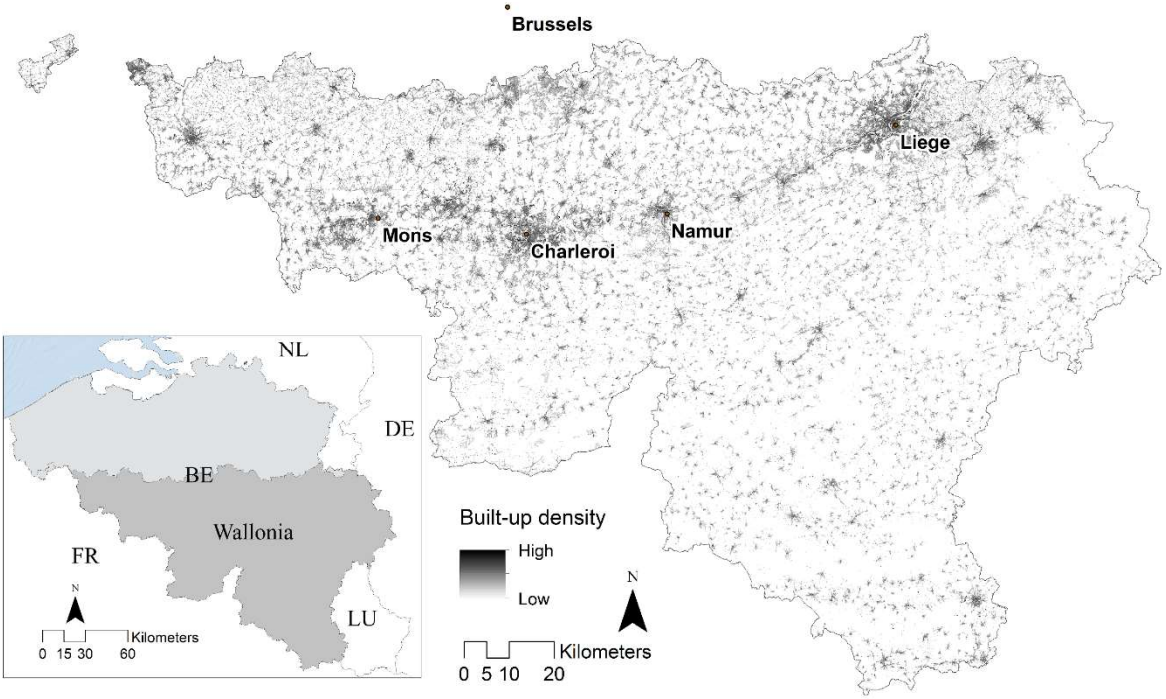

Figure 1.1: Study area.

We employ a multinomial logistic regression (MNL) model to examine the relationship between expansion/densification and their controlling factors. The MNL model allows for the consideration of several classes as the dependent variable (Y_n), using a set of independent explanatory variables (X_s). When working with MNL models, three kinds of dependent variables should be considered: (i) the nominal Y responses; (ii) the categorical responses with natural ordering; and (iii) the nested responses when one category is nested in the previous one. In this research, the dependent variable for the model is initially treated as categorical under the assumption that the levels of dependent status have a natural ordering (i.e., low to high density). To evaluate this assumption, the test of the proportional odds assumption is performed. The significance of the chi-squared statistic of the test is <0.001, which implies that the assumption of having a natural ordering in the dependent variable is violated. We then employ a nested MNL model with two levels: (i) urban vs non-urban; and (ii) three urban densities. The inclusive values (IVs) for the two nested levels are 0.8 and 3.9. Since at least one of the IVs is outside the 0–1 range, we decided not to opt for the nested MNL, as the parameter estimates are only consistent with utility maximization for a certain value range of the explanatory variables (Ortúzar and Willumsen, 1994). Accordingly, a nominal MNL model is adopted for this study.

The general form of the MNL model can be represented as:

$$\begin{aligned} \log(k_1) &= \alpha_{k_1} + \beta_{k_1 1} X_1 + \beta_{k_1 2} X_2 + \ldots + \beta_{k_1 v} X_v \\ &\ldots \\ \log(k_n) &= \alpha_{k_n} + \beta_{k_n 1} X_1 + \beta_{k_n 2} X_2 + \ldots + \beta_{k_n v} X_v \end{aligned} \qquad (1.1)$$

where *log(k_n)* is the natural logarithm of class k_n vs the reference class k_0, *X* is a set of explanatory variables (X_1, X_2,…, X_v), α_{k_n} is the intercept term for class k_n vs the reference class, and $\beta$is the slopes for the classes (the coefficient vector). Thus, the probabilities of each class can be obtained using the following formula:

$$\begin{aligned}
((P_c)_{ij}, Y = k_0) &= \frac{1}{1 + \exp(\log(k_1)) + \exp(\log(k_2)) + \ldots + \exp(\log(k_n))} \\
((P_c)_{ij}, Y = k_1) &= \frac{\exp(\log(k_1))}{1 + \exp(\log(k_1)) + \exp(\log(k_2)) + \ldots + \exp(\log(k_n))} \\
&\ldots \\
((P_c)_{ij}, Y = k_n) &= \frac{\exp(\log(k_n))}{1 + \exp(\log(k_1)) + \exp(\log(k_2)) + \ldots + \exp(\log(k_n))}
\end{aligned} \qquad (1.2)$$

where $((Pc)_{ij}, Y=k_n)$ is the probability of change from the reference class to class k_n occurring in cell *ij*. The MNL model employs the maximum likelihood estimation method to achieve the best-fit sets of coefficients for each *X*.

The model is performed for two observed periods, 1990–2000 and 2000–2010, using Belgian cadastral data. A comparison of the two periods allows the measurement of the stability of the role of the different factors over time. The MNL outcomes are a set of coefficients that define the contribution of each controlling factor to the urban development, as well as a map of probability of being urban for each class, which is generated by plugging the coefficients of the MNL model into Equation (1.2). The MNL model assesses overall model performance and the significance of individual *X* variables. The *X* variables were selected by entry testing based on the significance of the score statistic (*P*-value), which was set to $P \leq 0.05$. Only variables significant at $P \leq 0.05$ on at least one class were included in the final MNL model.

The goodness-of-fit of the model runs was evaluated using the relative operating characteristic (ROC) method. The ROC is an excellent method to estimate the quality of a model that predicts the occurrence of an event by comparing a probability map depicting the likelihood of change occurring and a binary map showing where the changes actually occurred (Hu and Lo, 2007). A ROC value of 0.5 means completely random discrimination and 1 means perfect discrimination.

Dependent variables

The dependent variables for the MNL model are defined using the cadastral dataset (CAD). CAD is a vector dataset representing buildings in two dimensions as polygons, made available by the Land Registry Administration of Belgium. CAD provides the construction date for each building. This information was used to generate three urban maps for 1990, 2000, and 2010. CAD vector data were then rasterized at a very fine cell dimension of 2×2 m.

One of the independent variables, elevation (DEM), is available at 10×10 m cell size and therefore we should aggregate the rasterized CAD data to at least 10×10 m (representing a building of 100 m). The computational time and resources required to process the 10×10 m datasets, about 400,000,000 cells, are huge. Data aggregation can efficiently reduce the computational resources of our model. Still the modifiable areal unit problem (MAUP) should be considered when aggregating spatial data (Openshaw, 1984; Openshaw and Taylor, 1979). To examine the effects of aggregation in the context of the MAUP, we performed a series of the first-lag autocorrelation analyses based on Moran's I test following Jelinski and Wu (1996). The conceptualization of spatial relations is based on King's (queens) case analysis, which considers a neighborhood window of eight cells. As a result of this sensitivity analysis (Figure 1.2), we selected an aggregated cell of 100×100 m, which appears as the best combination between aggregation dimension and Moran's I. Moreover, the 100×100 m cell size is commonly used in regional land use models (e.g. Mustafa et al., 2017; Poelmans and Van Rompaey, 2010).

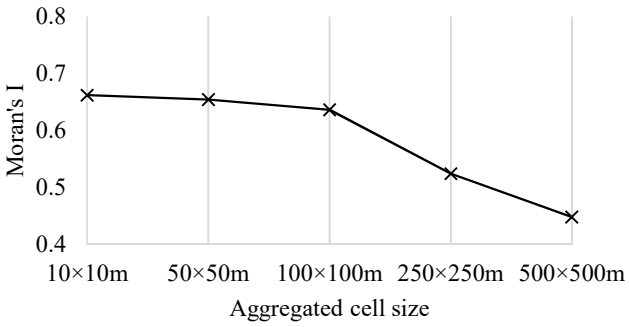

Figure 1.2: Effects of data aggregation on spatial autocorrelation (Moran's I) resulting from aggregation procedures for cadastral dataset.

Each aggregated cell has a density value that exhibits the number of 2×2 m cells located within its boundary. This density value will be used as a built-up density index for each aggregated 100×100 m cell. The minimum density value adopted for considering 100×100 m cells as built-up is 25. The threshold of 25 (representing a building of 100 m²) corresponds to an average-sized residential building in Belgium (Tannier and Thomas, 2013). The density value is then used to represent four classes: (class-0) non-urban, (class-1) low-density, (class-2) medium-density, and (class-3) high-density urban.

The natural breaks classification method was used to set the thresholds that define the different classes. This method effectively ensures a high internal homogeneity among classes (Fraile et al., 2016). The natural breaks method uses the Jenks optimization algorithm (Jenks and Caspall, 1971), which identifies breaks by the arrangement of classes that best groups similar values. This is done by minimizing the average deviation of each class from its mean and maximizing that average deviation from the means of the other classes. Table 1.2 presents the resulting thresholds, which define the different densities for the model implementation. The low-density and scattered built-up landscape of Wallonia resulted in low thresholds for medium and high densities.

Table 1.2. Range of built-up classes in the number of 2×2 cells.

Class	Minimum	Maximum	% of cells in 1990
Class-0 (non-urban)	0	24	85.13%
Class-1 (low-density)	25	264	10.69 %
Class-2 (medium-density)	265	735	3.56 %
Class-3 (high-density)	736	2500	0.62 %

Urban development controlling factors

The accessibility factors included in this study are the Euclidian distance to Road1 (highways), Road2 (main roads), Road3 (secondary roads), Road4 (local roads), railway stations, large-sized Belgian cities (population >90,000), and medium-sized Belgian cities (population 20,000–90,000). For the topological factors, slope and elevation are included. Employment rate is considered as a socioeconomic factor. The number of existing built-up cells from each density class within a 5×5 cell neighborhood is included in this study to consider local interaction effects. The selection of the neighborhood size was made because previous studies found that the defined neighborhood using all surrounding cells within a radius of one to eight cells can capture the operational range of the local processes being modeled (Hu and Lo, 2007; Roy Chowdhury and Maithani, 2014). Table 1.3 gives the complete list of the selected controlling factors, *Xs*. All data used in this study are represented as a 100×100 m raster grid. X variables are measured in different units so we standardized all continuous X variables. If some X variables relatively measured the same phenomena, strong collinearities would cause an erroneous estimation of the MNL model's parameters. Consequently, a multicollinearity test was examined in the initial stage using variance inflation factors (VIF). Montgomery and Runger (2003) recommended that the VIFs should not exceed 4.

X variables may exhibit spatial autocorrelation, which would bias the results of the regression analysis (Overmars et al., 2003). To address this issue, logistic regression land-use models are commonly calibrated based on a data sampling approach (e.g. Cammerer et al., 2013; Huang et al., 2010; Puertas et al., 2014). An alternative solution is the autologistic regression model, which considers an autocorrelative term in the regression model. A number of studies have argued that autologistic models outperform logistic models (e.g. Lin et al., 2011; Shafizadeh-Moghadam and Helbich, 2015). In contrast, some authors (e.g. Dormann, 2007) have reported that the logistic regression model tends to outperform the autologistic model in terms of estimation of model parameters. However, comparison of both modeling approaches (logistic vs autologistic) is beyond the scope of the present research. Our model was calibrated through a data sampling approach, which is commonly used in land-use change modeling. The selection of samples is based on 100 runs of the MNL model with different random samples. The best sample set, evaluated by ROC, was then selected.

Table 1.3. List of selected urbanization controlling factors.

Factor	Name	Type	Unit	SD*	Source
X1	Elevation (DEM)	Continuous	Meter	148.8	Belgian National Geographic Institute
X2	Slope	Continuous	Percent rise	5.6	Own calculation based on DEM
X3	Dist. to Road1	Continuous	Meter	8264.8	Own calculation based on NAVTEQ 2002 map
X4	Dist. to Road2	Continuous	Meter	3740.1	Own calculation based on NAVTEQ 2002 map
X5	Dist. to Road3	Continuous	Meter	1419.5	Own calculation based on NAVTEQ 2002 map
X6	Dist. to Road4	Continuous	Meter	834.7	Own calculation based on NAVTEQ 2002 map
X7	Dist. to railway stations	Continuous	Meter	5690.2	Own calculation based on WALPHOT s.a. data
X8	Dist. to large-sized cities	Continuous	Meter	25688.1	Own calculation based on WALPHOT s.a. data
X9	Dist. to med-sized cities	Continuous	Meter	12865.4	Own calculation based on WALPHOT s.a. data
X10	Number of class1 cells within a 5x5 window	Continuous	Number	4.1	Own calculation based on CAD data
X11	Number of class2 cells within a 5x5 window	Continuous	Number	2.5	Own calculation based on CAD data
X12	Number of class3 cells within a 5x5 window	Continuous	Number	1.1	Own calculation based on CAD data
X13	Employment rate	Continuous	Percent	5.3	Own calculation based on Belgian statistics
X14	Zoning	Categorical	Binary	0.4	Own calculation based on Wallonia authorities data

* standard deviation

1.4. Results and discussion

Figure 1.3 shows the spatial distribution pattern of density classes in 1990. High-density cells are concentrated in existing metropolises, whereas medium-density cells tend to be located in their surroundings and low-density lands are likely to be found in rural and remote locations. Table 1.4 summarizes class-to-class transitions from 1990 via 2000 to 2010. It can be seen that the transition from non-urban to low-density developments (i.e., class-0 to class-1) largely dominates over both periods. However, a progressive trend toward infill development, namely densification of urban areas, can also be identified from this table. This trend should be amplified especially in the transitions from medium- to high-density developments (i.e., class-2 to class-3) in those areas that are best located in terms of accessibility to transport and services. This finding can be related to some recent spatial policies. Since 2005, the definition of a new zone to be urbanized in the regional zoning plan in Wallonia must be compensated by the downzoning of a similar-sized area that was to be urbanized beforehand to a nonurban zone (Prokop et al., 2011).

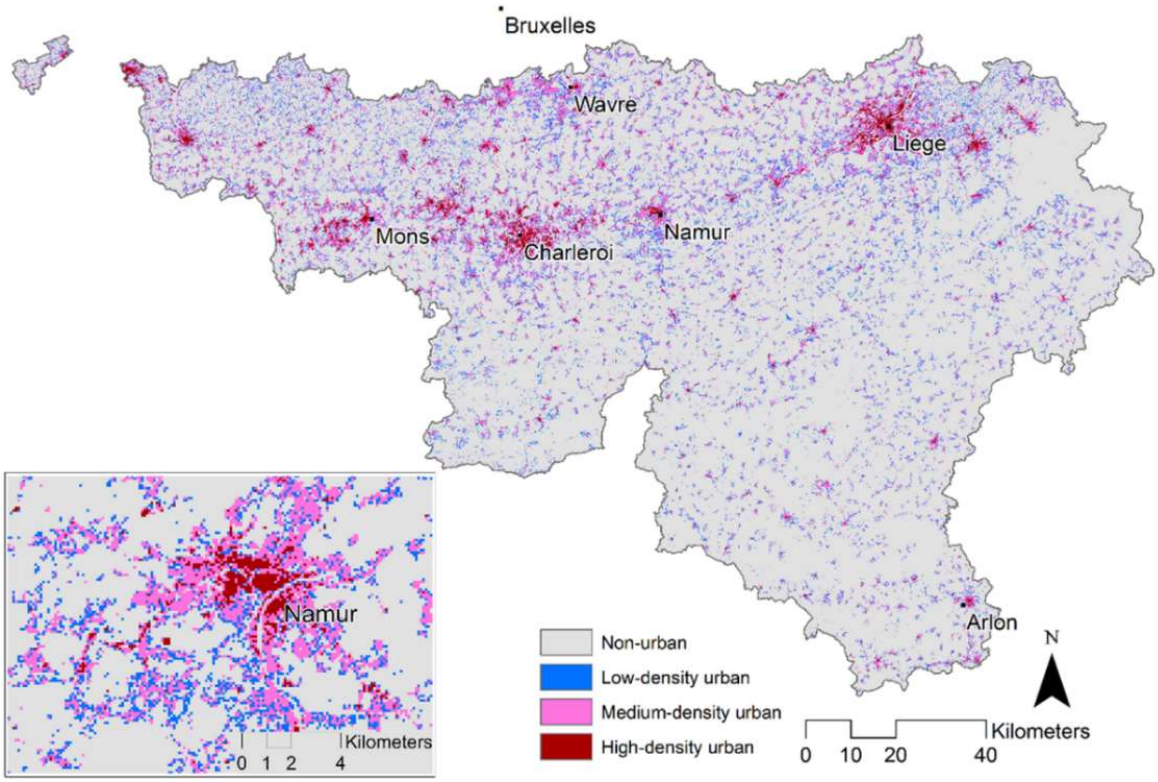

Figure 1.3: Urban density classes in 1990.

Table 1.4 shows that the transitions from class-1 to class-3 over the study period are marginal. Thus, densification is considered as the transitions from class-1 to class-2 and from class-2 to class-3, whereas expansion is seen as the transitions from class-0 to classes 1–3. The VIF test values (<1.59) for all standardized explanatory variables suggest that all X variables can be incorporated in the MNL model.

Table 1.4. The number of cells representing class-to-class changes (% of total changes).

1990-2000	Class-1	Class-2	Class-3
Class-0	14675 (60.91%)	1785 (7.41%)	550 (2.28%)
Class-1	-	6327 (26.26%)	102 (0.42%)
Class-2	-	-	653 (2.71%)
2000-2010	Class-1	Class-2	Class-3
Class-0	9665 (58.45%)	1202 (7.27%)	340 (2.06%)
Class-1	-	4714 (28.51%)	91 (0.55%)
Class-2	-	-	524 (3.17%)

1.4.1. Urban expansion

Table 1.5 presents the results of the expansion process, i.e., transitions from non-urban cells with a density of 0–24 to cells with urban density classes 1–3. For the relative measurement of the contribution of each controlling factor to the expansion process, the odds ratio (OR), which equals $exp(\beta)$, is calculated. An OR >1 (coefficients greater than 0) indicates a positive effect, i.e., the probability of development increases with an increasing OR of the variable, whereas an OR <1

indicates a negative effect. The results indicate that the impact of the different controlling factors varies along with density.

Expansion of all density classes is highly correlated with zoning status (X_{14}), which is in line with findings by Poelmans and Van Rompaey (2010). In both periods, the result shows a gradual upward trend in the zoning status from low density to high density. For instance, in 1990–2000, the expansion of classes 1, 2, and 3 is respectively around 11, 20, and 68 times more likely to be located in zones designated for urban use than in zones designated for other land uses. To minimize administrative and financial risks, high-density developments are typically located in areas where the legally binding plan allows such developments. In contrast, urban developments in areas adjacent to urban cores (medium density) such as suburbs do not strictly follow land-use plans. The impact of zoning on transitions to low-density classes is lower than the one observed in other classes. Such transitions can be considered as remote areas, consisting of scattered buildings (1–3 buildings/ha), which can sometimes deviate from existing zoning plans, especially in agriculture-related zones.

In both periods, elevation (X_1) is a positive determinant for low- and medium-density expansions, whereas slope (X_2) has a remarkable negative effect on all expansion processes, as in Poelmans and Van Rompaey (2010), especially on the expansion of medium- and high-density classes. The model predicts that a 5.6% rise in slope decreases the odds of expansion by a factor of 0.4 for the medium-density class, and by 0.3 and 0.4 for the expansion of the high-density class in 1990–2000 and 2000–2010, respectively.

All statistically significant distances to road classes have OR values <1 implying that the closer to roads, the higher the expansion probability, as reported in Cammerer et al. (2013), and Poelmans and Van Rompaey (2010). Distance to high-speed roads (X_3 and X_4) has a notable impact on the development of high-density areas, although it should be considered that a number of urban cores are directly accessible via high-speed roads in Wallonia. Distance to secondary roads (X_5) contributes to the expansion of different density classes, especially the medium-density class, whereas distance to local roads (X_6) has a remarkable impact on the expansion of low-density areas in both periods, which is what can be expected, as many low-density areas are only accessible via local roads. The findings suggest that the new developments of medium- and high-density projects are likely to be located near train stations (X_7) in 1990–2000 and 2000–2010.

Interpretation of the contribution of distance to large- and medium-sized cities (X_8 and X_9) in Wallonia indicates a decentralizing and suburbanizing trend over time. In 1990–2000, the impact of distance to large-sized cities positively affected high-density expansion. In 2000–2010, the distance to large-sized cities had a positive impact on low- and high-density classes. This means that the likelihood of low- and high-density developments increased with increasing distance to

large-sized cities in both periods. In contrast, distance to medium-sized cities was a negative determinant of medium- and high-density expansion in 1990–2000 and remained positive on low-density expansion in 2000–2010.

The increasing number of existing low-density cells within a neighborhood of 5×5 size (X_{10}) reveals a strong relationship with low-density expansion: every four low-density neighbors increase low-density expansion odds by around four times in 1990–2000 and 2000–2010. The probability of medium-density expansion is greater by increasing the number of existing low-, medium-, and high-density cells (X_{10}, X_{11}, X_{12}), whereas the probability of high-density expansion is greater by increasing the number of existing medium- and high-density cells (X_{11}, X_{12}) within a neighborhood.

Table 2.5. The coefficients (β) of the MNL model for urban expansion (reference: class-0). Sample size 16,360.

Factor	1990-2000			2000-2010		
	Coefficients β (Odds Ratio)			Coefficients β (Odds Ratio)		
	Class-1	Class-2	Class-3	Class-1	Class-2	Class-3
Intercept	-1.106	-3.669	-6.402	-1.106	-3.526	-6.288
X1	0.217*	0.129*	-0.054	0.135*	0.154*	-0.064
	(1.242)	(1.138)	(0.947)	(1.144)	(1.167)	(0.938)
X2	-0.218*	-0.951*	-1.307*	-0.234*	-0.845*	-1.000*
	(0.804)	(0.386)	(0.271)	(0.791)	(0.429)	(0.368)
X3	-0.058	-0.134	-0.564*	-0.100*	-0.261*	-1.170*
	(0.944)	(0.874)	(0.569)	(0.905)	(0.771)	(0.310)
X4	-0.042	-0.236*	-0.539*	0.033	-0.251*	-0.505*
	(0.959)	(0.790)	(0.583)	(1.034)	(0.778)	(0.603)
X5	-0.133*	-0.334*	-0.263*	-0.098*	-0.252*	-0.093
	(0.875)	(0.716)	(0.769)	(0.907)	(0.778)	(0.911)
X6	-0.214*	-0.157*	-0.211	-0.205*	-0.144*	-0.026
	(0.807)	(0.855)	(0.810)	(0.814)	(0.866)	(0.975)
X7	0.017	-0.161*	-0.301*	0.021	-0.129*	-0.365*
	(1.017)	(0.851)	(0.740)	(1.021)	(0.879)	(0.694)
X8	0.005	-0.059	0.186*	0.105*	0.044	0.271*
	(1.005)	(0.942)	(1.204)	(1.110)	(1.045)	(1.311)
X9	-0.028	-0.168*	-0.237*	0.064*	0.002	0.126
	(0.972)	(0.845)	(0.789)	(1.066)	(1.002)	(1.134)
X10	1.286*	0.619*	0.098	1.260*	0.512*	0.255*
	(3.619)	(1.856)	(1.103)	(3.524)	(1.669)	(1.290)
X11	0.306*	0.433*	0.289*	0.485*	0.709*	0.529*
	(1.358)	(1.541)	(1.336)	(1.623)	(2.031)	(1.697)
X12	0.009	0.204*	0.287*	0.040	0.286*	0.432*
	(1.009)	(1.227)	(1.333)	(1.041)	(1.331)	(1.541)
X13	N.S.	N.S.	N.S.	N.S.	N.S.	N.S.
X14	2.371*	2.974*	4.216*	2.446*	2.967*	4.103*
	(10.705)	(19.576)	(67.728)	(11.539)	(19.437)	(60.546)
ROC	0.903	0.887	0.959	0.906	0.889	0.973

* Indicate significance at P≤ 0.05 level
N.S. non-significant at P≤ 0.05 level

The lack of significant contribution of employment rate (X_{13}) to the expansion processes indicates that it was not a limiting factor of the urban expansion processes, as it was the case in Hu and Lo (2007), and Poelmans and Van Rompaey (2010).

1.4.2. Urban densification

Urban densification is defined as transitions from low- to medium-density class, as well as transitions from medium- to high-density class. As such, it corresponds to infill development. In general, the magnitude of the unique effects of land-use policies (zoning) and accessibility factors declined along with the densification process. Table 1.6 lists the MNL model's results of the densification process. The slope's OR values (X_2) <1, as in densification processes, signify that the process of conversion from lower to higher densities tends to occur in flat areas. The estimated coefficients of slope in both periods highlight that slope—the only variable that has a statistically significant impact on all urban development processes—continues to play an important role in explaining both expansion and densification processes, compared with other variables in our model. When considering infill development policies, it could be expected that some variables, such as distance to train stations or accessibility to employment areas, would play a more significant role in driving urban development, by contributing to reducing home-to-work distances and increasing the use of sustainable modes of transport. Our results indicate that in Wallonia this is not yet the case; urban development processes continue to be determined by physical factors, i.e., low slope areas that are scattered across the entire region.

Distance to high-speed roads (X_3 and X_4) negatively contributes to all densification processes. Other distance-related factors have no impact except for secondary roads, which contributed to the densification of low-density areas in 1990–2000, and distance to large-sized cities, which contributed to the densification of low-density areas in 2000–2010. Neighborhood plays a significant role in densification processes. In both periods, the odds of conversion of low-density lands into medium density are increased by a factor of 1.1 for every four low-density neighbors. Each medium-density neighbor increases the odds of low-density densification by ~0.5 times. The odds of conversion of medium density into high density are increased by ~1.2 for each high-density neighbor. These findings suggest that existing high-density locations will generally experience a higher densification rate. Unlike the expansion processes, where the employment rate is not significant, the employment rate (X_{13}) contributes positively to the densification of medium-density areas. However, the contribution of this variable to the densification process is small compared with the other variables. The nonsignificant role of employment rate could be explained by the fact that many commuters (even car users) can deduct their transport costs from their income tax (De Decker, 2008). Together with the density of the road network, this may encourage people to choose to live in low-density settlements far from their workplaces. Interestingly, the

magnitude of the zoning status effect (X_{14}) on the densification process decreases compared with the expansion process. The effect of zoning status on the change from medium- to high-density class is not significant. It also shows a moderate effect on the change from low to medium density in both periods.

The ROC values differ between the distinct processes of urban development. The expansion process shows a relatively high goodness-of-fit with ROC values of 0.89–0.97. Estimation of the potential urban densification process produced many false-positives, which were estimated at ROC values of 0.74–0.76. This implies that the densification process is less predictable than the urban expansion process, which can be explained by the fact that most of the selected controlling factors were not statistically significant. The ROC values for 1990–2000 and 2000–2010 were almost identical, indicating that there were no major changes in the urban development trend over the study period.

Table 1.6. The coefficients (β) of the MNL model for urban densification.

	1990-2000		2000-2010	
Factor	Coefficients β (Odds Ratio)		Coefficients β (Odds Ratio)	
	Reference: class-1 Sample size: 9000	Reference: class-2 Sample size: 1000	Reference: class-1 Sample size: 9000	Reference: class-2 Sample size: 1000
	Class-2	Class-3	Class-2	Class-3
Intercept	-1.507	-0.174	-1.547	-0.173
X1	N.S.	N.S.	N.S.	N.S.
X2	-0.431 (0.650)	-0.256 (0.774)	-0.467 (0.627)	-0.424 (0.654)
X3	-0.106 (0.900)	-0.397 (0.672)	-0.165 (0.848)	N.S.
X4	-0.091 (0.913)	N.S.	-0.095 (0.909)	-0.282 (0.754)
X5	-0.054 (0.948)	N.S.	N.S.	N.S.
X6	N.S.	N.S.	N.S.	N.S.
X7	N.S.	N.S.	N.S.	N.S.
X8	N.S.	N.S.	0.059 (1.061)	N.S.
X9	-0.110 (0.895)	N.S.	N.S.	N.S.
X10	0.089 (1.093)	-0.448 (0.639)	0.073 (1.075)	-0.458 (0.632)
X11	0.271 (1.311)	N.S.	0.276 (1.318)	N.S.
X12	N.S.	0.183 (1.201)	N.S.	0.230 (1.259)
X13	N.S.	0.078 (1.081)	N.S.	0.195 (1.216)
X14	1.123 (3.074)	N.S.	1.314 (3.723)	N.S.
ROC	0.738	0.762	0.738	0.757

* Indicate significance at P≤ 0.05 level
N.S. non-significant at P≤ 0.05 level

1.5. Conclusions

Using a multinomial logistic regression model, this study explores the relationship between urban expansion/densification and their controlling factors. It considers the three classes of urban densities of low, medium, and high density. Previous urban expansion models assumed a binary process of expansion, i.e., urban vs non-urban. Tables 1.5 and 1.6 show that the assumption of a binary approach may lead to inaccurate conclusions as the relative importance of the controlling factors typically varies with density, for both expansion and densification processes.

This study highlights significant factors that control low-density development, which is one of the main characteristics of urban sprawl. Spatial planning, road accessibility, and neighborhood interactions are important determinants of the low- and medium-density developments in Wallonia, Belgium. This finding is in line with those of other studies conducted in other regions of the world (e.g. Aguayo et al., 2007; Hu and Lo, 2007).

Our results indicate that there is a progressive shift from expansion to densification in Wallonia even though expansion processes remain very active. The densification processes show a nonsignificant relationship with railway stations, which means that infill development does not yet follow a transit-oriented development approach that would foster high-density developments around train stations. Proximity to medium- and large-sized cities does not appear to be a key factor in densification processes, even though it is certainly where infill development is most expected in terms of both real estate value and contribution to sustainable development. This phenomenon may be related to the fact that densification appears highly correlated with neighborhood characteristics, which may conceal the effect of proximity to medium- and large-sized cities where denser neighborhoods may be expected.

Our study reveals that infill development is mainly driven by local factors in Wallonia and that expansion remains controlled by the zoning plan. In contrast, the influence of zoning on densification is not major. Infill development does not obey an official spatial policy adopted at the regional level that is articulated along clear sustainability principles. Hence, the impact of zoning on expansion and densification appears counterproductive in some respects, which is quite unsatisfactory in terms of land-use policy. It should be stressed that zoning documents were drawn up in the 1970s and 1980s in Wallonia, well before the current sustainability agenda. Even though these documents have been partially revised since then, areas open to urban development remain overabundant in some parts of the region. A mechanism for the transfer of development rights should be designed to better allocate urban zones to places/nodes where infill development can be supported. At the same time, streamlining the modification of land-use plans and planning permission procedures in selected areas of the region may provide appropriate support for those processes.

The results of this study emphasize that the MNL model incorporating various classes of urban densities provides useful information for policy makers who want to explore the relationships between spatial drivers of infill development. Contrasting the drivers underlying expansion and densification processes is essential for designing spatial policies that support improved land recycling and infill development.

1.6. Key contributions

- The relative importance of the drivers behind urban development typically varies with density.
- One can observe a slight increase of densification processes over time in Wallonia. Still, expansion keeps by far the dominant process.
- Densification processes are mainly driven by self-organization dynamics. It does not follow a clear land-use policy following infill development at regional level.
- Expansion processes are strongly controlled by the zoning plan.

PART 2: Projecting Future Urbanization. Modelling Approach, Calibration, and Validation

Chapter 2: Modelling Urbanization with Multinomial Logistic Regression and Cellular Automata

2.1. Introduction[1]

Urban development is the most typical form of land-use change. Without policy interventions, urban development may cause destructive impacts on the environment, on natural resources and on human health (Zhang et al., 2011). Consequently, modelling urbanization is attracting attention of scientists, urban planners and politicians alike. Most urban expansion models (e.g. Han and Jia, 2016; Liao et al., 2014; Liu et al., 2014; Puertas et al., 2014; Vermeiren et al., 2012) are raster-based with a coarse cell space ranging from 30 m× 30 m to 300 m × 300 m. Whilst many authors advocate a larger grid cell for land-use modelling, for example 100×100m (e.g. Jiang et al., 2007; Munshi et al., 2014; Poelmans and Van Rompaey, 2010), land-use cells with these dimensions usually comprise a mix of different land-uses (Omrani et al., 2015). For example, a cell classified as built-up land may be occupied by 80% built-up surface and 20% arable surface. With increases in the spatial resolution of data, researchers have begun to use grid cells as small as 10 m × 10 m, such as Berberoğlu et al. (2016) model for Adana city (Turkey). However, the drawback to using such a fine resolution is that it requires intensive computational resources to model larger study areas such as regions where 100 m × 100 m cell dimensions are commonly used (e.g. Omrani et al., 2015; Poelmans and Van Rompaey, 2010). One solution to address the trade-off between coarse regular cell spaces and heterogeneity is examining several built-up densities instead of a binary classification (i.e. urban/non-urban). Although urban densification processes, transitions from low-density to high-density, is critically important for policy makers who are concerned with restricting sprawl (Nabielek, 2012; Tachieva, 2010), the literature on urban expansion models highlights that many of the models focus only on expansion process (e.g. Poelmans and Van Rompaey, 2009; Wang et al., 2013). However, there are a limited number of studies that consider the expansion of several urban densities and/or densification in a variety of ways. Mustafa et al.

[1]This chapter is based on: Mustafa, A., Heppenstall, A., Omrani, H., Saadi, I., Cools, M., & Teller, J. (2018). Modelling built-up expansion and densification with multinomial logistic regression, cellular automata and genetic algorithm. *Computers, Environment and Urban Systems*, 67, 147–156.

(2015a), Robinson et al. (2012), Sunde et al. (2014), Xian and Crane (2005), Yang (2010), and Zhang et al. (2011) model the expansion of different urban/built-up densities. Crols et al. (2015), Loibl and Toetzer (2003) and White et al. (2015, 2012) model the processes of urban expansion as well as of densification. They define densification as an increase in population and/or several economic sectors density.

One of the most popular techniques of existing urban expansion models which are employed to analyze and/or predict the urban landscape is cellular automata (CA) (e.g. Berberoğlu et al., 2016; Feng et al., 2011; Han et al., 2009; Tian et al., 2016; Wang et al., 2013). CA is a dynamic discrete space and time bottom-up modelling approach. CA is widely used in urbanization modeling due to its simplicity, transparency and powerful capacities for dynamic spatial simulation (Clarke and Gaydos, 1998). Aburas et al. (2016) and Santé et al. (2010) reviewed CA urbanization models concluding that the CA modelling approach is one of the most appropriate techniques for simulating urban landscape. However, key challenges in CA are calibrating the transition rules of urban development probability as a function of (i) a series of controlling factors and (ii) spatial (neighborhood) characteristics. Early methods for CA calibration are based on trial and error (e.g. White and Engelen, 1997) and/or a visual test, to determine the model's parameters (e.g. Clarke et al., 1997; Ward et al., 2000). Recently, a variety of automated methods based on statistics (e.g. García et al., 2013), machine learning (e.g. Rienow and Goetzke, 2015), artificial neural networks (e.g. Berberoğlu et al., 2016) and search algorithms for optimization such as genetic algorithms (e.g. Al-Ahmadi et al., 2009) and particle swarm optimization (e.g. Feng et al., 2011) have begun to be widely employed.

Validation of CA models is another challenge. A common validation method is based on pixel-by-pixel location agreement (e.g. Poelmans and Van Rompaey, 2009). This approach cannot discriminate between "near-miss" and "far-miss" errors which limits its ability to detect spatial patterns (Mustafa et al., 2014). Another approach is based on spatial metrics (Roy Chowdhury and Maithani, 2014). Spatial metrics can be potentially misleading, for example, two areas with distinctly different infrastructures may show the same spatial index (White and Engelen, 2000). A third method is based on a fuzzy set theory. Fuzzy map comparison provides a method of dealing and comparing maps containing a complex mixture of spatial information (Ahmed et al., 2013). It takes into account local variations meaning that matches found at shorter distances are given a higher agreement. It measures the similarity of a cell in a value between 0 (fully-distinct) and 1 (fully-identical). Thus, it can easily distinguish areas of minor errors from areas of major errors. (van Vliet et al., 2016) present a comprehensive survey of calibration and validation practices in land use change modeling.

This study contributes to research efforts that model urban expansion and densification processes. We model the urban expansion (non-urban to one of urban density classes) and densification

(lower urban densities to higher ones). The model is based on a hybrid approach which integrates logistic regression and CA modelling approaches. It is applied to Wallonia (Belgium) as a case study. Belgian cadastral data (CAD) are used to generate three urban land-use maps for the years 1990, 2000 and 2010. These maps represent four urban classes: non-urban (class-0), low-density (class-1), medium-density (class-2) and high-density (class-3). Three maps can define one calibration interval (1990-2000) and one validation interval (2000-2010). The model considers a set of static controlling factors related to accessibility, geo-physical features, policies and socio-economic factors. Another important factor is neighborhood interactions because of the fact that urbanization can be regarded as a self-organizing system (Poelmans and Van Rompaey, 2010).

The model's parameters are calibrated based on a logistic regression model and genetic algorithm. The logistic regression is employed to set the parameter of 12 urbanization controlling factors: elevation, slope, zoning status, employment rate, richness index and Euclidian distances to highways, main roads, secondary roads, local roads, railway stations, large-sized and medium-sized Belgian cities. The richness index is calculated as the average income per capita for each municipality divided by the average income per capita in Belgium. The dependent variable for the logistic regression model represents the changes from class-0 to class-1, class-2 or class-3, the changes from class-1 to class-2 and the changes from class-2 to class-3.

A multi-objective genetic algorithm (MGA) is employed to calibrate the neighborhood interactions on a dynamic basis. García et al. (2013) reported that the GA is one of the most robust heuristic automated methods to solve optimization problems. A number of studies have used GA to calibrate CA models (e.g. Al-Ahmadi et al., 2009; García et al., 2013; Shan et al., 2008). The MGA objective function is the maximization of allocation accuracy rates for all urban classes. The accuracy rate function is defined as a fuzzy membership function of exponential decay with a halving distance of two cells and a neighborhood window of four cells. The accuracy rate function is also employed to validate the model.

2.2. Materials

2.2.1. Datasets

The urban maps for 1990, 2000 and 2010 are generated based on the Belgian cadastral database (CAD) in a shapefile format. CAD vector data were rasterized at a cell size of 2 m × 2 m. The rasterized cells were then aggregated to a 100 m × 100 m raster-grid. The density values were calculated for the aggregated cells (100 m²) by counting the smallest cells (2 m²). All aggregated cells with density values less than 25 were considered as non-urban cells.

Table 2.1. Urban density classes range in number of 2×2 cells (% of 100x100 cell area).

Class	Minimum	Maximum
Class-0 (non-urban)	0	24 (1%)
Class-1 (low-density)	25	102 (4.1%)
Class-2 (medium-density)	103	499 (20%)
Class-3 (high-density)	500	2500 (100%)

Table 2.2. The number of cells representing class-to-class changes (% of total changes).

1990-2000	Class-1	Class-2	Class-3
Class-0	10841 (37.21%)	5153 (17.69%)	1016 (3.49%)
Class-1	-	10102 (34.67%)	151 (0.52%)
Class-2	-	-	1872 (6.43%)
2000-2010	Class-1	Class-2	Class-3
Class-0	7120 (34.99%)	3450 (16.96%)	637 (3.13%)
Class-1	-	7535 (37.03%)	107 (0.53%)
Class-2	-	-	1497 (7.36%)

Table 2.3. List of selected urban controlling factors.

Factor	Name	Type	Unit
X1	Elevation (DEM)	Continuous	Meter
X2	Slope	Continuous	Percent rise
X3	Dist. to Road1	Continuous	Meter
X4	Dist. to Road2	Continuous	Meter
X5	Dist. to Road3	Continuous	Meter
X6	Dist. to Road4	Continuous	Meter
X7	Dist. to railway stations	Continuous	Meter
X8	Dist. to large-sized cities	Continuous	Meter
X9	Dist. to med-sized cities	Continuous	Meter
X10	Employment rate	Continuous	Percent
X11	Richness index	Continuous	Percent
X12	Zoning	Categorical	Binary (0 non-urban, 1 urban)

All 100 m × 100 m cells have a density index ranging between 0 and 2500. The density index is then used to set four classes: non-urban (class-0), low-density (class-1), medium-density (class-2) and high-density (class-3). A geometrical interval classification method is used to set the density ranges that define the different classes. This classification method works very well on continuous data (Arlinghaus and Kerski, 2013). The resulting density ranges are listed in Table 2.1. Table 2.2 gives the actual urban transitions over the modeled period for four density classes. The urban development causative factors were operationalized to be included in the MNL. Table 2.3 gives the selected controlling factors for this study.

2.3. Methodology

This section discusses the main characteristics of the model. The quantity of change during calibration (1990-2000) and validation (2000-2010) phases was constrained to the actual quantity of new urban lands, Table 2.1, divided evenly by 10 (the number of years).

2.3.1. The transition rules

The quantity of change is spatially allocated based on a transition rule which has two components. The first component concerned the main urbanization controlling factors as determined using MNL. The second component dealt with the neighborhood characteristics (section 2.3.1.1). The transition potentials *P* for a cell *ij* changing its state from non-urban to one of urban densities or low density urban to a higher one at specific time-step is calculated as follows:

$$P_{ij} = \sqrt{\left(P_c\right)_{ij} \times \left(P_n\right)_{ij}^{\sigma}} \qquad (2.1)$$

where $(P_c)_{ij}$ is the urbanization probability based on controlling factors, $(P_n)_{ij}^{\sigma}$ is the neighborhood effect on the cell *ij* and σ expresses the relative importance of the neighborhood effect. Figure 2.1 demonstrates an example of how the final transition potential *P* matrix is calculated.

The model selects the top-scoring cells from the built-up transition potentials matrix for each density class and changes their state to the appropriate class until meeting the required quantity. The transition potential matrices are calibrated for 1990-2000. The calibration results are then used to simulate 2000-2010 urban pattern. The simulated map of 2010 is compared against the actual 2010 map to validate the model allocation ability (section 2.3.2).

0.31	0.97	0.88
0.42	0.92	0.76
0.02	0.94	0.52

$\odot$

14.1^2	2^2	6.2^2
16.2^2	2.8^2	7.1^2
7.8^2	4.2^2	8.6^2

$\rightarrow$

7.9	2	5.8
10.5	2.7	6.2
1.1	4.1	6.2

Figure 2.1: An example of urban transition potentials matrix (right) which equals the square root of pairwise multiplication of P_c (left) and P_n (middle) matrices. The σ of P_n is assumed to be 2.

Cell neighborhood calibration

Neighborhood interactions can also be calibrated in MNL model by including them as part of the explanatory variables (e.g. Hu and Lo, 2007; Verburg et al., 2004). However, because MNL models are not temporally explicit, they cannot reveal the path-dependent and self-organizing development which is typical for urban expansion (Poelmans and Van Rompaey, 2010; Wu, 2002). The most common approach to explicitly calibrate the neighborhood interactions on a dynamic basis is by using a cellular automata (CA) modelling approach.

In some studies (e.g. Chen et al., 2014; Poelmans and Van Rompaey, 2009; Wu, 2002) the neighborhood is defined as a square region, the Moore neighborhood, around the central cell with many square sizes from 3×3 to 11×11. Chen et al. (2014), and Poelmans and Van Rompaey (2009) analyzed several square sizes and concluded that the model run with the 3×3 neighborhood window produces a land-use pattern that most fits the actual pattern. These studies use a coarse cell resolutions. However, it might be different for finer cell resolutions. In this study, a 3×3 neighborhood window is used to consider neighborhood interactions. The $(P_n)_{ij}$ is calculated according to the method proposed by White and Engelen (2000):

$$\left(P_n\right)_{ij} = \sum_k \sum_x \sum_d w_{kxd} \cdot I_{kxd} \qquad (2.2)$$

where w_{kxd} is the weighting parameter assigned to a cell with class k, which represents one of the built-up classes listed in Table 2.2, at position x at distance zone d and I_{kxd} is 1 if a cell in distance d is occupied by class k or 0 otherwise.

Our objective is to define the CA parameters that achieve the best allocation accuracy rate for the expansion process (transitions from class-0 to class-1, class-2 and class-3 simultaneously) and for the densification process (transitions from class-1 to class-2 and transitions from class-2 to class-3). In order to automatically calibrate the neighborhood weighting parameters, a multi-objective genetic algorithm (MGA) is used for the expansion and a genetic algorithm (GA) is used for the densification process. The genetic algorithm is a highly effective algorithm for solving both constrained and unconstrained optimization problems that has been inspired by the mechanisms of evolution and genetics (Al-Ahmadi et al., 2009; Holland, 1975). MGA attempts to portray a trade-off among multiple, possibly conflicting objectives at once. In this research, MGA is a variant of a non-dominated sorting genetic algorithm II (NSGA-II) proposed by Deb (2001). NSGA-II favors individuals with an elitist strategy and individuals that can help increase the diversity of the population (Yijie and Gongzhang, 2008). The output of the MGA is a set of solutions that is also known as Pareto front optimized solutions, among which we can select the most preferable solution. Pareto front is a set of feasible solutions that are non-dominated to each other but are significantly better than the rest of solutions.

The MGA/GA initializes a random initial population in which many solutions participate in an iteration (generation). It then uses stochastic operators to generate new generations and direct a searching process based on a fitness function. Each individual in the population corresponds to a chromosome made up of a set of genes, where each gene represents one parameter that requires calibration. In each generation, every individual in the population is evaluated through a fitness function. Once the initial population is generated and evaluated, the parents for the next generation are selected by using a tournament procedure based on a relative fitness score. The

tournament randomly selects two individuals, and the individual with the highest fitness value becomes a parent. Each two parents are combined based on a crossover operator. We proposed that the crossover operator generates two children that lie on the line representing both parents and inherit at least 70% genes from the parent with the better fitness value. Once the new generation is obtained, each child is then perturbed in its vicinity by a mutation operator that adds a small random number to each gene.

This study tries to achieve a proper balance between exploration and exploitation ability of the MGA/GA. Exploration enables the MGA/GA to explore a broader search space, while exploitation enables MGA/GA to focus on one direction which is an optimal solution or close to it (Hansheng and Lishan, 1999). The mutation operator is used to provide exploration ability whereas the crossover operator is used to lead the population to the global optimal solution so far. In our case, the mutation operator selects a random number from a Gaussian distribution with a center of zero and a standard deviation of 2 at the first generation. This standard deviation is shrunk to 0 linearly as the last generation is reached. Consequently, the MGA/GA explores much more search space at the beginning of the optimization process and ensures the convergence of the population towards the global optimal solution by the end of the process.

MGA/GA is initialized with a random population. Stochastic operators are applied to this population and a large number of generations evolved to obtain a favorable solution. Each individual solution takes about 19 seconds in case of MGA and 8 seconds in case of GA to be evaluated using a good PC (Intel Core i7-4700 CPU @ 2.4GHz) implying that large population and generation numbers require considerable time to be processed. To minimize the computing time, we implement a two phase MGA/GA. First, the MGA/GA starts with a low number of population and generations. Second, the outcome of the first run is used to set the initial population, initial range and number of generations. In addition, the first run is used to determine values for the crossover and mutation operators. Based on this, a set of 500 generations (300 for expansion, 100 for densification of class-1 and 100 for densification of class-2) with 500 individuals for each generation are used for the final MGA/GA.

The objective function for the genetic algorithms for the calibration is based on a fuzzy membership function, as discussed further below. The parameter values that maximize the objective function will be selected as the best calibration outcome.

2.3.2. Validation

The ability of the model to locate transitions from non-urban to one of urban densities and lower densities to higher densities is validated by comparing the simulated map of 2010 with the actual map of 2010. The comparison considers only new urban transitions between 2000 and 2010. The fuzziness index of a cell location depends on the cell itself and the cells in its neighborhood.

There is no universally agreed extent to which the neighboring cells influence the fuzzy representation and a type of decay function among land-use modelers. Although it may be advantageous to experiment with different neighboring sizes and decay functions to define the best alternative, this experiment is beyond the scope of this research as it would require too much space to adequately discuss such analyses. However, a number of authors proposed an exponential decay function with a halving distance of two cells and a neighborhood with a four-cell radius to evaluate (e.g. Ahmed et al., 2013; Hagen, 2003; Loibl et al., 2007). Likewise, the average fuzziness similarity rate used in this research is an exponential decay with a halving distance of two cells and a neighborhood with a four-cell neighbor extent and calculated as follows:

$$FSR_k = \frac{\sum_{x_k \in X_{k,sim}} \left| I_{x_k 0} \cdot (1/2)^{0/2}, I_{x_k 1} \cdot (1/2)^{1/2}, ..., I_{x_k d} \cdot (1/2)^{d/2} \right|_{\max}}{X_{k,actul}} \qquad (2.3)$$

where FSR_k ($0 \le FSR_k \le 100$) is the fuzziness similarity rate for class k, $I_{i_k d}$ is 1 if cell i_k in the simulated map at zone d ($0 \le d \le 4$) has the similar land-use class to one cell at zone d in the observed map otherwise is 0, $X_{k,sim}$ equals the change amount of class k in the simulated map and $X_{k,obsr}$ equals the change amount of class k in the observed map. The FSR is also employed as the objective function for MGA/GA.

2.4. Results and discussion

In this section, the urban landscape resulted from classification of CAD data, the calibration results and the validation of the model are discussed. In general, the urban landscape visible in Wallonia resembles the classical urban pattern from across a wide range of regions worldwide (e.g. Kumar et al., 2012). A high level of built-up density was found in the major urban cores surrounded by medium-density areas. A large majority of low-density lands are likely to be found in scattered rural areas and remote locations. Figure 2.1 illustrates different densities for Charleroi and Namur metropolitan areas as an example.

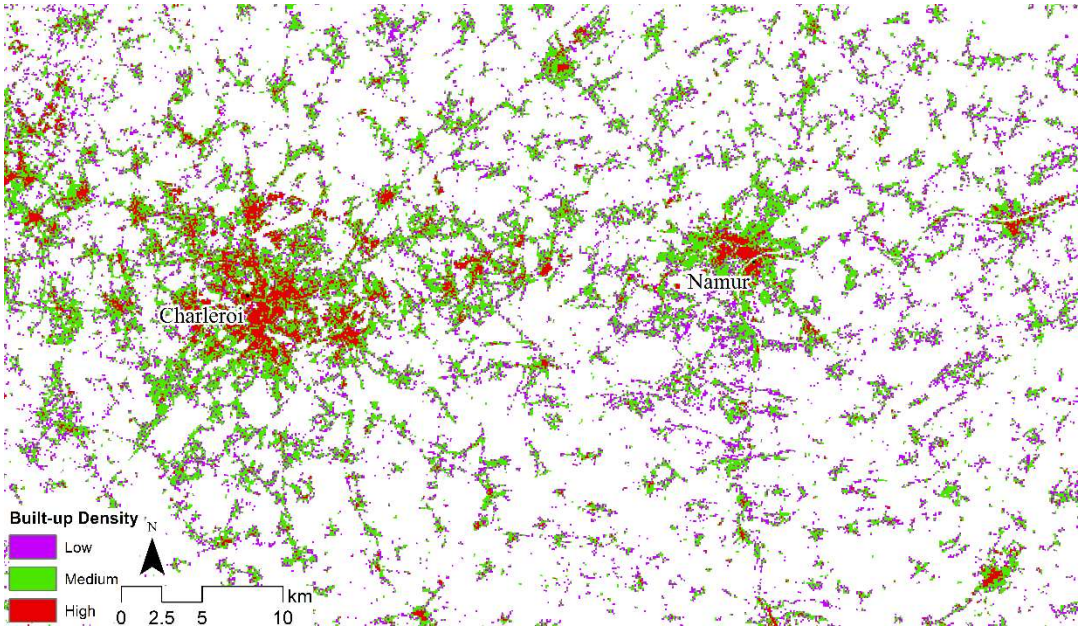

Figure 2.1: Urban classes of 2010 for Charleroi and Namur metropolitan areas.

Variance inflation factors test, with values of less than 1.33, shows no problems with multicollinearity suggesting that all causative factors can be incorporated in the MNL model. The MNL parameter sets calibrated in the 1990–2000 are shown in Figure 2.2.

The GA optimization module for the densification of class-1 and class-2 began to converge when reaching iteration 56 and 50 respectively (Figure 2.3). After 228 iterations, average change in the spread of Pareto solutions for MGA was less than 0.00001. The MGA/GA optimal weighting values that define neighborhood interactions are given in Figure 2.4 (a, b and c). The calibration shows that the likelihood of low-density expansion is highly increased by increasing the number of existing low-density and medium-density lands and decreasing the number of high-density lands in the immediate neighborhood of the cell. The probability of medium-density expansion is increased with increasing number of all land-uses, especially medium-density cells. This study finds a positive relationship between expansion of high-density and the number of existing high-density cells in the neighborhood of the cell. In contrast, the expansion of high-density lands is negatively impacted by increasing the number of non-built-up, low and medium-density lands.

The probability of low to medium-density urban transitions is positively linked with the existing non-urban, low and medium-density urban neighbors and negatively linked with high-density neighbors, whereas the densification of medium-density areas is negatively related to the increasing number of non-urban and low-density cells and positively related to the increasing the number of high-density cells in the neighborhood of the cell. Together, these findings suggest that existing residents of low and medium-density areas tend to protest dense developments near their homes, whereas most new densified areas are located within or close to already high-density neighbors. This causes a highly fragmented and low-density urban landscape. One of the main

factors leading to this situation is the spatial planning policy (Dieleman and Wegener, 2004; Poelmans and Van Rompaey, 2009).

The ROC values of the MNL outcomes are 0.81, 0.85, 0.94, 0.73 and 0.72 for class-0 to class-1, class-0 to class-2, class-0 to class-3, class-1 to class-2 and class-2 to class-3 respectively. ROC values higher than 0.70 are considered as a reasonable fit and the estimates can be used in further analyses (Cammerer et al., 2013; Jr and Lemeshow, 2004).

The calibration and validation of allocation accuracy rates are given in Figure 2.4 (d). The relative importance of the neighborhood effect (σ) parameter is calibrated using MGA. The MGA of σ converges when reaching iteration 35 for expansion process, 27 and 24 respectively for densification of class-1 and class-2. The value of parameter σ shows neutral effect, i.e. equals 1, on the expansion of class-2, class-3 and the densification of class-2. For the expansion and densification of low-density class the values of σ are 1.97 and 0.53 respectively.

The calibration accuracy rates are larger than the validation rate. The possible source of this variation is potentially due to the uncertainty associated with the future values of modeling parameters. Most CA models (e.g. Al-Ahmadi et al., 2009; García et al., 2013) introduced a stochastic disturbance term to represent unknown errors and uncertainty. The extension of this study necessitates a more comprehensive framework that explicitly models uncertainty related to future values of the model's parameters.

The fuzziness similarity rates for the major metropolitan area (Liege), as an example, are shown in Figure 2.5. This figure demonstrates a majority of allocated cells has a high FSR. Table 2.4 lists the number of allocated cells in each FSR class. According to Table 2.4, the model spatially allocates more than 75% and 70%, in 1990-2000 and 2000-2010 respectively, of new cells in the right location or in the immediate neighbor.

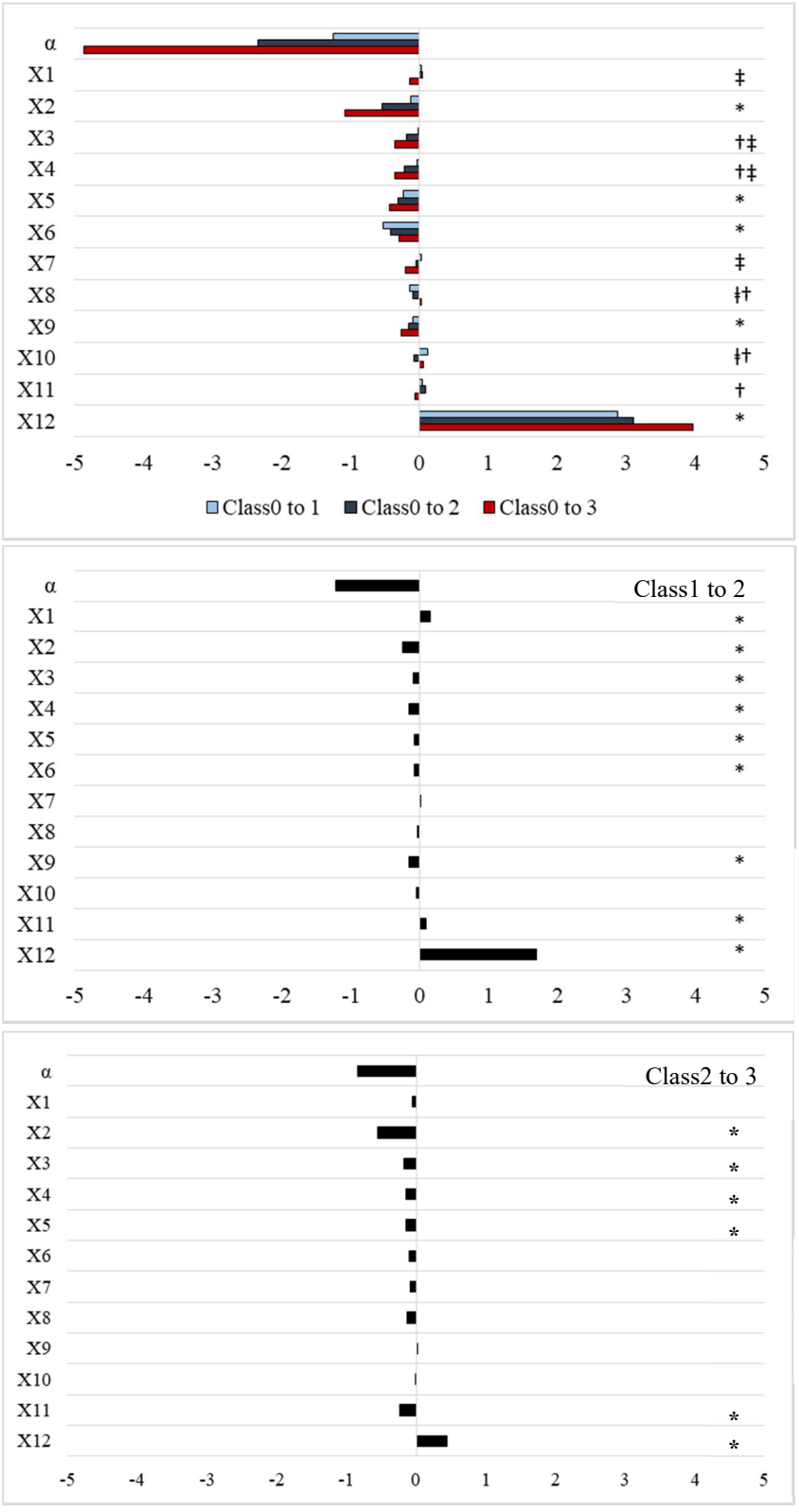

X1: Elevation
X2: Slope
X3: Dist. to Road1
X4: Dist. to Road2
X5: Dist. to Road3
X6: Dist. to Road4
X7: Dist. to railway stations
X8: Dist. to large-sized cities
X9: Dist. to med-sized cities
X10: Employment rate
X11: Richness index
X12: Zoning

Significance at p-value ≤ 0.05 for
* all transitions
ǂ class-0 to class-1 transitions
† class-0 to class-2 transitions
‡ class-0 to class-3 transitions

Figure 2.2: The MNL parameters coefficients for 1990-2000.

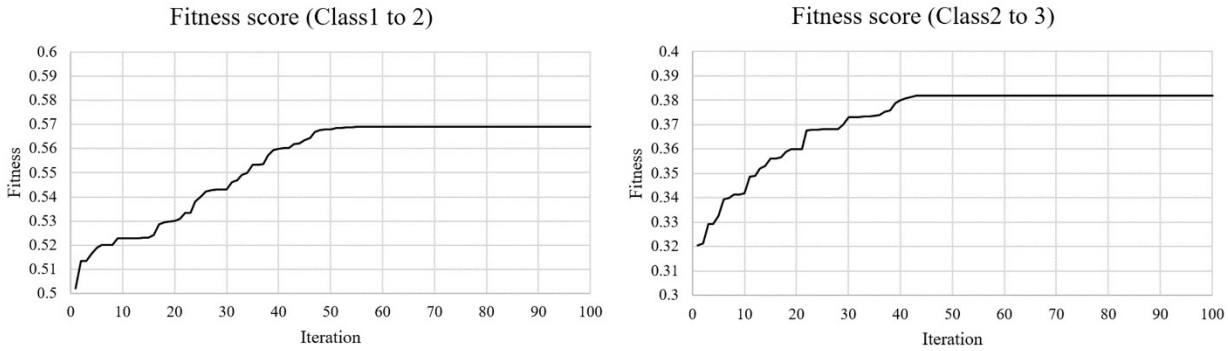

Figure 2.3: The convergence of the fitness score during the GA optimization.

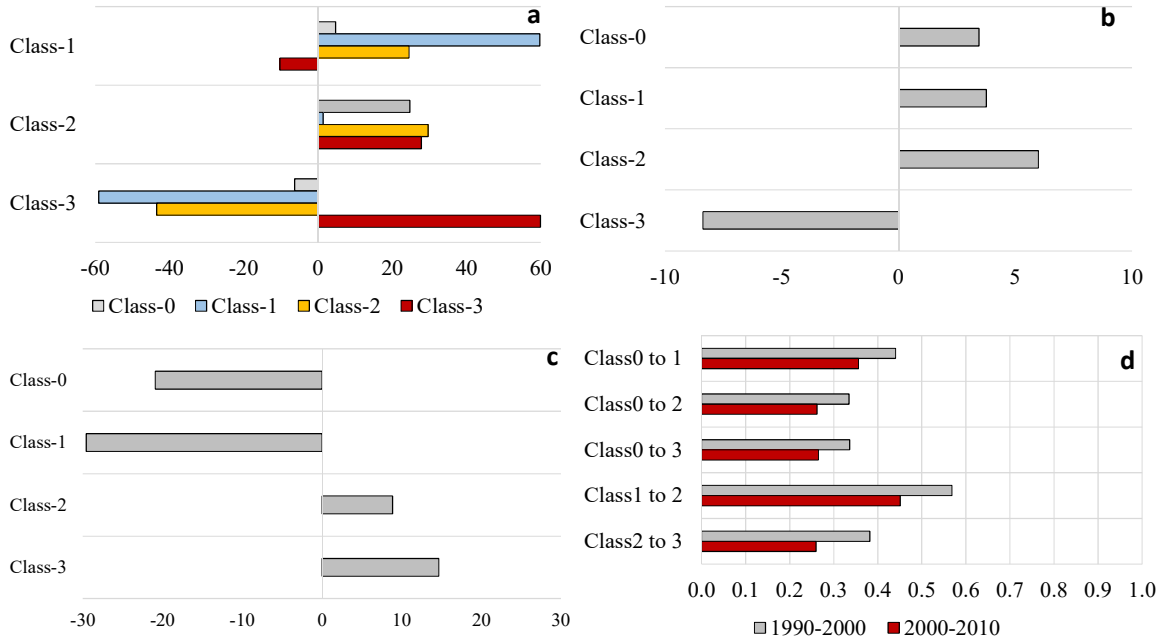

Figure 2.4: Weighting values that define neighborhood parameters values for (a) transitions from class-0 to class-1, class-2 and class-3, (b) transitions from class-1 to class-2 and (c) transitions from class-2 to class-3. (d) The average fuzzy similarity rates for calibration and validation.

Table 2.4. The number of allocated new cells with each fuzziness similarity rate (FSR) (% of total changes).

FSR	1990-2000	2000-2010
0	2683 (9.21)	3169 (15.58)
0.25	1038 (3.56)	807 (3.97)
0.35	1391 (4.77)	975 (4.79)
0.5	1952 (6.70)	1228 (6.04)
0.71	17076 (58.61)	11529 (56.66)
1	4995 (17.14)	2638 (12.97)

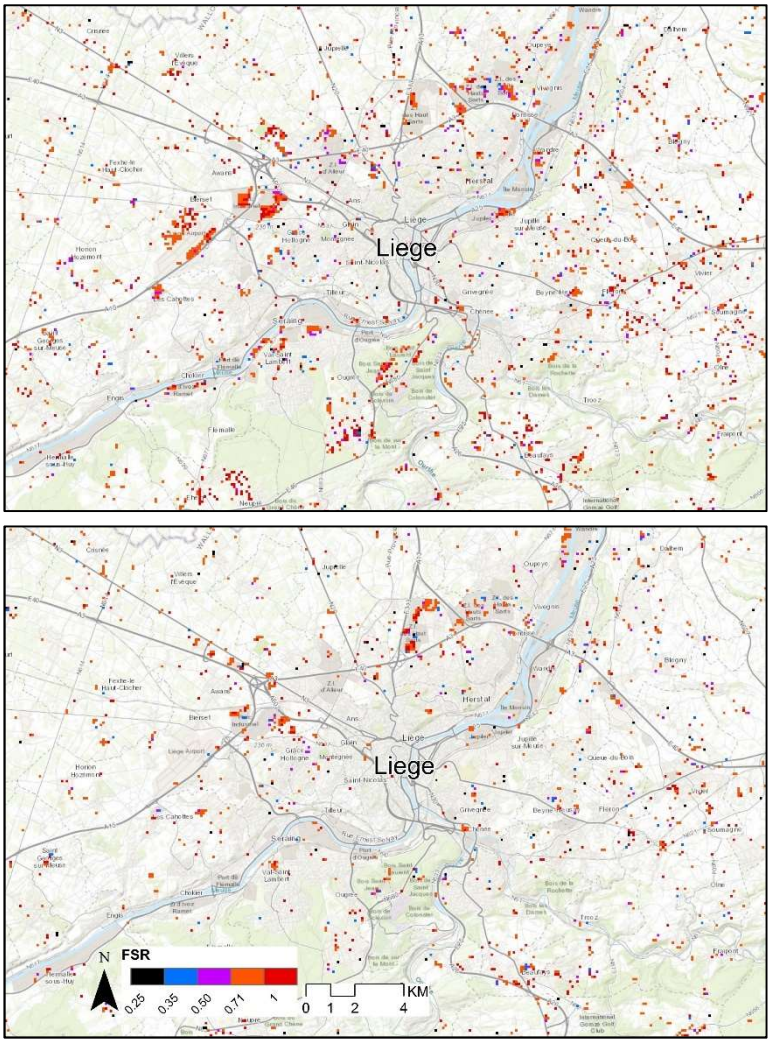

Figure 2.5: The fuzziness similarity rate (FSR) for Liege metropolitan.

2.5. Conclusions

One of the central limitations of most existing urban expansion models is that urbanization is considered as a binary process (urban vs non-urban). This research has demonstrated that the urban development process is heterogeneous, with links between density and the impact of different urban development drivers. We propose an integrated multinomial logistic regression (MNL) and cellular automata (CA) model to examine the urbanization trends in Wallonia. The urban development considers both expansion and densification. Considering the densification is an essential component of sprawl-fighting land-use policies. In this study, urban densities (non-urban, low-density, medium-density and high-density) for 1990, 2000 and 2010 and geophysical and socioeconomic data that are referred to as controlling factors were gathered and processed. The MNL allows to automate the calibration of the controlling factors whereas the CA model is used to simulate the neighborhood interactions. A multi-objective/genetic algorithm is employed to calibrate neighborhood interactions parameters. The calibration is done for urban transitions

between 1990 and 2000. The calibration results are then used to validate the model by simulating the 2010 urban pattern and compare it with the actual 2010. The model evaluates the MNL outcomes using relative operating characteristic and validates the simulated built-up patterns by means of fuzzy set theory. The model reveals a good overall accuracy. However, calibration and validation processes provide information on the uncertainties in the model outcomes over time. In later work we intend to pursue the analysis further by modelling uncertainty in the future urban simulations. Therefore, our model can effectively develop future urbanization scenarios considering the uncertainty.

The neighborhood effect weights imply that the densification occurs in already dense areas whereas low-density and medium-density areas tend to retain their densities over time. Public authorities clearly should play a role in the development of a more balanced densification policy, considering the densification of very accessible (transport, services, etc) low/medium density nodes besides a further densification of already dense areas. This is not contradictory with a concentration spatial policy provided that low/medium density nodes where densification occurs are well connected to city centers (as for instance promoted through transit-oriented development).

Our analysis does not consider building use or height. There are several missing of buildings uses and heights within the cadastral data. Consequently, population and employment density indices cannot be considered here. However, this study prompts a series of further research questions regarding the relation between built-up density and land-use policy, spatial, geophysical, and socioeconomic factors. Hopefully this study should provide a useful context for policy makers and the ongoing research.

2.6. Key contributions

- A multi-objective Genetic Algorithm considering multiple density classes has been successfully integrated a CA model to calibrate it.
- Our CA model allows to predict future land-use considering different urban densities according to neighborhood and global factors.
- It further confirms earlier observations, as densification and sprawl are inherently related to previous levels of density at the neighborhood scale.
- An average fuzziness similarity rate has been implemented and tested for the validation of multi-density models.

Chapter 3: An Integrated Cellular Automata and Agent-Based Model to Simulate Future Urbanization

3.1. Introduction[1]

Urban environment is a complex system, which includes a large number of contradictory parameters and several actors (e.g. households, developers, government, etc.). The complexity of such a system is well explored in Batty (2008, 2007). Urban expansion model is a tool to gain insight into the mechanisms of the urban environment. These models can project the expected future demands of urban lands and/or a spatial distribution of these demands. Urban expansion models have wide range applications, which expands from global warming (e.g. Haggert, 1995) to response to flood risks (e.g. Beckers et al., 2013; Mustafa et al., 2016; Poelmans et al., 2010).

Several statistical and geospatial approaches have been proposed and developed to model urban expansion, including logistic regression models (logit) (e.g. Hu and Lo, 2007; Vermeiren et al., 2012), cellular automata (CA) (e.g. Al-Ahmadi et al., 2009; Mitsova et al., 2011) and agent-based models (AB) (e.g. Hosseinali et al., 2013; Zhang et al., 2010). Often, the urbanization likelihood of a non-urban land is determined by static drivers related to accessibility, geophysical features, policies and socio-economic factors. Another important driver is neighborhood interactions because of the fact that urbanization can be regarded as a self-organizing system (Poelmans and Van Rompaey, 2010). The relative importance of different drivers as determinants of the urbanization likelihood can be based on different approaches such as logit and CA.

Logit models are a common approach to model urban expansion. They predict the outcome of a categorical variables using a set of quantitative and/or qualitative predictors. Logit can include geophysical as well as socio-economic factors. The model's ability to include as many factors as necessary allows us to better understand the main drivers behind urbanization processes.

[1]This chapter is based on:
Mustafa, A., Cools, M., Saadi, I., & Teller, J. (2017). Coupling agent-based, cellular automata and logistic regression into a hybrid urban expansion model (HUEM). *Land Use Policy*, 69C, 529–540.
Mustafa, A., Bruwier, M., Archambeau, P., Erpicum, S., Pirotton, M., Dewals, B., & Teller, J. (under review) Effects of spatial planning on future flood risks in urban environments. *Journal of Environmental Management*.

Neighborhood interactions can also be captured in Logit models by including them as part of the explanatory variables as in Hu and Lo (2007) and Verburg et al. (2004). However, because logit models are not temporally explicit, they cannot reveal the path-dependent and self-organizing development which is typical for urban expansion (Poelmans and Van Rompaey, 2010; Wu, 2002). The most well-known approach to calculating the neighborhood interactions on a dynamic basis is cellular automata (CA) based model, in which the neighborhood state is updated during each simulation step. Cellular models are simple and widely available (Clarke and Gaydos, 1998). However, pure CA models focus on the calculation of urbanization transitions by explicitly consider the immediate neighbors of each landscape unit, i.e. cell, rather than on the interpretation of drivers of urban expansion. Several studies try to overcome this limitation of pure CA models by integrating CA with other modeling methods to consider several urbanization drivers. In this context, logit and CA are commonly combined to create a so-called 'CA-logit model', which considers both the urbanization static drivers and the dynamic neighborhood interactions (Poelmans and Van Rompaey, 2010).

One of the clear drawbacks of CA-logit approach is related to the lack of theoretical links between the spatial transitions rules and agents within the urban environment and their decisions. Agent-Based (AB) models offer a way of incorporating the influence of human decision-making on land use change by simulating agents as goal-oriented entities capable of responding to their environment and interacting with each other. Agents in the model can play a role of individuals or groups of people, institutions, etc. They can exhibit different characteristics: they can be heterogeneous (e.g. economic state, age, family structure), autonomous (they take their own decisions based on prescribed rules and/or analytical functions) and dynamic (they can learn and adapt to different conditions) (Valbuena et al., 2008). The agents are commonly grouped into homogeneous sets of individuals with comparable characteristics and behaviors. Generally, the decision-making criteria of agents require a large amount of data stemming from surveys that depict people's choices and utilize experts' knowledge. In a large study area, such an intensive data gathering is limited by the presence of a large number of agents (Valbuena et al., 2008). In order to overcome data limitations, a number of studies used empirical data, such as distance to road network, slope etc., to represent agents decision-making for which we have no behavioral information (Mustafa et al., 2017a; Robinson et al., 2012).

In this chapter, we propose an integrated cellular automata and agent-based model (CA-AB), inspired by the work of Mustafa et al. (2017a), to allocate the necessary new urban development. It considers two development processes: expansion and densification. In addition, this chapter compares the performance of MNL-CA model (chapter 2) with the proposed CA-AB model.

3.2. Methods

The model is applied to Wallonia (Belgium). The urban land use maps of 1990, 2000, and 2010 and all explanatory factors described in chapter 2 are introduced in CA-AB.

The model is a 100×100 m² grid-based whereby urbanization are simulated through the interaction between several agents (Figure 3.1).

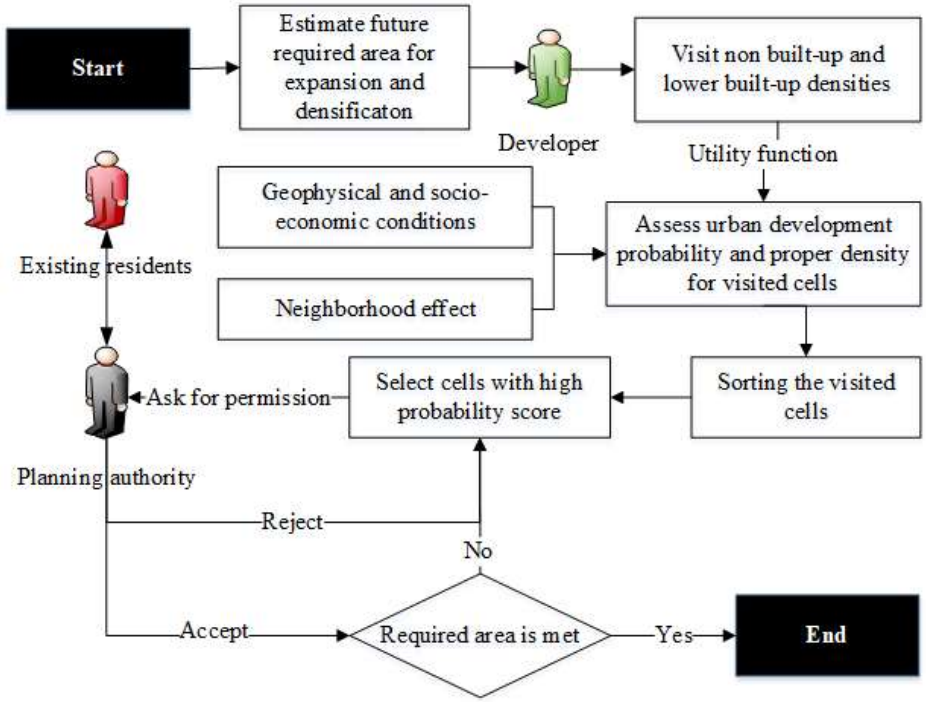

Figure 3.1: The overall framework of CA-AB model.

The agents are categorized into three groups with different characteristics and goals: developer (DevAG), existing resident (ExtAG) and planning permission authority (PPA). At each time step, corresponding to one year, a number of DevAGs select locations to develop. The selection of target location is a spatial knowledge-based decision that is provided by regional and local attractiveness. Regional attractiveness factors are listed in Table 3.1. They are in line with the controlling factors presented in chapter 2.

The relationship between existing residents and developer agents is often conflicting. On the one hand, each developer agent tends to build within the existing urban area (densification) or close to it in order to benefit from existing services and low risk of his/her investment. On the other hand, existing residents usually want to live in low density areas and do not prefer their neighborhood to be developed (Rand et al., 2005). In this study, a 3×3 neighborhood window is used to represent the DevAGs preferences regarding local attractiveness.

Table 3.1. List of regional attractiveness factors.

Factor	Name
X1	Elevation (DEM)
X2	Slope
X3	Dist. to Road1
X4	Dist. to Road2
X5	Dist. to Road3
X6	Dist. to Road4
X7	Dist. to railway stations
X8	Dist. to large-sized cities
X9	Dist. to med-sized cities
X10	Employment rate
X11	Richness index

Each DevAG determines transition potential from one class to another for a location according to the following equation:

$$UF_{DevAG} = \left(P_c\right)_{ij} \times \left(P_n\right)_{ij}^{\sigma} \tag{3.1}$$

where UF_{DevAG} is the utility function for Dev_{AG}, P_c is the regional attractiveness, P_n represents the developer agents local attractiveness, and σ is a variable indicates the relative importance of the neighborhood preferences. The P_c is determined according to the following equation:

$$\begin{aligned}(P_c)_{ij} = a_{AG} \times X1 + b_{AG} \times X2 + c_{AG} \times X3 + d_{AG} \times X4 + e_{AG} \times X5 + f_{AG} \times X6 + g_{AG} \times X7 \\ + h_{AG} \times X8 + i_{AG} \times X9 + j_{AG} \times X10 + k_{AG} \times X11\end{aligned} \tag{3.2}$$

where a_{AG} to k_{AG} are specific weights assigned to utility function variables listed in Table 3.1. The P_n is dynamically computed at each time-step using an embedded CA model according to the method proposed by White and Engelen (2000):

$$\left(P_n\right)_{ij} = \sum_k \sum_x \sum_d w_{kxd} \cdot I_{kxd} \tag{3.3}$$

where w_{kxd} is the weighting parameter assigned to a cell with class k, which represents one of the urban classes listed in Table 2.2, at position x at distance zone d and I_{kxd} is 1 if a cell in distance d is occupied by class k or 0 otherwise.

After the respective developer has selected a cell to develop or densify and at which density, it has to ask for a development permission from the planning permission authority (PPA). The PPA determines to grant the development permission according to two factors: (i) land-use zoning regulations, and (ii) the resistance of existing residents against proposed new development. Frist, the PPA sets three zones categories: (1) permitted (urban zones), (2) severely restricted (arable lands, grasslands, forests, and other classes) and (3) forbidden (water bodies) according to the authorized zoning plan. If a cell is located in a permitted or in a forbidden zone, PPA will

instantaneously grant or reject the permission respectively. Otherwise, if the cell is located in a severely restricted zone, PPA will give permissions for a specific percentage of the change amount (allowed rate) each time-step as follows:

$$PPAZ = \begin{cases} grant, & Dt \leq ARt \\ reject, & otherwise \end{cases} \quad (3.4)$$

where *PPAZ* is the PPA decision on a development proposal for a cell within severely restricted zones, *Dt* is the number of developed cells within severely restricted zones in previous time-steps and *ARt* is the allowed rate. Second, PPA considers the local residents protest as follow:

$$PPADec = \begin{cases} grant, & AvDt_k \leq AcD_k \\ reject, & otherwise \end{cases} \quad (3.5)$$

where *PPADec* is the *PPA* final decision, $AvDt_k$ average density at time-step *t* for a 3×3 neighborhood window in which a density class *k* occupies ≥ 50 % of the total cells within the neighborhood window, and AcD_k is the accepted average density value for a neighborhood with a density *k*.

The model is calibrated with urban development that was observed between 1990 and 2000. The calibration results are then used to validate the model with the development between 2000 and 2010. A genetic algorithm (GA) is employed to calibrate the model parameters (Equations 3.1 to 3.5). GA is one of the recent automatic calibration methods used to calibrate urban expansion models (e.g. Al-Ahmadi et al., 2009; García et al., 2013; Mustafa et al., 2017). In order to set GA parameters such as the number of individual in each generation, the number of generations, the selection of the parents for each generation, the crossover, and the mutation operators we performed a number of empirical experiments on different values of the parameters and selecting the best ones.

The GA objective function is the maximization of allocation accuracy rates for all density classes. The accuracy rate function is defined as a fuzzy membership function of exponential decay with a halving distance of two cells and a neighborhood window of 4×4 cells, Equation (2.3).

3.3. Results and discussion

Figure 3.2 illustrates the spatial distribution of new development across Wallonia. The region borders with other countries show a remarkable effect of urbanization in Wallonia especially the metropolitan of Lille (France). The development of new low-density overwhelmed Namur municipality and the south of Wallonia through the last couple of decades. The 2000-2010 period, however, shows lower development of low-density lands in the north of the region. Interestingly, the densification of low-density area follows upward trend over the past two decades. The

construction of new high-density areas is largely situated in the east of Wallonia. Whereas the transitions from medium-density to high-density areas clearly affect the major urban cores.

Table 3.2 lists the calibration result for the model parameters. In this table, X1 to X11 are the calibrated weights for parameters involved in Equation 3.2. X12 to X15 represent the effect of urban density class-0, class-1, class-2, and class-3 within the neighborhood, Equation 3.3. X16 is the weight assigned to variable σ in Equation 3.1. X17 is the allowed rate *ARt* in Equation 3.4. X18 to X20 show the *AcD* in Equation 3.5, the accepted average density value for a neighborhood with a dominant density of class-1, class-2, and class-3 respectively.

Referring back to the results of the MNL-CA model, chapter 2, the calibration results reveal some differences. Generally, the effect of accessibility factors has increased whereas the geophysical factors have gone in the opposite direction. The results highlight the role of planning authorities in enforcing zoning planning. The calibration of the allowed rate *Art* shows that some transitions from non-urban to low-density (163 ha/year) does not follow the zoning plan. This is also the case for the transitions from low-density to medium-density (61 ha/year). Almost all high-dense developments are located within urbanizable zones (only 4 ha/year from non-urban, and 7 ha/year from medium-density are located outside urbanizable zones). For the rest, the conclusions are in line with the findings of chapter 2.

Performance comparison of MNL-CA and CA-AB models, by means of the average fuzzy similarity rates, is given in Table 3.3. The results imply that CA-AB always outperforms MNL-CA. Although the performance of CA-AB model is slightly better than MNL-CA in terms of calibration (1990-2000), the performance assessment in the validation phase (2000-2010) is much higher. This is an important result as it implies that CA-AB is more stable than MNL-CA model and therefore CA-AB is more robust in terms of future forecasting. Both models extrapolate the calibration results (1990-2000) to simulate future land-use (2000-2010). This offers one explanation of why the improved performance of the validation period over the calibration one. MNL-CA follows only a few rules to change the state of the cells depending on some socioeconomic, geophysical, accessibility, policy factors, and neighborhood states. On the other hand, CA-AB relates the allocation process to the decisions of several actors: developers, residents, and authorities. The latter is seen as an opportunity in MNL-CA by involving zoning plan as a factor in MNL, while it is a barrier in CA-AB.

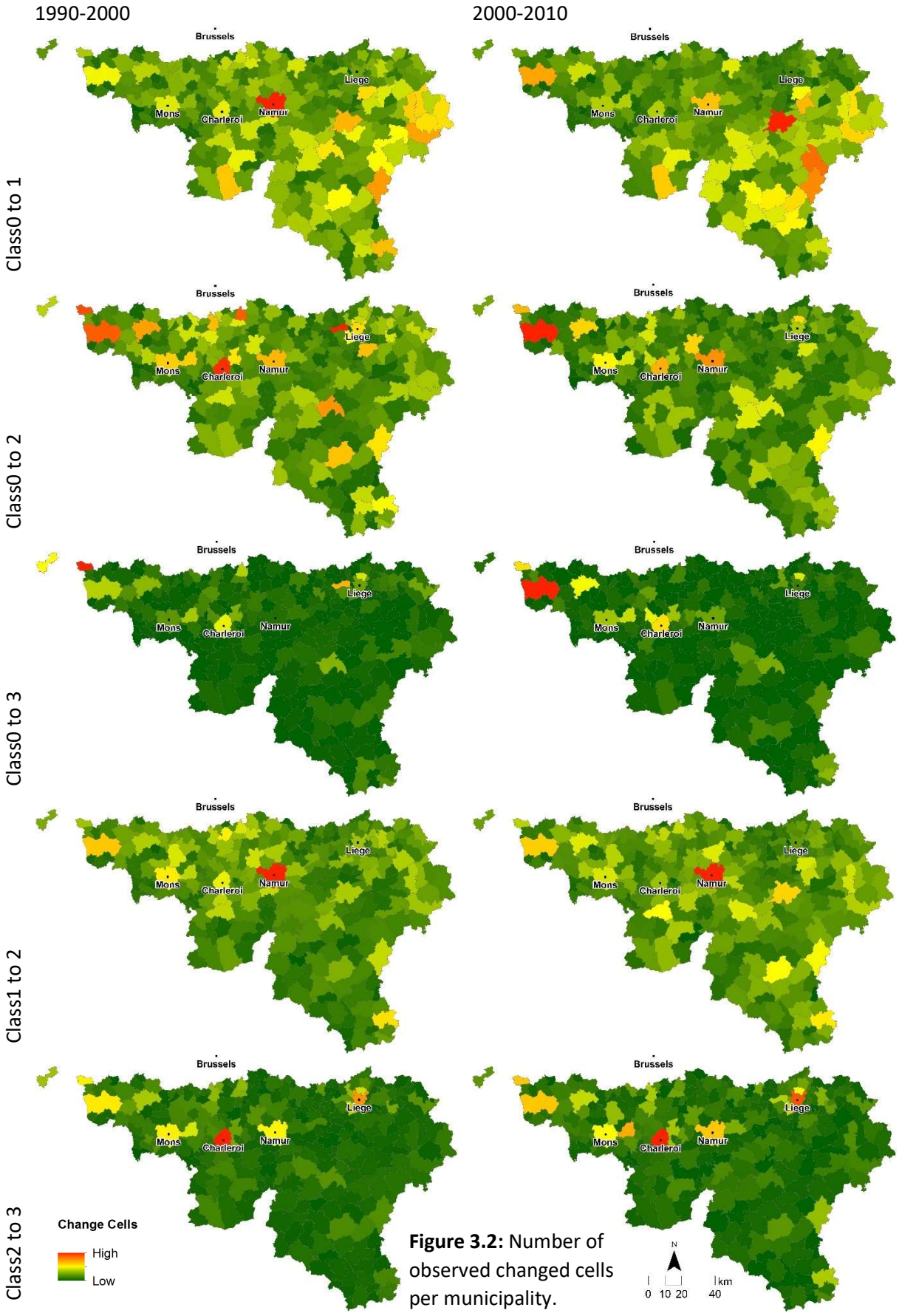

Figure 3.2: Number of observed changed cells per municipality.

Table 3.2. Calibrated weights for the model's parameters**.**

Parameter	Class 0 to 1	Class 0 to 2	Class 0 to 3	Class 1 to 2	Class 2 to 3
Elevation	0.002	0.079	0.005	1.094	0.044
Slope	-0.168	-0.577	-0.111	-0.413	-0.688
Dist. to Road1	-0.124	-0.886	-0.429	-0.109	-0.307
Dist. to Road2	-0.017	-0.254	-0.017	-0.578	-0.711
Dist. to Road3	-0.237	-0.077	-0.003	-0.142	-0.689
Dist. to Road4	-0.987	-0.004	-0.037	-0.06	-0.219
Dist. to railway stations	0.071	-0.049	-0.058	-0.372	-0.019
Dist. to large-sized cities	0.105	-0.083	-0.131	-0.427	-0.397
Dist. to med-sized cities	0.094	-0.068	-0.001	-0.299	-0.352
Employment rate	0.759	0.137	-0.005	0.436	0.118
Richness index	0.046	-0.015	-0.058	0.716	0.033
Class 0 neighbors	0.009	0.542	0.039	-0.198	-0.443
Class 1 neighbors	1.192	-0.062	-0.044	1.313	0.128
Class 2 neighbors	0.912	0.797	-0.039	1.718	0.881
Class 3 neighbors	-0.805	0.773	0.152	-0.383	1.531
σ (Eq. 3.1)	1.019	1.343	0.772	1.506	1.497
ARt (Eq. 3.4)	0.152	0.069	0.035	0.057	0.036
AcD_1 (Eq. 3.5)	1.45	1.10	1.45	1.42	1.25
AcD_2	1.95	1.95	1.56	1.95	1.42
AcD_3	2.00	2.20	2.90	2.45	2.63

Table 3.3. Average fuzziness similarity rate (FSR) for newly urban cells**.**

	CA-AB model		MLN-CA model	
	1990-2000	2000-2010	1990-2000	2000-2010
Class 0 to 1	0.45	0.39	0.44	0.36
Class 0 to 2	0.38	0.34	0.33	0.26
Class 0 to 3	0.36	0.33	0.34	0.27
Class 1 to 2	0.58	0.48	0.57	0.45
Class 2 to 3	0.40	0.32	0.38	0.26

3.4. Conclusions

This chapter has introduced a coupled cellular automata agent-based model (CA-AB) for simulating urbanization processes. Three groups of agents have been defined in the model: developers, existing residents, and planning authority. The model has been calibrated using empirical data related to geophysical, accessibility, and socioeconomic factors. Furthermore, a CA module has been embedded into the model structure for calculating the preferences of developers in terms of their local neighbors. By means of fuzziness accuracy, we have compared the performance of the proposed model and MNL-CA model presented in chapter 2. The results confirm that the CA-AB model outperforms the logit-CA model. Most importantly, the CA-AB model is more stable than the logit-CA model over time.

It is important to keep in mind that the abstraction for the current version of CA-AB is simple, with only three agent classes, and thus some key variables may be missed. In addition, the model is calibrated using empirical data that essentially provide an abstract representation of the agent's reasoning without any insight into the agent's behavior changes. Further research should consider

including more agent groups and developing more adaptive and learning-oriented agents. In spite of these limitations, the major contribution of CA-AB is to provide more flexibility in simulating policymaker decisions on the allowed rate of new development outside urbanizable zones and dealing with the protest of existing residents against new developments which is not the case in the typical logit-CA model.

3.5. Key contributions

- A coupled CA-AB model outperforms MNL-CA model.
- It has been demonstrated that CA-AB is more robust than logit-CA in urbanization forecasting.
- CA-AB allows to simulate and evaluate a broader choice of policy options. It may be used to include uncertainty factors in the model, through the behavior rules attributed to agents.

Chapter 4: Addressing Uncertainty in Land-use Change Dynamic

4.1. Introduction[1]

One of the primary goals of land use change models is to forecast possible future land states. Although uncertainty is an inherent feature of any forecast, few land-use change models considered uncertainty as a component of the model structure. According to a comprehensive review of 114 land use change applications, van Vliet et al. (2016) found that only 17% of the reviewed applications addressed uncertainty. Uncertainties may arise from many sources. One source relates to the errors in the model's input data which were investigated in a number of studies (e.g. Tayyebi et al., 2014). The estimation of the future change amount (quantity uncertainty), which is usually determined exogenously (Santé et al., 2010), is another source of uncertainty. This type of uncertainty was captured in various land-use models by simulating different scenarios differ in the quantity of change (e.g. Cammerer et al., 2013; Landuyt et al., 2016). Another common source of uncertainty is the potential nonstationary character of the spatial allocation of land use changes. Generally, land-use models extrapolate allocation calibration results to simulate future landscape. Thus, these models implicitly assume that the calibrated parameter set is valid for the future and do not consider the nonstationary feature of the land-use allocation that is related to the political, economic, and/or environmental conditions which are known to be nonstationary (van Vliet et al., 2016). Figure 4.1 depicts the difference between quantity uncertainty and allocation uncertainty. Our main focus in the present study is related with land-use allocation uncertainty. The uncertainty in the allocation process was addressed in many studies by means of fuzziness (e.g. Wang et al., 2013) or randomness (e.g. Yang et al., 2008). The randomness, however, ensures that each run can produce a different landscape and that some patterns can be proper by chance (Brown et al., 2005; van Vliet et al., 2016). Many of the current techniques for embedding allocation uncertainty in land-use change models are inspired by introducing a stochastic disturbance (SD) term or a Monte-Carlo Simulation (MC) method into the model. Feng (2017), Mustafa et al. (2014), and Yang et al. (2008) introduced an

[1]This chapter is based on: Mustafa, A., Saadi, I., Cools, M., & Teller, J. (under review). A Time Monte-Carlo method for addressing uncertainty in land-use change dynamic. *International Journal of Geographical Information Science*.

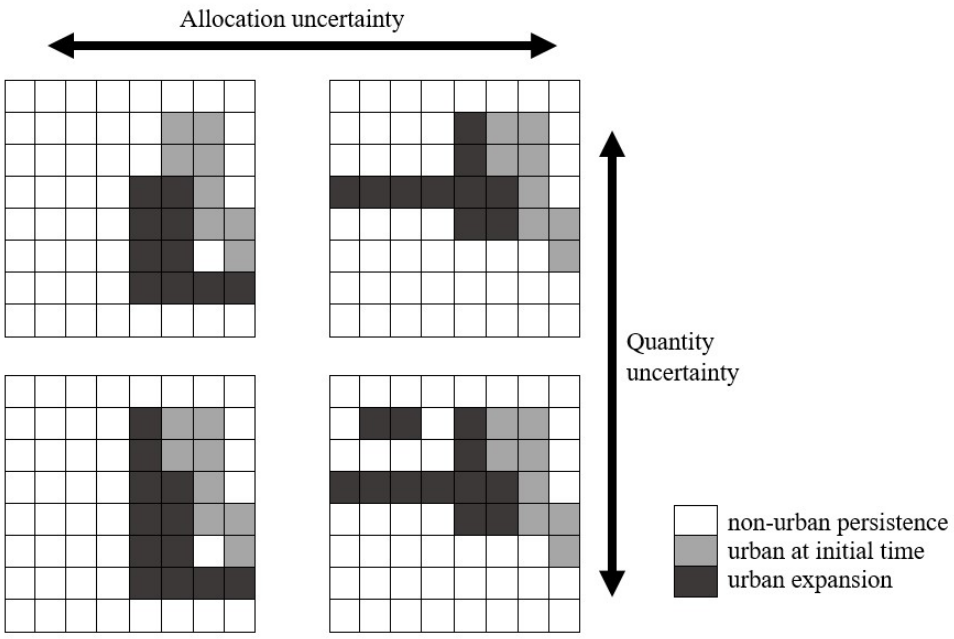

Figure 4.1. Quantity and allocation uncertainties in land-use change models.

SD term, proposed by White and Engelen (1993), whereas Li and Liu (2006), Liu et al. (2008a), and Wu (2002) used an MC method in their models to consider uncertainty.

The main contribution of this research is that it introduces an approach to tune uncertainty degree over time so that it differentiates the uncertainty degree between the immediate future and the distant future. Our approach compares the transition probability from one land-use to another of each land unit to a random number as in Wu (2002). Yet, a major differentiation of our work lies in generating a uniform random number that is drawn over a dynamic range associated with transition probabilities from one state to another and this range is increased over time.

We incorporate our method in a cellular automata (CA) model to simulate urban expansion in Wallonia (Belgium) from 1990 to 2010. After calibrating and validating the model, a comparison of the results obtained by our method and by the two most widely used methods, SD and MC, is performed. The comparison demonstrates the robustness of our method against SD and MC methods.

This research is structured as follows. In section 4.2, we review SD and MC methods and then describe our method. Section 4.3 presents the land-use change model, study area, and data. In section 4.4, we show and discuss our results. Finally, section 5 presents our conclusions.

4.2. Modeling land use allocation uncertainty

In this section, we review the SD method proposed by White and Engelen (1993) and the MC method proposed by Wu (2002) for incorporating uncertainty into land-use change models. Thereafter, we introduce our method, which we refer to as time Monte-Carlo (TMC) method.

Once the transition probability is computed for each unit in the landscape, the SD term perturbs each probability score in its vicinity by a random number that can be calculated as follows (White and Engelen, 1993):

$$SD = 1 + (-\ln \gamma)^{\sigma} \tag{4.1}$$

where γ is a uniform random number between 0 and 1, and σ is a parameter that allows to controlling the magnitude of the SD. When σ is set at 0, the model will behave deterministically. In contrast, when σ is set at high positive values, the model will become a random process. Introducing an SD term in the transition probabilities may cause a bias in the model outcomes, because those cells with very low transition probabilities can also change their state (García et al., 2011; Wu, 2002). Wu (2002) proposed an alternative method which employs a Monte-Carlo Simulation procedure for modeling allocation uncertainty. In this approach, after computing the transition probabilities, a cell in the landscape is randomly selected and its probability is compared with a random number uniformly distributed between 0 and 1, such that the state of a cell is changed if its probability score is greater than the random number. One of the shortcoming of this approach is that it does not allow controlling of the degree of randomness. Therefore, Wu (2002) transformed the transition probability of each cell by comparing it with the best available probability at each time-step, as follows:

$$Pi'^{t} = Pi^{t} \exp[-\delta(1 - Pi^{t}/\max(P^{t})] \tag{4.2}$$

where Pi'^{t} is the updated transition probability for cell i at time-step t, Pi^{t} is the original probability, δ is a dispersion term, and max(P^{t}) finds the maximum transition probability at time-step t. The dispersion term, δ, in Equation (4.2) plays a role equivalent to σ in Equation (4.1). When δ is set at high values, this will decrease transition probabilities, in particular for cells with a lower probability score, away from the maximum probability at each time-step. Thus, a strong differentiation between cells with higher probabilities and for those with lower probabilities is gained, and there will be less chance for land-use change of the latter.

Although the two methods explained above are widely used to model allocation uncertainty in land-use change models, none of the methods ensure that the degree of uncertainty is changeable over time, which is the case in reality as the distant future involves more uncertainty about the economic value of the land, about actual communication means, about social/household

preferences etc. All these elements play a key role in land allocation and become less predictable in a distant future. The contribution of this research lies in being one of the first attempts to control uncertainty degree over time in land-use change models.

The proposed TMC method uses an MC procedure as in Wu (2002). At each time-step, a cell is selected at random and its computed transition probability is compared to a uniform random number within a dynamic range. The key difference between the proposed method and the method of Wu (2002) is that Wu defines this range between the minimum and maximum probabilities, i.e. 0 and 1. We propose that this range varies so as to tune the degree of uncertainty over time. At each time-step, the computed transition probabilities are sorted in descending order, with the most suitable cell at the top of the list. Typically, the top-scoring cells from the sorted list change their state until meet the requested change quantity. In order to consider uncertainty, the model randomly selects one cell in a set of cells with best probabilities, the size of which is initially determined by the quantity of change and subsequently increased to include more cells. Thereafter, the model compares the transition probability of the selected cell with a uniform random number and the cell change its state according to the following equation:

$$Si^{t+1} = \begin{cases} change, & Pi^t > rand \\ non-change, & otherwise \end{cases} \quad (4.3)$$

where Si^{t+1} is the state of the cell *i* at the next time-step, Pi^t is the computed transition probability at the time-step *t*, and *rand* is a uniform random number within a range (*randmin* ≤ *rand* ≤ *randmax*). We set *rand_max* and *rand_min* as follows:

$$\begin{aligned} rand_{max} &= \max(P^t), \\ rand_{min} &= trans(q + (t \times \phi \times q)) \end{aligned} \quad (4.4)$$

where $max(P^t)$ returns the maximum probability at time-step *t*; and $trans(q+(t\times\phi\times q))$ returns the transition probability of a cell during time-step *t* from the sorted list which it is location determined by *q*, the change quantity pre time-step, and ϕ is a specific percentage of *q*. Figure 4.2 illustrates an example of the method. By doing so, the model behaves deterministically at the beginning and slowly turns to behave more and more stochastically as the model operates over time.

4.3. Land-use change model

In this study, we apply a grid-based cellular automaton (CA) land-use change model to simulate urban expansion in Wallonia (Belgium) between 1990 and 2010. Urban land-use maps of 1990 and 2000 are used to calibrate the model parameters. The calibrated parameters are then used to simulate 2010 urban pattern. We validate our model by comparing the simulated 2010 pattern with the observed pattern of 2010. The model has two main modules: the demand module and

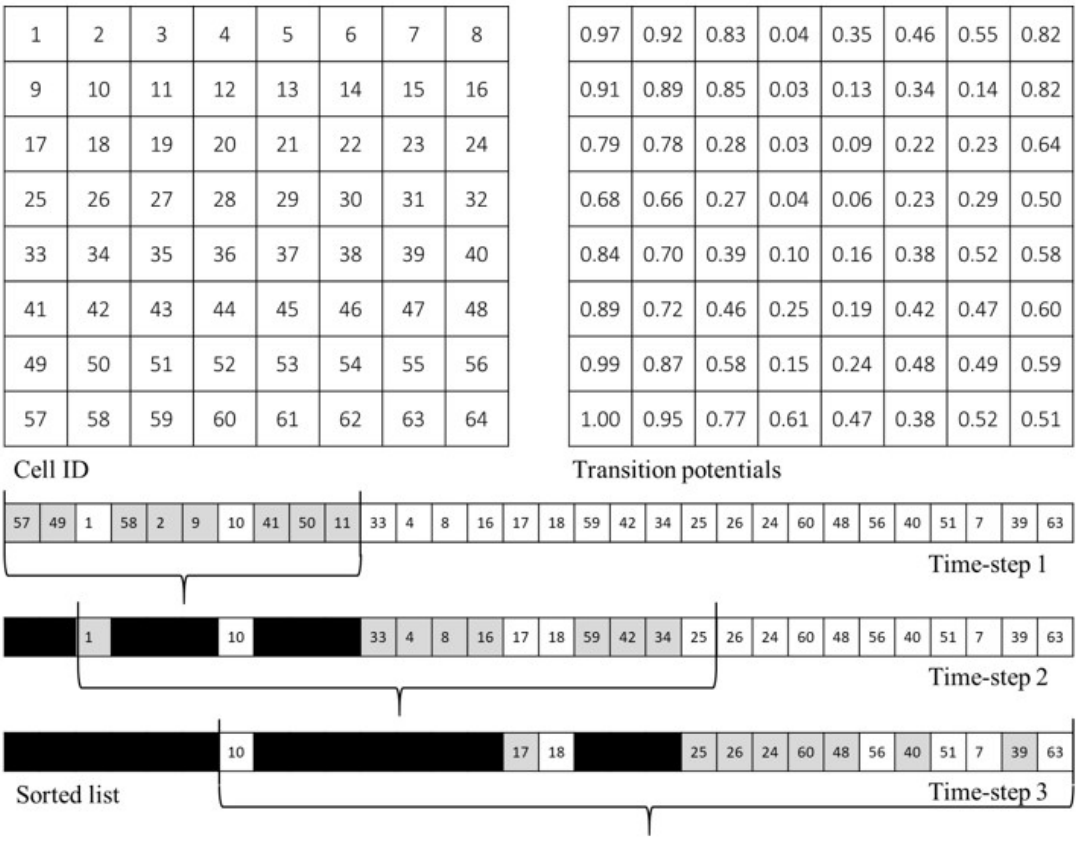

Figure 4.2. Example of the TMC method. Assuming that q=8 and ϕ=25%, the model randomly selects 8 cells out of 10, 8 cells out of 12, and 8 cells out of 14 in the time-steps 1, 2, and 3 respectively according to Eq. 3. White: no-change, gray: changes done in the current time-step, and black: changes done in the previous time-septs.

the allocation module. Our emphasis is not on the quantity uncertainty, but rather on the allocation uncertainty and therefore the demand module was fed with the actual quantity of new urban divided by 10 (the number of time-steps).

The allocation module allocates new urban cells based on transition probabilities. Two major components shaped the probabilities as in Wu (2002), Poelmans and Van Rompaey (2010), and Mustafa et al. (2018). The first is based on a set of urbanization diving forces. The second component concerns the dynamic interaction between neighborhood land-uses. The transition probability *P* for cell *i* at time-step *t* is computed as follows:

$$Pi^{t} = \left(Pi_{d}\right) \times \left(Pi_{n}\right)^{t} \times con(.) \tag{4.5}$$

where (Pi_d) is the urbanization probability based on of urbanization driving forces, $(Pi_n)^t$ is the neighborhood interaction, and *con(.)* is restrictive conditions for land-use change. The (Pi_d) is calculated as:

$$(Pi_d) = \frac{\exp(\alpha + \beta_1\chi_1 + \beta_2\chi_2 + \cdots + \beta_n\chi_n)}{1 + \exp(\alpha + \beta_1\chi_1 + \beta_2\chi_2 + \cdots + \beta_n\chi_n)} \quad (4.6)$$

where α is the intercept, ($X_1, X_2, \ldots, X_n$) are the land-use change driving forces and ($\beta_1, \beta_2, \ldots, \beta_n$) the weights of the driving forces. Logistic regression model (logit) is employed to calibrate the weights β_n. We consider the same set of driving forces listed in Table 2.3.

The $(Pi_n)^t$ is calculated as follows (Feng et al., 2011; Wu, 2002):

$$\left(Pi_n\right)^t = \frac{count(s = urban)}{n \times n - 1} \quad (4.7)$$

where *count(s=urban)* represents the number of urban cells amongst the Moore n×n neighborhood. In each time-step, representing one year, the model converts the non-urban cells according to Equation (4.3), until meeting the required change amount.

4.3.1. Validation

The validation process involves assessing the goodness of fit of the logit model, and the allocation accuracy of the model. The goodness of fit of the logit model is assessed using the McFadden pseudo R-square (PR^2) and the relative operating characteristic (ROC) procedure (Pontius Jr. and Schneider, 2001). The PR^2 mimics the R-squared statistic of linear regression models. A value of 1 shows a perfect fit, whereas a PR^2 of 0 indicates a random fit. We evaluate the allocation performance in terms of both allocation and pattern accuracy. Allocation accuracy evaluates the model's ability to allocate new changes to the proper locations, whereas pattern accuracy evaluates the configuration or the structure of the landscape (Hagen-Zanker and Martens, 2008). The common approach to assess location accuracy is the spatial overlay which depends on the cell to cell location accuracy (e.g. Mustafa et al., 2017a; Wu, 2002). This approach cannot differentiate between near-miss and far-miss errors (Mustafa et al., 2014). Pattern accuracy is often measured by a set of spatial metrics (Mustafa et al., 2014; Roy Chowdhury and Maithani, 2014). Yet, the spatial metrics can show misleading results, for example, two landscapes with different patterns may give the same spatial index (White and Engelen, 2000). Some other methods of accuracy assessment can differentiate between near and far misses, such as multi-resolution analysis (Pontius et al., 2004) and a fuzzy similarity method (Hagen, 2003). Although, these methods are location accuracy methods, they also can be classified as a measure of pattern accuracy as they operate at larger scales than the cell. In this research, we assess the accuracy of calibration and validation phases using a fuzzy similarity method. The fuzziness similarity rate (FSR) used here is calculated as follows (Hagen, 2003; Mustafa et al., 2018):

$$FSR_k = \frac{\sum_{x_k \in X_{k,sim}} \left| I_{i_k 0} \cdot (1/2)^{0/2}, I_{i_k 1} \cdot (1/2)^{1/2}, ..., I_{i_k d} \cdot (1/2)^{d/2} \right|_{\max}}{X_{k,obsr}} \times 100 \qquad (4.8)$$

where FSR_k ($0 \le FSR_k \le 100$) is the fuzziness similarity rate for class k, $I_{i_k d}$ is 1 if cell i_k in the simulated map at zone d ($0 \le d \le 4$) has the identical land-use class to one cell at zone d in the observed map otherwise is 0, $X_{k,sim}$ equals the change amount of class k in the simulated map and $X_{k,obsr}$ equals the change amount of class k in the observed map.

4.4. Results and discussion

In this section, we briefly state the result of the logit calibration and then we turn our attention to the allocation uncertainty. The estimated coefficients of the logit model are shown in Table 4.1. The PR^2 of the logit model is 0.295 indicating a good fit (Clark and Hosking, 1986). The transition probability map generated by the logit model shows a very good fit with ROC value of 0.833.

Table 4.1. The logit coefficients.

Factor	Name	Coefficient β
	Intercept	-0.9030
X_1	Elevation (DEM)	0.0623*
X_2	Slope	-0.2183*
X_3	Dist. to Road1	-0.0744*
X_4	Dist. to Road 2	-0.0819*
X_5	Dist. to Road 3	-0.2734*
X_6	Dist. to Road 4	-0.5558*
X_7	Dist. to railway stations	-0.0042
X_8	Dist. to large-sized cities	-0.1351*
X_9	Dist. to med-sized cities	-0.1661*
X_{10}	Employment rate	0.0003
X_{11}	Richness index	-0.0002
X_{12}	Zoning	3.0348*

*Significant at a 95% confidence level

The FSR (fuzziness similarity rate) without randomness for the calibration, simulated 2000 vs actual 2000, and for the validation, simulated 2010 vs actual 2010, are 48.52 and 39.33 respectively with a loss of about 10% between 2000 and 2010. We propose to set ϕ in Equation (4.4) at 1% corresponding to the FSR loss per year between 2000 and 2010. In addition, we examine other values of ϕ including 2%, 5%, 10%, 50%, 100%, and 200%.

In order to compare the performance of the TMC with the SD and the MC methods, we examine the model performance with respect to each single method. The SD is introduced in the model by updating Equation (4.5) as follows:

$$Pi^t = \left(Pi_d\right) \times \left(Pi_n\right)^t \times con(.) \times SD \quad (4.9)$$

We use different values of σ, Equation (4.1), to investigate its effect on the model. Regarding the MC method, Wu (2002) suggests that the range of δ is usually from 1 to 10. Accordingly, we set δ at 1, 2, 4, 6, 8, and 10. With higher values of δ, the model tends to produce a strong skewed probabilities which causes the computation time to increase exponentially. For example, when setting δ at 20 the cells with original probabilities of 0.9426 and 0.5854 will become 0.5121 and 0.0002 after implementing Equation (4.2). The computing time with high δ value is large, to give an idea, one run using δ=15 is about 1.6 hours, and using δ=20 is about 23.2 hours. Table 4.2 presents the average computation time per run for each method. We implemented our model in MATLAB, running on a desktop computer clocked at 3.60GHz with 32.0 GB RAM. The results indicate that the TMC method is significantly faster than the SD and the MC methods.

Table 4.2. The average run-time per run.

Method	Run time (Seconds)
Original model (deterministic)	3
TMC ϕ = 0.01 (1%)	24
TMC ϕ = 2 (200%)	4
SD σ = 0.01	34
SD σ = 2	28
MC δ = 1	40
MC δ = 10	271

Many simulations are required to investigate the properties of the model in the dynamic environment of different random noises and thus we run the model 9,500 times (500 runs per configuration). The simulated varying FSR for new urban cells is given in Table 4.3. Based on the experimental results, introducing the TMC with ϕ = 0.01 in the model slightly improves the average FSR. This is also the case for the SD with σ=0.01 and 0.05. Increasing the magnitude of both ϕ and σ decreases the average FSR as the model involves more randomness. In contrast, in the MC method the average FSR increasing with higher values of δ. This can be explained by the fact that δ controls the exponential curve that scales the transition probability and therefore higher values of δ cause more skewed curve. As a result, the chance of the cells with higher transition probability values to change their state will be higher than other cells. However, the results indicate that it is difficult to get comparable results to the model performance without randomness using the MC method even with higher values of δ.

Figure 4.3 illustrates the future urban patterns for 2030 and 2100. The number of new urban cells in each time-step, one year, is constrained to the observed quantity of new developed cells between 2000 and 2010 divided evenly by 10.

Table 4.3. The fuzziness similarity rate for newly urban cells for 9,500 runs.

		1990-2000			2000-2010		
		Maximum	Average	Minimum	Maximum	Average	Minimum
	Deterministic model	48.52	-	-	39.33	-	-
TMC	ϕ = 0.01	48.60	48.53	48.46	39.46	39.35	39.27
	ϕ = 0.02	48.57	48.51	48.43	39.45	39.33	39.23
	ϕ = 0.05	48.57	48.49	48.41	39.43	39.28	39.11
	ϕ = 0.1	48.56	48.47	48.34	39.59	39.31	39.09
	ϕ = 0.5	48.27	48.04	47.77	39.29	39.02	38.64
	ϕ = 1	47.86	47.51	47.16	39.08	38.65	38.17
	ϕ = 2	47.09	46.56	46.25	38.60	38.05	37.58
SD	σ = 0.01	48.59	48.53	48.46	39.38	39.34	39.26
	σ = 0.05	48.62	48.52	48.39	39.47	39.34	39.10
	σ = 0.1	48.56	48.40	48.30	39.49	39.28	39.01
	σ = 0.5	48.13	47.85	47.57	39.17	38.82	38.53
	σ = 1	46.84	46.52	46.23	38.11	37.69	37.10
	σ = 2	42.50	41.98	41.45	34.21	33.49	32.62
MC	δ = 1	36.47	36.05	35.74	28.23	27.55	26.68
	δ = 2	38.60	38.08	37.61	30.48	29.49	28.87
	δ = 4	42.17	41.62	40.93	33.69	33.02	32.35
	δ = 6	44.57	44.13	43.64	36.00	35.49	34.73
	δ = 8	45.91	45.63	45.38	37.59	36.99	36.48
	δ = 10	46.99	46.59	45.95	38.41	37.74	37.22

Figure 4.3 demonstrates that the MC method cannot produce simulations somewhat similar to the ones without considering any randomness. Furthermore, this becomes more difficult with lower values of δ. On the contrary, the SD method with very low degree of σ produces simulations similar, with marginal differences, to the ones without randomness which can be expected as the model tends to evolve to a stable state with lower degrees of σ. By increasing the degree of σ the model produces simulations quite different from the ones produced in a deterministic way. From the qualitative analysis of Figure 4.3, it is confirmed that the proposed TMC method well inherits the randomness in the model. It produces simulations similar to the ones produced without randomness at the earlier time-steps and slightly tunes the simulations far from the deterministic-based simulations over time. One could ask why the SD method is not used since it produces comparable results to the TMC method and we can increase the degree of randomness over time via σ. One key feature of the TMC method is that it keeps the original transition probabilities which is not the case with the SD method. This enables the model to simulate an important land-use change process in which the landowners may resort to speculative motives for hoarding land, in anticipation of potential development in the future. Consequently, some cells with high transition potentials have a great chance of changing their state in the later time-steps. When it comes to the magnitude of uncertainty, which controlled by ϕ or σ, Table 4.4 shows that the TMC method controls the degree of randomness more efficiently than the SD method.

Table 4.4. The new urban cells allocation difference (%) between 500 simulations for each configuration.

	2030			2100		
	Maximum	Average	Minimum	Maximum	Average	Minimum
TMC | ϕ = 0.01	1.37	1.21	0.99	5.76	5.38	4.96
TMC | ϕ = 2	34.45	33.75	32.99	36.55	36.17	35.78
SD | σ = 0.01	1.35	1.14	0.94	1.05	0.76	0.89
SD | σ = 2	62.06	61.17	60.18	35.72	35.28	34.79
MC | δ = 10	38.64	37.99	37.22	31.59	31.16	30.66
MC | δ = 1	85.70	85.32	84.93	62.44	62.12	61.76

Table 4.4 gives the results of the allocation differences for the new urban cells between 500 simulations for each configuration. The main aim of this table is to indicate the dependence of model results on the magnitude of the randomness parameter. Surprisingly, the results reveal that both SD and MC methods generate landscape patterns for 2100 that are more similar to each other than the patterns generated for 2030. This is against expectation because distant future is more uncertain than the near ones. In the SD and the MC methods, we have constant change amount per time-step whereas the available number of cells that can change their state decreasing with increasing the time-steps. If the number of the available cells is fewer, as the case in 2100, the opportunity of these cells to be randomly selected during each run is higher. Contrariwise, in the TMC method we have a fixed change amount and the number of cells that can change their state is increasing with time. As a result, our method is able to increase the randomness magnitude over time.

If the simulations are uniform, a specific number of cells will change their state in most of the simulations resulting in lower differences in the allocation process. On the other hand, if the simulations are very variable, many cells will change towards another state during each simulation and therefore the difference between each simulation is high. It is difficult to forecast and interpret the future simulations if the model generates landscape patterns that are highly different from each other. With a lower magnitude of randomness, the model generates landscape patterns for distant future that are very similar to each other, as in SD with σ = 0.01, such that the future simulations can be considered as an extrapolation of the past trends. The TMC with ϕ = 0.01 method produces patterns with low differences for the near future and higher difference for the distant futures. In addition, by 2100, the method is still able to generate patterns that can be considered because they are not very different from each other.

4.5. Conclusions

We proposed a method, which we refer to as TMC, to introduce randomness in land-use change models with a purpose of modeling allocation uncertainty. The method is based on a Monte-Carlo simulation in which a cell in the landscape is randomly selected and its transition

probability from one state to another is compared with a random number uniformly distributed within a dynamic range that increases over time. We compared the proposed method with the widely used methods to introduce randomness in land-use change forecasting: Stochastic Disturbance, and Monte-Carlo Simulation. The three methods were introduced into a cellular automata model that was developed to simulate urban expansion in Wallonia (Belgium) between 1990 and 2000.

Our analysis reveals that the TMC produces results comparable with existing methods over the short-term validation period (2000-2010). Further on it is capable of tuning uncertainty on longer-term time horizon. Controlling the degree of randomness over time is an important feature of the TMC as the distant future is characterized by more uncertainty than the near future.

The proposed method assumes that all projections are exposed to the same source of allocation uncertainty. Therefore, more research in how to quantify several allocation uncertainty sources such as uncertainties related to the model structure, model simplification, and model parameter estimates need to be conducted. For example, our model was calibrated and validated with 1990-2010 data. Throughout this period, there were no major urban transition breaks and the land-use dynamics can be regarded as rather consistent over times. By contrast, applying our model over the distant past, e.g. 1950-2010 would allow to analyze uncertainties related with major development breaks, as for instance the shift from a train-based to a car-based city model in the 1950ies and 1960ies, the succession of diverging economic cycles or the adoption of legally-binding land-use regulation in the late 1970ies.

4.6. Key contributions

- Our proposed method, Time Monte-Carlo (TMC), tunes the uncertainty over time.
- The uncertainty magnitude tends to decrease over time with traditional methods, stochastic disturbance and Monte-Carlo Simulation, which is against expectation.
- Introducing some randomness in land-use change models tends to improve the performance of predictions when compared to the purely deterministic predictions, even on short-term, e.g. 10 years, time horizons.

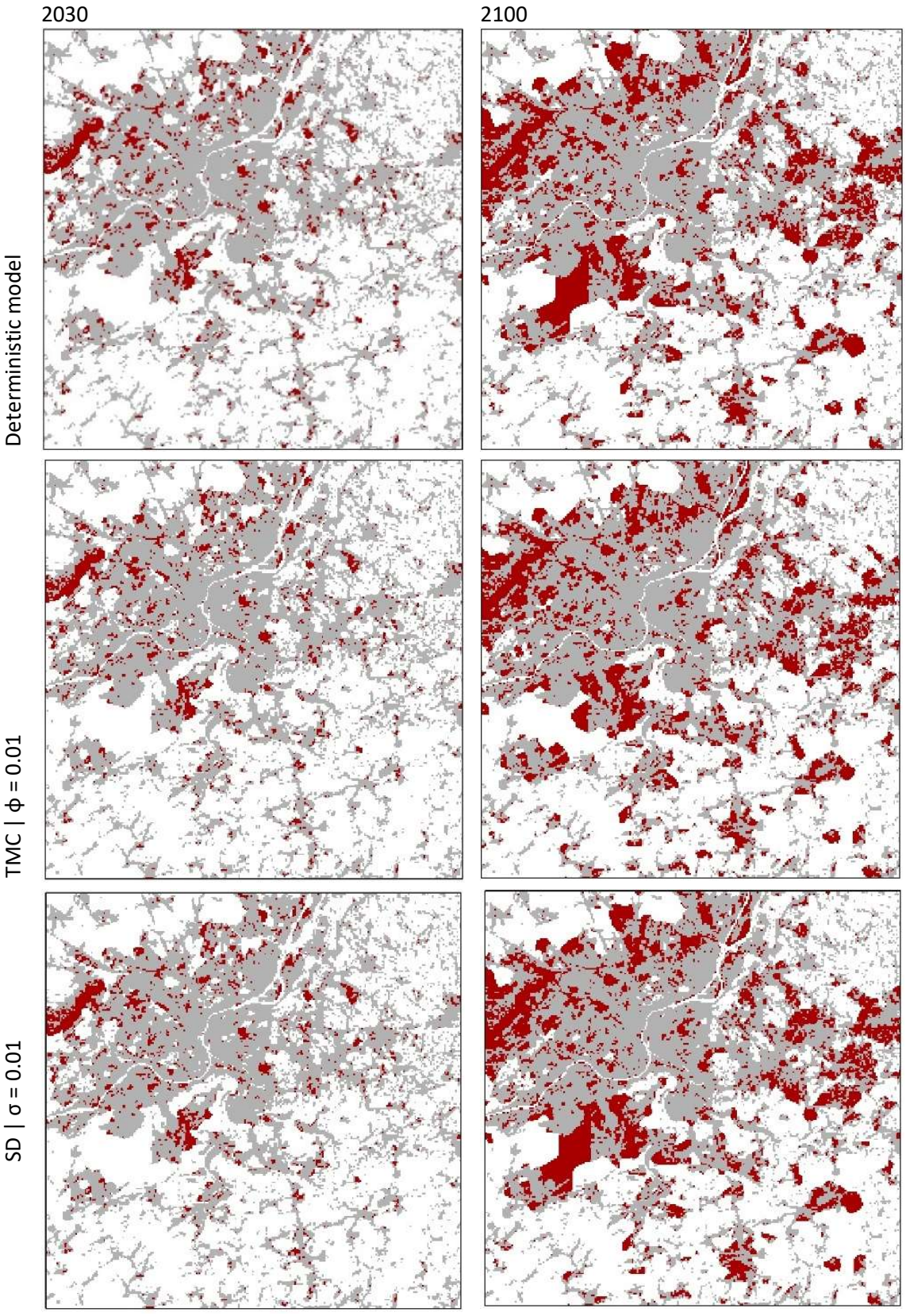
2030
2100
Deterministic model
TMC | ϕ = 0.01
SD | σ = 0.01

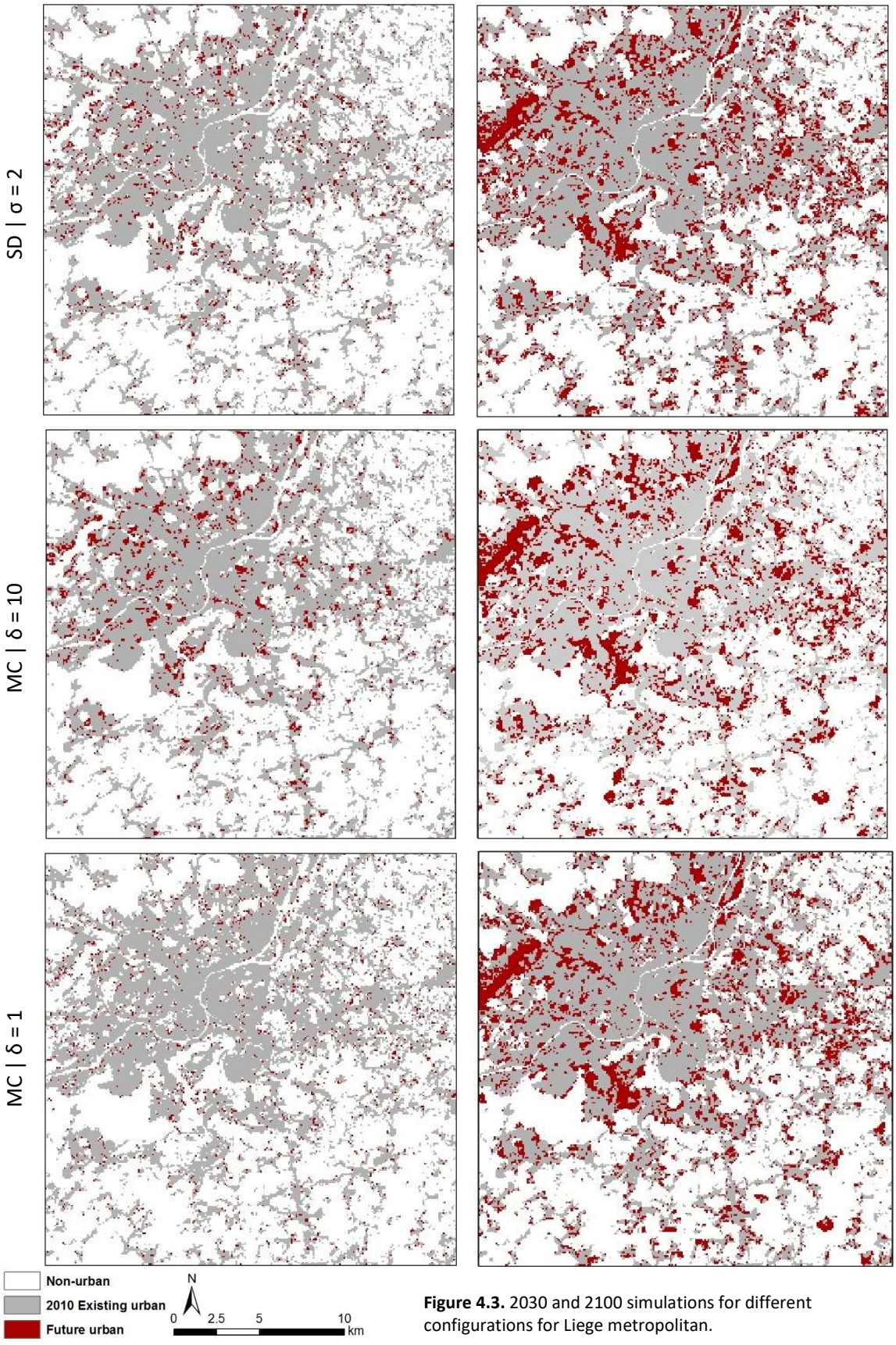

Figure 4.3. 2030 and 2100 simulations for different configurations for Liege metropolitan.

PART 3: Impact of Future Urbanization on Floods

Chapter 5: Effects of spatial planning on future flood risks in urban environments

5.1. Introduction[1]

The magnitude and frequency of floods, particularly river floods, are currently increasing in northwest Europe (Moel and Aerts, 2010). Climate change and urban development are key elements contributing to increased flood damage (Poelmans et al., 2011). Urbanization increases the damage due to flood exposure caused by the increasing population and infrastructure within flood-prone zones. In addition, transforming natural surfaces into artificial surfaces causes an increase in flooding frequency because of poor infiltration and increased exposure to the elements (Huong and Pathirana, 2013). Recent studies have shown different effects of climate change and urban development on flood risk. The Intergovernmental Panel on Climate Change claimed, with low confidence, that climate change has affected the frequency and magnitude of flooding (IPCC, 2014). Poelmans et al. (2011) and Beckers et al. (2013) investigated the relative impact of both climate change and future urban expansion on floods. Poelmans et al. (2011) found that the potential flood-related damage was mainly influenced by urbanization on the floodplains. Similar results were obtained by Beckers et al. (2013) in a "dry" climate scenario, while climate change is more influential in a "wet" scenario. Hannaford (2015) found that changes in peak flows could not be directly attributed to climate change across the United Kingdom. Cammerer et al. (2013) analyzed potential changes in future flood exposure because of different land use developments and found that the range of potential changes in flood-exposed residential areas varies from no further change to 159% increase depending on the spatial planning scenarios.

Previous studies that coupled urban development scenarios with hydrological models using a spatial resolution between 50 m and 100 m (e.g., Beckers et al., 2013; Cammerer et al., 2013; Poelmans et al., 2010; Tang et al., 2005) considered only urban expansion processes, i.e., transitions from nonurban to urban land use. Such a binary process may fail to estimate the damage related to floods properly because it neglects the different densities of urban cells and the

[1]This chapter is based on: Mustafa, A., Bruwier, M., Archambeau, P., Erpicum, S., Pirotton, M., Dewals, B., & Teller, J. (under review). Effects of spatial planning on future flood risks in urban environments. *Journal of Environmental Management*.

variation in density over time. However, spatial planning policies designed to foster infill development are now increasingly targeting low- and medium-density urban areas, with significant densification capacities in terms of both available land and services.

This study investigates the possibility of flood damage related to different urban development scenarios in Wallonia (Belgium) if there is no further climate change. The main contribution of our study is the evaluation of the impacts on flood damages from spatial planning policies that consider expansion versus densification processes compared with spatial planning policies oriented towards development restrictions in flood-prone zones.

5.2. Study area

Wallonia covers an area of 16,844 km^2 in southern Belgium (Figure 5.1). Its hydrographic network is structured along four hydrographic districts (Meuse, Rhine, Escaut Scheldt or Seine basin), 15 hydrographic subbasins and 6,208 so-called PARIS sectors, each of which correspond to a river stretch with relatively homogeneous characteristics in the main riverbed and in the floodplains. In this study, we only consider the two main districts of Meuse and Escaut, which cover 73% and 22% of Wallonia, respectively. The areas of most subbasins in the Meuse district are larger than in the Escaut district, while the population density is generally lower in the former. The Meuse aval subbasin is the largest in Wallonia and the most densely inhabited in the Meuse district. Four subbasins in the Meuse district have a population density lower than 100 inhabitant/km², while it is higher than 175 inhabitant/km² for all subbasins in the Escaut district (DGO3 2015a, 2015b). The Meuse district is mainly covered by agricultural uses and forests while the Escaut district is mainly covered by agriculture and built-up uses. In both districts, high flows generally occur in winter and low flows in summer, following the rainfall–evaporation regime.

Table 5.1: Hydrographic sub-basins in Wallonia in the Meuse and Escaut districts and their respective main river, area and population density (DGO3/SPW, 2015a, 2015b).

District	Sub-basin	Main river	Area (km²)	Density in 2009 (inh/km^2)
Meuse	Meuse aval	Meuse	1,924	373
	Meuse amont	Meuse	1,923	116
	Ourthe	Ourthe	1,843	83
	Semois-Chiers	Semois	1,759	74
	Sambre	Sambre	1,703	361
	Lesse	Lesse	1,343	52
	Amblève	Amblève	1,077	72
	Vesdre	Vesdre	703	305
Escaut	Dyle-Gette	Dyle and Gette	944	273
	Haine	Haine	802	512
	Escaut-Lys	Scheldt	766	287
	Dendre	Dender	673	175
	Senne	Senne	569	372

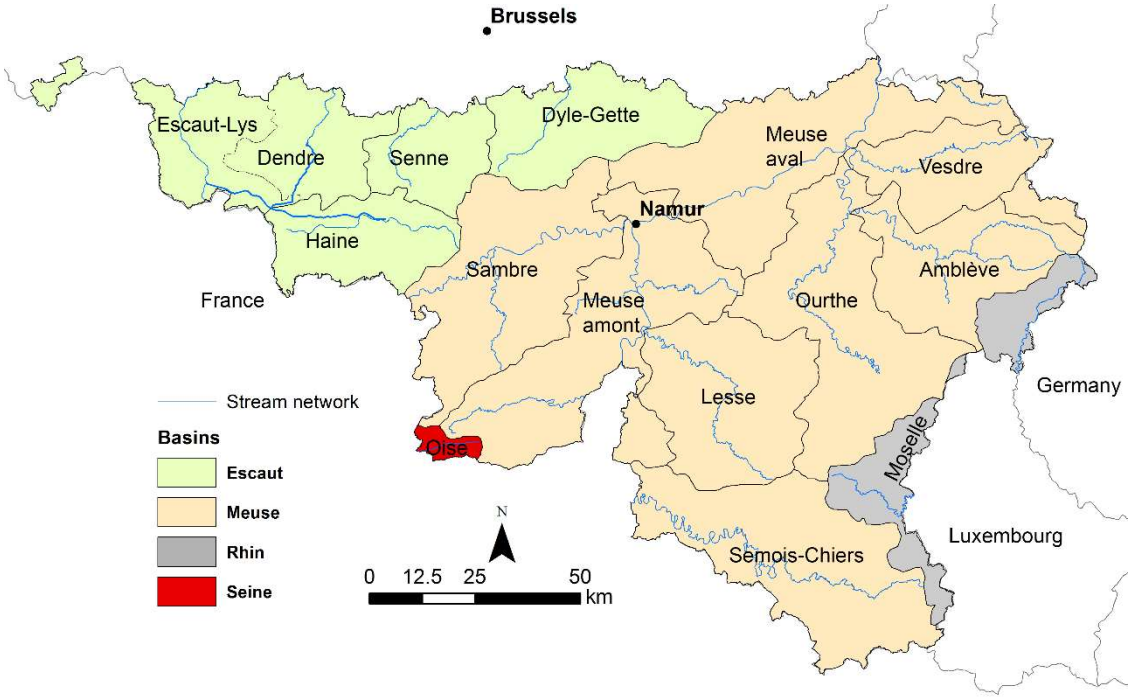

Figure 5.1: Representation of the 4 hydrographic districts and 15 hydrographic sub-basins in the Walloon region.

5.3. Methods

Our methodology to assess flood damage for different urbanization scenarios consists of three main steps. Firstly, urban land-use data for 1990, 2000 and 2010 were generated based on Belgian cadastral data (CAD). Secondly, following chapters 3 and 4, the CA-AB is employed to simulate future urban land-use (2030, 2050, 2070 and 2100). In order to define the appropriate number of urban density classes from hydrological point of view, a sensitivity of the computed flood damage to the number of classes is examined. The model focuses on two sources of uncertainties, (i) the expected future quantities of changes, and (ii) the developer agents' behaviors when selecting specific land to develop. The first source of uncertainties is often influenced by dynamics that occur at large spatial and temporal scales and involving macro-economic and demographic changes (Veldkamp and Lambin, 2001). Commonly, the estimates of quantity uncertainty are based on simulation of different scenarios according to any assumption of extrapolation of the past quantity of changes, population expansion and/or socio-economic transitions (e.g. Cammerer et al., 2013; Mustafa et al., 2016; Poelmans et al., 2010). Using linear extrapolations of the observed expansion and densification rates between 1990, 2000 and 2010 in Wallonia, three change rates are proposed for the future: low-, medium- and high-demand. These scenarios were derived by extrapolating respectively the trends between 2000 and 2010 (low), 1990 and 2010 divided by 2 (medium), and 1990 and 2000 (high-demand). Regarding the parameter weights that define developer agents' behaviors when selecting specific land to develop, we propose to introduce a uniform random variable in the model to consider uncertainty due to allocation as proposed in

chapter 4. Finally, the Wolf2D hydraulic model (Bruwier et al., 2015; Ernst et al., 2010; Erpicum et al., 2010b) was used to compute inundation extents and water depths for each future urban pattern.

5.3.1. Hydrological characteristics

The computation of inundation extents and water depths for the generation of flood hazard maps in Wallonia was performed for steady flows corresponding to return periods of 25, 50 and 100 years, using the 2D hydraulic model, WOLF 2D, with a cell size of 5 m × 5 m.

In this study, we only consider the water depth to determine the flood damage. Flood damage is influenced by additional factors such as the flow velocity, the flood duration, transport of sediments, and early warning. In this study, however, flow velocity remained low, which is typical in floodplains of lowland rivers. Therefore, it has a negligible influence on the damage (Kreibich et al., 2009; Pistrika and Jonkman, 2010). We use stage-damage functions, which were developed for relatively long-duration floods (Kreibich et al., 2010), which is consistent with the flood events of interest in this study. Water depth is widely recognized as the factor with the greatest influence on flood damage estimation (Büchele et al., 2006; Merz et al., 2007; Kreibich et al., 2009), whereas the specific contribution of additional factors remains incompletely understood and, no generally accepted procedure exists for quantifying their influence in large-scale damage modelling as undertaken in this study.

Maps of inundation extents and water depths were computed for several hundreds of kilometers of rivers throughout Wallonia (Figure A-1 in the Appendix). In the Escaut district, only a limited portion of all sectors was computed, except for the Escaut-Lys subbasin where results are available all along the Scheldt river (Escaut). No river was computed in the Haine subbasin. In the Meuse district, computations were performed all along the rivers Amblève, Meuse, Ourthe, Sambre, Vesdre, and Viroin rivers. In the Lesse and Semois-Chiers subbasins, results are only available for some reaches of the Lesse and Semois rivers.

5.3.2. Flood damage assessment

Figure 5.2 shows the overview of our workflow. The result is a map giving the spatial distribution of direct and tangible flood damage at a mesh-resolution of 5 m × 5 m, representative of the resolution of the hydraulic computation. The land-use category of each floodplain cell was determined from the land-use map at a resolution of 100 m × 100 m. Only damages related to buildings are computed in this study and we do not consider damages related to other land-uses like infrastructure, agriculture, and forest.

The susceptibility of a building to flooding was assessed by a stage-damage function giving the relative damage, i.e., the share of the total value of a building that is damaged by the flood, as a function of the water

depth. In this study, we used the stage-damage functions for residential and industrial categories defined by the FLEMO (Kreibich et al., 2010). The damage assigned to residential and industrial buildings is split between mobile and immobile assets. Figure 5.3 illustrates the single FLEMO stage-damage function used for both assets for residential buildings and the two functions for industrial ones.

The determination of flood damage in monetary value requires the assignment of a specific value to the buildings. In our study, the monetary values of residential and industrial buildings were chosen so that in the baseline scenario, the estimated flood damages are similar to those computed by Beckers et al. (2013) along the Meuse river for a 100-year flood. We used identical monetary values for both residential and industrial categories and assume that immobile values are four times higher than mobile ones, which respects the ratios proposed by Beckers et al. (2013). In Table 5.2, the resulting immobile and mobile values are significantly higher than the values used by Beckers et al. (2013). These results were obtained from the type of elements for which the monetary values are assigned: i.e., parcels for Beckers et al. (2013) and buildings in this study.

Table 5.2: Prices of the residential and industrial categories.

	Beckers et al. (2013)		The present study	
Element at risk	Parcel		Building	
	Immobile	Mobile	Immobile	Mobile
Residential	389 €/m^2	119 €/m^2	2000 €/m^2	500 €/m^2
Industry	343 €/m^2	90 €/m^2	2000 €/m^2	500 €/m^2

The United Nations defines risk as the combination of the probability of an event to occur and its negative consequences (UNISDR, 2009). Considering N flood events with a return period T_i and causing a damage D_i, the risk R was evaluated by Ernst et al. (2010) as the expectation value of damage by the following expression:

$$R = \sum_{i=1}^{N} \left[\left(\frac{1}{T_{i-1}} - \frac{1}{T_i} \right) \frac{D_{i-1} + D_i}{2} \right] \tag{5.1}$$

Equation (5.1) was computed based on the three return periods T_{25}, T_{50} and T_{100} without extrapolation neither to lower nor to higher return periods for which data are not available consistently for all the considered river reaches. As a result, Equation (5.1) gives an indicator of the flood risk and not the risk itself since the risk curve should be integrated over the entire range of flood probability. This indicator is, however, useful for the determination of the impact of urbanization on flood damage with a single scalar value representative of the damage occurring in-between the three return periods considered in this study.

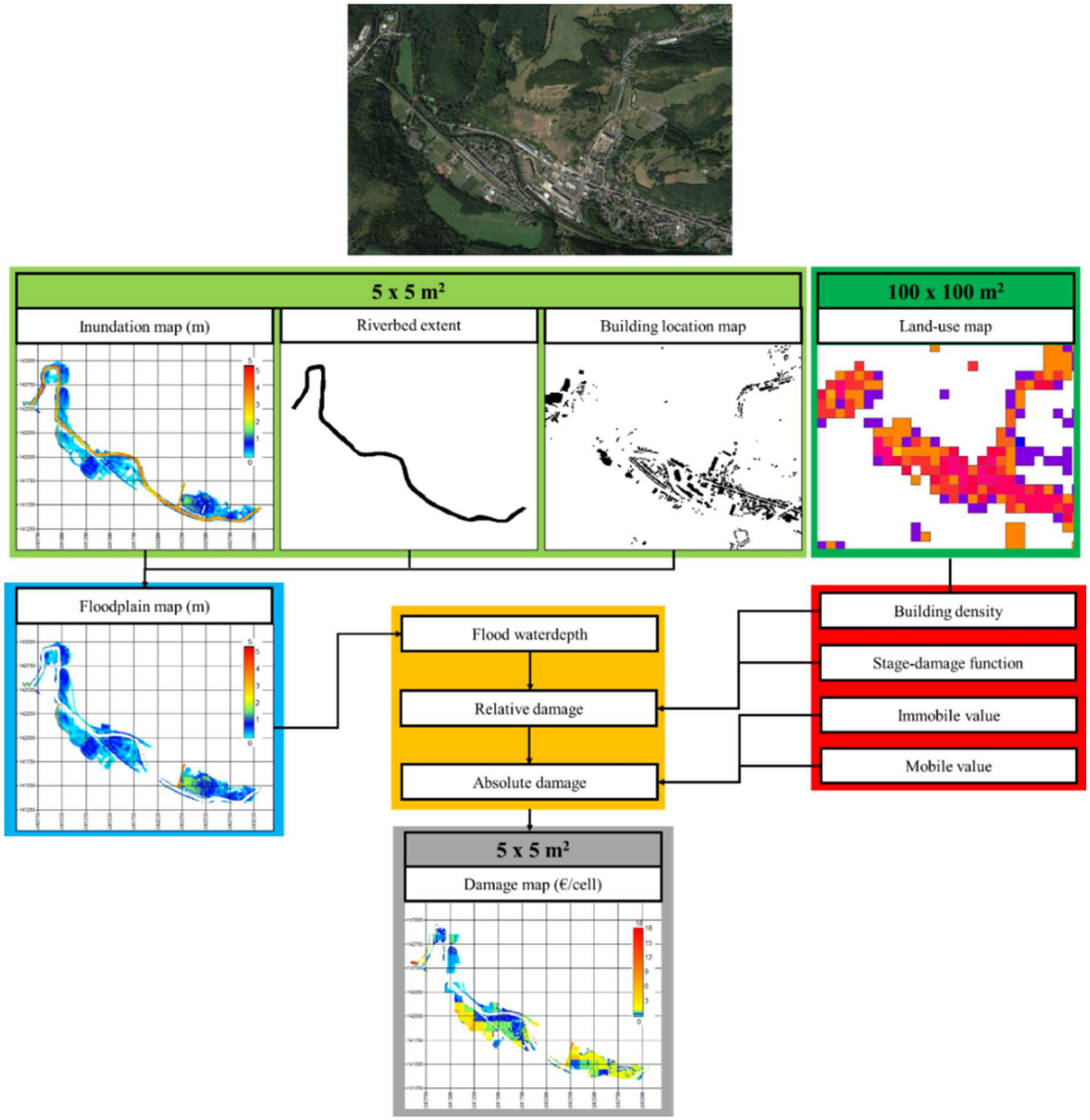

Figure 5.2: Methodology for the estimation of flood damage.

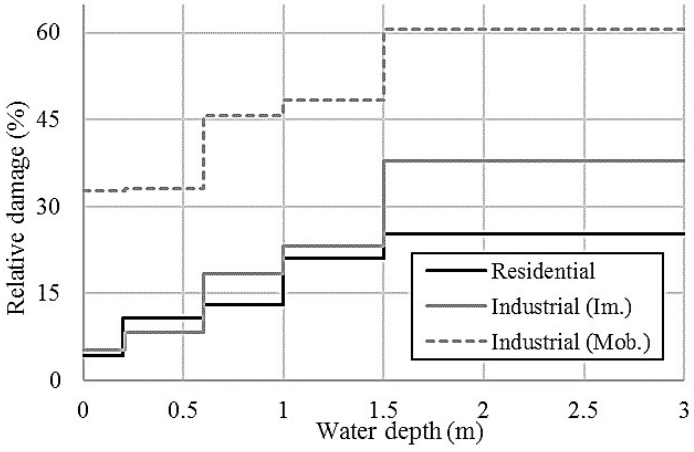

Figure 5.3: FLEMO stage-damage functions for residential and industrial land use categories.

5.3.3. Influence of the number of urban density classes

The sensitivity of the computed flood damage to the number of density classes is assessed for flood discharges Q_{25} and Q_{100}. We examine 1 to 9 density classes for each land-use category, the flood damage D_d computed with d classes of density is compared to the results obtained with the highest number of classes, i.e. D_9, using the following relative difference E_d:

$$E_d = \frac{D_d - D_9}{D_9} \tag{5.2}$$

The computed flood damages are overestimated by 48% to 105% when a single class of building density is used (Figure 5.4). When the number of classes is increased, the value of the computed flood damage converges rapidly towards values close to D_9, and fluctuates slightly around this value. When five classes of densities are used, the relative error remains lower than 5% for the two flood discharges Q_{25} and Q_{100}. Beyond this number of classes, the relative difference E_d does not seem to decrease significantly. Therefore, we used five classes of density for each land use category (i.e., residential and industrial) using the natural-breaks technique (Jenks and Caspall, 1971). Table 5.3 gives an estimation of the number of buildings per 100 m × 100 m land assuming that the average-sized residential building in Belgium is 100 m² (Tannier and Thomas, 2013). Table 5.3 demonstrates that about 80% of built-up land is related to very low-density urban classes (class-1 and 2), whereas only 5% are highly dense areas in 2010 observed data. This offers a strong potential to increase density of the existing urban areas.

Table 5.3. Urban density classes range in percentage of 100m×100m cell area.

Class	Minimum	Maximum	Number of cells in observed 2010 (% of Wallonia area | % of built-up area)
Class-0 (non urban)	0	1	1410959 (83.5 | 0)
Class-1 (lowest-density)	1	5.8	129232 (7.6 | 46.4)
Class-2	5.8	13.8	91148 (5.4 | 32.7)
Class-3	13.8	26.1	41447 (2.5 | 14.9)
Class-4	26.1	48.6	14109 (0.8 | 5.1)
Class-5 (highest-density)	48.6	100	2847 (0.2 | 1)

5.3.4. Future urbanization scenarios

As detailed in Table 5.4, 24 different urbanization scenarios were generated by varying the urbanization rate, the spatial policies (densification with/without expansion), and different levels of flood management policies. In this respect, we consider three zones represented in the official inundation maps (Erpicum et al., 2010a):

- zones of “low flood hazard”, referred to hereafter as “zone 1”;
- zones of “medium flood hazard”, referred to hereafter as “zone 2”;
- zones of “high flood hazard”, referred to hereafter as “zone 3”;

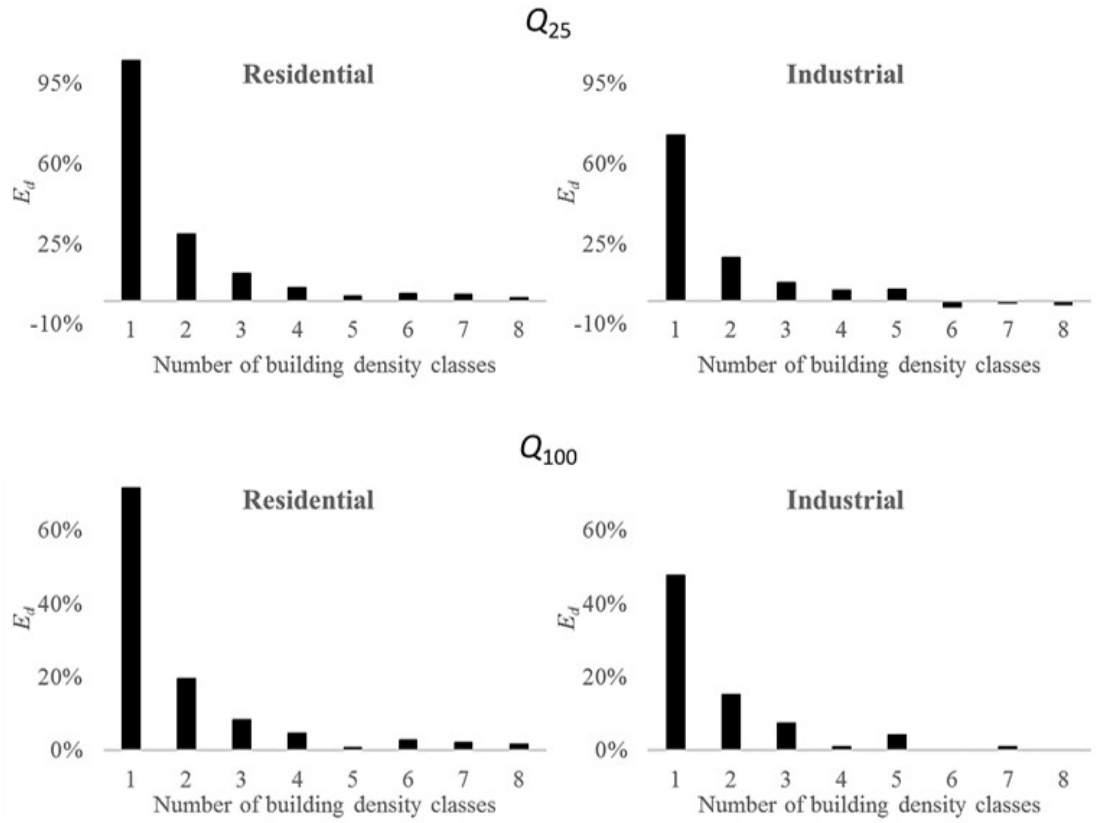

Figure 5.4: Sensitivity of the total flood damage computed with different numbers of classes of building density, for flood discharges Q25 and Q100.

The business-as-usual scenario is in line with the recent urban developments. In the densification scenarios, we assume that the expansion process is blocked and the required new areas for expansion are taken from the next density level. For instance, the expansion from class-0 to class-1 and class-2 is substituted by densifying the same area from class-1 to class-2. In cases where the available area of a specific class is not sufficient to be further densified, the model densifies the required expansion area from the next density class. After simulating each density class, the model assigns an urban use (residential or industrial) for each cell according to the official zoning plan of Wallonia.

Table 5.4. Urbanization scenarios.

	Urbanization rate Ban on new developments	High (1990-2000)	Medium (1990-2010)	Low (2000-2010)
Business as usual	None	BH	BM	BL
	In zone 3	BHR-3	BMR-3	BLR-3
	In zones 2 and 3	BHR-23	BMR-23	BLR-23
	In all zones	BHR-123	BMR-123	BLR-123
Densification	None	DH	DM	DL
	In zone 3	DHR-2	DMR-2	DLR-2
	In zones 2 and 3	DHR-23	DMR-23	DLR-23
	In all zones	DHR-123	DMR-123	DLR-123

5.4. Results and discussion

5.4.1 Future urban land-use

The proposed ABM generates a series of future possible urbanization scenarios. The validation of the model, simulated 2010 vs observed 2010 map, shows a comparable results to those reported in the literature (e.g., Han and Jia, 2016; Long et al., 2013; Wang et al., 2013) with Kappa indices of 0.88, 0.87, 0.90, 0.92 and 0.92, for classes 1-5 respectively..

Table 5.5 lists the actual urban transitions over the modeled period. The table indicates that the predominant urbanization processes have been the development of low and medium density areas (class-1 and 2). The observed class changes further suggest that transitions from class 1 to classes 4 and 5, class 2 to class 5, and class 3 to class 5 over the study period are marginal. Therefore, we set the densification as the transitions from class 1 to classes 2 and 3, from class 2 to classes 3 and 4, from class 3 to class 4, and from class 4 to class 5.

Figure 5.5 illustrates the simulated maps for 2030 and 2100 considering BH and DH scenarios. In business-as-usual scenarios, the development of new low and medium density land are occurring continually and therefore Wallonia will experience highly fragmented urban landscape in the future. On the other hand, there are sufficient low and medium density urban areas that could accommodate future urbanization demands. As mentioned above, we assumed that, in the densification only policy, the required new areas for expansion are taken from the next density class. If the available area of a specific class is not sufficient to be further densified, the model densifies the required expansion and densification area from the next density class. Consequently, the area of class-1 and class-2 will decreases over time. Figure 5.6 shows the percentage of change for each class comparing with the 2010.

Table 5.5. Class to class transitions.

1990-2000	Class-1	Class-2	Class-3	Class-4	Class-5
Class-0	12548	2753	973	464	211
Class-1	-	9469	517	71	9
Class-2	-	-	3364	151	8
Class-3	-	-	-	820	23
Class-4	-	-	-	-	130
2000-2010	Class-1	Class-2	Class-3	Class-4	Class-5
Class-0	8277	1851	628	289	127
Class-1	-	7195	320	55	15
Class-2	-	-	2598	116	10
Class-3	-	-	-	594	10
Class-4	-	-	-	-	80

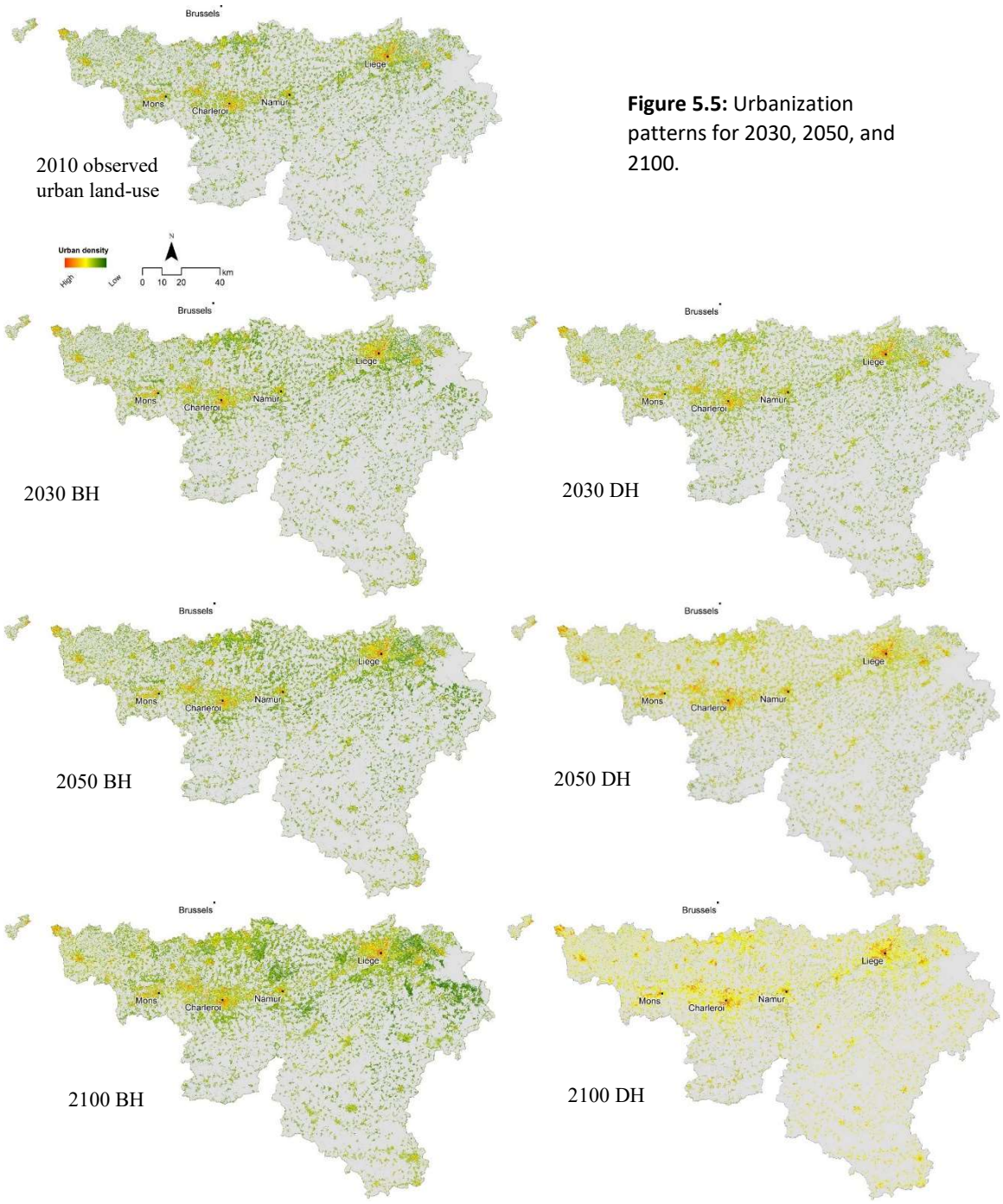

Figure 5.5: Urbanization patterns for 2030, 2050, and 2100.

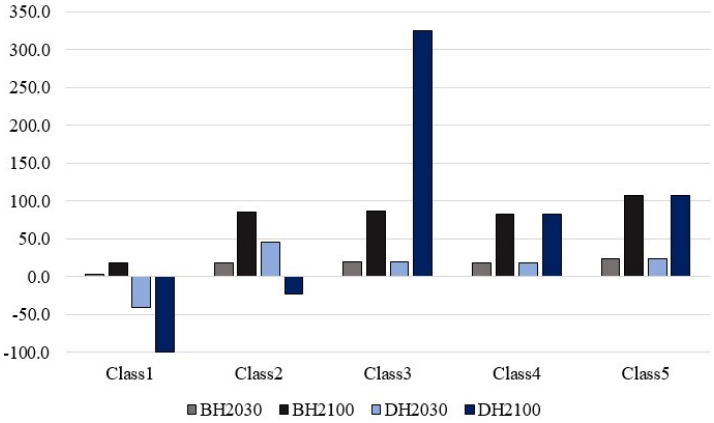

Figure 5.6: Change rate (%) of the area of each urban class related to its area in 2010.

5.4.2. Flood risk

The uncertainty in the computation of the flood risk indicator resulting from the adopted resolution of the land use information (100 m × 100 m) is expected to be significant, particularly for moderate events with limited flood extents such as the Q25 flood discharge. Consequently, the assessment of the flood risk in absolute monetary values should be interpreted with caution. Following Moel and Aerts (2010), we therefore use relative values of flood risk, taken as a percentage of a reference risk values (in the baseline scenario) computed with the same methodology.

Distribution of the flood risk between the sub-basins in the baseline scenario

Figure 5.8 illustrates the relative contributions of different sub-basins to the flood damages for the *Q25*, *Q50* and *Q100* flood discharges (respectively 445×106 €, 620×106 € and 830×106 €) and to the value of the flood risk indicator (18×106 €). For most sub-basins, the relative contributions are very similar for the different flood discharges as well as for the flood risk indicator. The variations are the highest for the Meuse aval sub-basin in which the contribution to the overall flood damages varies between 14% and 20% depending on the considered flood discharge. In what follows we only discuss the flood risk indicator since the conclusion can reasonably be extended to the flood damages for the three computed flood discharges.

The results show that:

- The Meuse amont, Meuse aval and Ourthe sub-basins have the highest contribution to the computed flood risk indicator. This is consistent with the high number of sectors which are computed in these sub-basins (Figure 5.8).
- The flood risk indicator in the Vesdre sub-basin is more than twice as high as in the Semois-Chiers, Lesse and Amblève sub-basins, despite a smaller sub-basin area and the existence of large reservoirs in the upper part of the Vesdre catchment. This is certainly related to the population density, which is four to six times higher in the Vesdre sub-basin than in the other ones.
- In the Escaut district (Dyle-Gette, Senne, Dendre and Escaut-Lys sub-basins), the computed flood risk indicator is the lowest because only a limited number of sectors are computed.

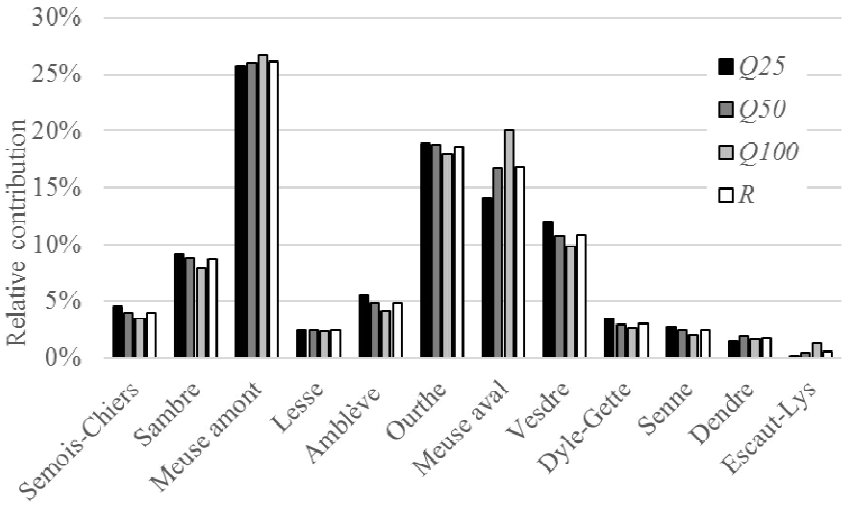

Figure 5.8: Relative contribution of each sub-basin to the total flood damages at the regional level and to the flood risk indicator (R) for the baseline scenario (2010 land-use map).

Influence of the urbanization scenarios on the magnitude of the total flood risk

In this section, we compare the influence of the spatial planning policies on the increase in the value of the flood risk indicator for the 2050 time horizon compared with the baseline scenario.

Table 5.5 shows that the increase in the total flood risk indicator ranges between 0% and 44% depending on the spatial planning scenario for a high demand rate and between 0% and 22% for a low demand rate. Banning new developments in flood-prone zones is by far the most influential spatial planning factor. A ban on new developments in flood-prone zone 3 would limit the increase in the flood risk indicator to roughly one-third of the values without any ban on new developments. Extending the ban to flood prone-zones 2 reduces the increase in flood risk indicator to only 1-2% when compared with 2010. Banning new developments in all flood-prone zones leads to no increase in flood damages for the computed flood discharges because their maximum inundation extents matches the maximum flood-prone zones. The effects of urban development restrictions in flood-prone zones on the increase in flood damage are of the same magnitude for both BAU and densification strategies.

In all cases, densification spatial planning policy leads to a higher flood risk indicator compared to BAU, especially in the case where no or moderate urban development restrictions are adopted in flood-prone zones. This is quite logical because the urban areas where densification may occur are predominantly located in valleys in Wallonia, following the pattern inherited from the industrial revolution. Without banning new developments or with a regulation in flood-prone zones 3, the rise in the flood risk indicator is respectively from 9 to 15 percentage points and from 2 to 3 percentage points higher in the densification scenario. Basically, this means that densification policies designed to curb sprawl should be accompanied by adequate restriction measures in flood-prone zones to mitigate the increased flood risk.

The influence of uncertainty related to the demand rate is lower than the effect of spatial planning policies. However, its impact remains significant because the increase in the flood risk indicator for a low urbanization rate scenario without regulation on new developments (with regulation in flood-prone zones 3) is 7 to 13 (2 to 3) percentage points lower than that obtained with a high demand rate scenario.

Table 5.5: Increase in the flood risk indicator for the 2050 time horizon based on different urbanization scenarios, compared to the baseline scenario (2010).

	Ban on new developments	High urbanization rate	Medium urbanization rate	Low urbanization rate
Business as usual	None	29%	27%	22%
	In flood zones 3	9%	8%	7%
	In flood zones 2 and 3	1%	2%	1%
	In all flood zones	0%	0%	0%
Densification	None	44%	37%	31%
	In flood zones 3	12%	11%	9%
	In flood zones 2 and 3	2%	2%	2%
	In all flood zones	0%	0%	0%

Influence of the urbanization scenarios on the distribution of the flood risk

The flood risk indicator in 2050 is strongly influenced by the spatial planning scenario (Table 5.5). In this section, we investigate the distribution of the increase in flood risk indicator among the subbasins depending on the spatial planning policy.

Figure 5.9-a indicates that in business-as-usual scenarios (BAU), the urbanization rate impacts poorly the distribution of the rise in flood risk between the sub-basin but modifies the magnitude of the flood risk. On the contrary, the distribution of flood risk is highly influenced by the spatial policies (BAU VS densification scenario). With the densification policy, the changes in flood risk are distinctively higher in the Meuse district (sub-basins from Semois-Chiers to Vesdre in Figure 5.9-a) than for the BAU scenario, while a reduction is observed in the Escaut district. Figure 5.9-b show the relative increase in flood risk for each sub-basin compared with its flood risk in 2010. It is clear that in the BAU scenarios, the flood risk in the north-west part of Wallonia is remarkably increased, whereas the flood damage is nearly equally increased in most of the sub-basins in the densification scenarios.

In all sub-basins, banning new developments in flood-prone zones 3 (Figure 5.9-c) has a high impact on the mitigation of the increase in flood risk (reduction from 4.8×106 € to 1.4×106 € of the rise in the flood risk indicator). Extending the ban to flood-prone zones 2 leads to marginal rises in flood risk in most sub-basins (rise in flood risk reduced to around 3×105 €). Only for the Meuse amont, Meuse aval and Dyle-Gette sub-basins, a significant additional mitigation of the flood risk can be obtained by an extension of the ban on new development in flood-prone zones 1 (roughly a reduction of 2.5×105 € for the rise in flood risk over the three sub-basins).

Along the Meuse River, Beckers et al. (2013) evaluated the increase in flood damage due to urbanization in-between 1 and 40% for a 100-year flood. In this study, the range of the increases in flood damage for Q100 is 0-40% for the BAU scenarios, while a maximum increase by 85% is computed for the densification scenario (DH).

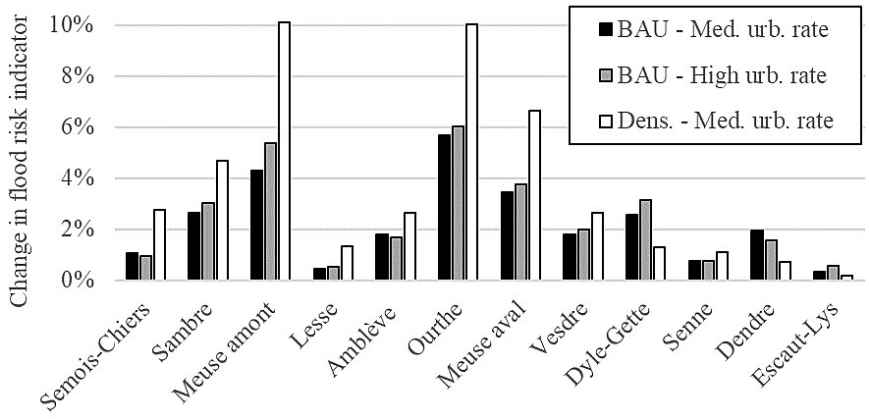

(a)

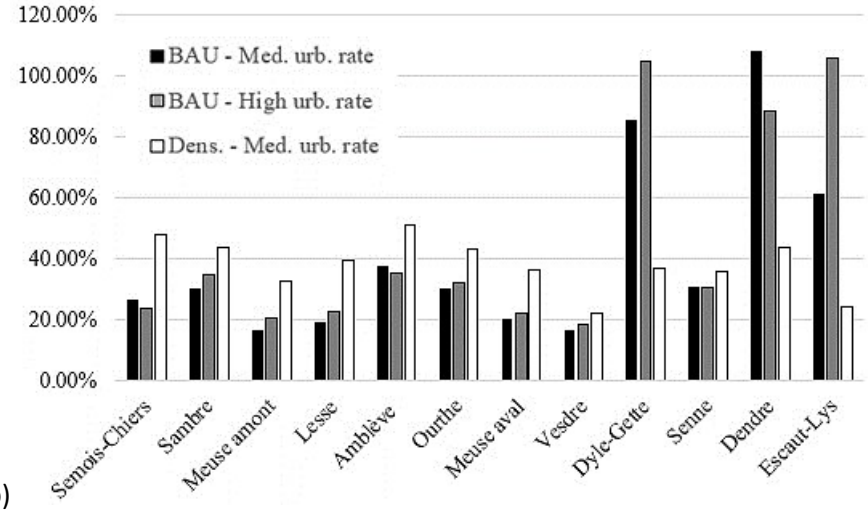

(b)

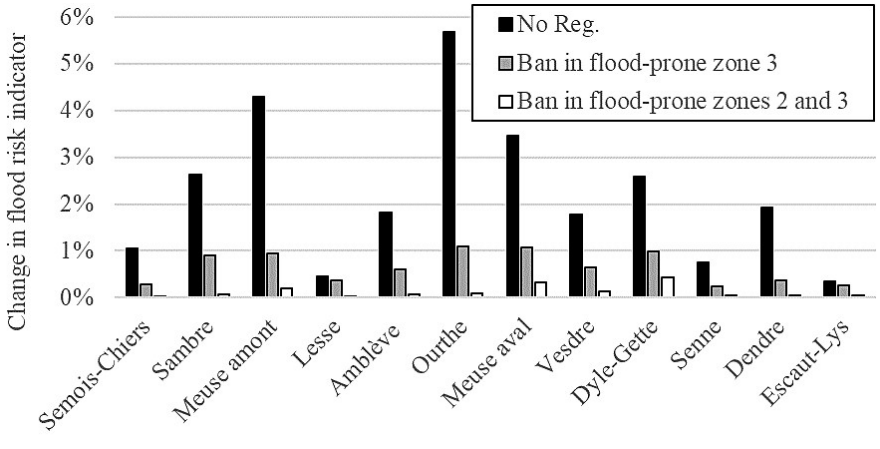

(c)

Figure 5.9: Changes in the values of the flood risk indicator in 2050 for each sub-basin compared to (a) the total flood risk in the baseline scenario, and (b) the flood damage for the sub-basin in the baseline scenario. (c) Changes in the flood risk indicator for each sub-basin compared to the total flood risk in the baseline scenario for BAU – Med. Urb. rate.

Increase in flood risk for different future time-horizons

In this section, the increase in flood risk is quantified for the time horizons 2030, 2050, 2070 and 2100 (Table 5.6) for the six following urbanization scenarios:

Table 5.6: Increase in the flood risk per decade in Wallonia.

Scenario	Flood risk increase (%)
BL	5.5
BH	7.5
DH	11
BLR-3	2
BLR-23	1
BLR-123	0

The first three scenarios are representative of the range of variation of the computed flood risk indicator without restrictions on urbanization in flood-prone zones. The comparison of the last three scenarios with the first enables to assess the effect of restrictions on new developments in flood prone-zones.

The distribution of changes in the flood risk indicator between the different subbasins are slightly affected by the time horizon. The variations of the relative contribution of a subbasin to the total flood risk indicator at the time horizon 2100 are the highest for the first urbanization scenario (BAU with a low urbanization rate and no regulation on new urbanization), in which the maximum change of the relative contribution is -4% points (Meuse amont subbasins) while the average absolute change is as low as 1.3% points.

Finally, it is worth mentioning that the coarse resolution, 100 m², of the land use maps and the assumption that flow characteristics do not change with urbanization are two limitations of this study. Furthermore, it should be stressed that the results of the present research are specific to a given territory where existing urban zones are somehow concentrated in flood-prone zones. The results may differ in those places where urban settlements did not initially develop along water channels. Nonetheless, we believe that the main findings of this research are significantly relevant contributions to sustainable flood risk management that pave the way for more flood-proof and resilient spatial planning. One of the significantly relevant of the current study for urban planners is that a spatial planning policy oriented towards densification without expansion should be accompanied by strict restriction measures in flood-prone zones to mitigate exposure to future flood risks.

5.5. Conclusions

This research investigated the effects of different spatial planning policies on future flood risks in Wallonia (Belgium), for flood discharges corresponding to return periods of 25, 50 and 100 years. A number of future urban patterns were generated with a spatial ABM considering several factors. This model simulated both urban expansion and densification process. By means of a sensitivity analysis, we showed the importance of considering urban density and not just binary data (urban/nonurban) in the estimation of flood damage.

The uncertainty related to the demand for future urban development strongly influenced the computed flood damages and on their spatial distribution. Without considering any ban on urban development in flood-prone zones, the increase in total flood risk varies by a factor of approximately two depending on the urbanization scenario. Quite importantly the sensitivity of the computed rise in flood damage to the spatial planning policy (BAU vs. densification) is shown to be much higher than to the demand rate. This highlights that spatial policies may have a substantial influence on future flood risk, even for a fixed demand rate.

For the future time horizons 2030 to 2100, the increase in flood risk is expected to be between 5.5% and 11% per decade compared with the current situation. Banning new developments in flood-prone zones would enables a strong reduction of expected increases. They would be reduced by a factor of 3 with a ban on new developments in flood-prone zones 3 (high flood hazard) and to values lower than 1% with an extension of the ban to other flood-prone zones, regardless of the spatial planning policy.

5.6. Key contributions

- The estimation of flood damage may be overestimated by 48% to 105% when models do not take into consideration urban densities.
- There is a sufficient area in low and medium urban density classes to accommodate the future demand of urban development up to 2100.
- Without flood management policies, the increase in total flood risk by 2100 varies by a factor of approximately two.
- The sensitivity of the flood risk to the urbanization policy (business-as-usual vs. densification) is shown to be high which highlights that the spatial policies may have a substantial influence on future flood risk, even for a fixed urbanization rate.

Chapter 6: Influence of Urban Layout on Inundation Flow in Floodplains of Lowland Rivers

6.1. Introduction[1]

The natural advantages of the floodplain and the trend towards urban densification and expansions has fomented that floodplain development continued apace, regardless of potential planning policies to control these factors (Moel and Aerts, 2010; White, 2008). Referring back to chapter 5, implementing a densification policy at the regional level would mean that many of new urban areas should be located within flood-prone areas. Consequently, the potential damage as a result of floods will continue to rise. Within this context, digitally-enhanced urban design has the potential to construct flood resistant urban layouts. Our approach is concerned with accommodating the unavoidability of floods through modifications to urban and architectural design.

Urban layout modeling has shown its research value in understanding, predicting and/or controlling effects of shape on many urban concerns such as urban planning (e.g. Vanegas et al., 2012; Weber et al., 2009), urban vehicular traffic (e.g. Garcia-Dorado et al., 2014; Sewall et al., 2011), crowd simulation (e.g. Feng et al., 2016), urban weather simulation (e.g. Garcia-Dorado et al., 2017) and water/fluid simulations (e.g. Bridson, 2015; Enright et al., 2002). Within this urban context, researchers and designers pay a lot of attention to flood mitigation. In this research, we establish a link between geometric urban layout design and urban flooding and assist in designing improved flood-sensitive cities. Table 6.1 lists some of existing tools simulate either fluid simulation or geometric modeling. Our key motivation is to create a procedural generation system that automatically generates 3D urban layouts that consider the influence of geometric urban characteristics (e.g. road width, orientation, and/or curvature) on flow properties during flood water simulations.

[1]This chapter is based on:
Bruwier, M., Mustafa, A., Aliaga, D. G., Archambeau, P., Erpicum, S., ... Dewals, B. (2018). Influence of urban pattern on inundation flow in floodplains of lowland rivers. *Science of the Total Environment*, 622-623, 446–458.
Mustafa, A., Wei Zhang, X., Aliaga, D. G., Bruwier, M., Nishida, G., Dewals, B., Teller, J. (under review). Procedural generation of flood-sensitive urban layouts. *Environment and Planning B: Urban Analytics and City Science*.

Table 6.1: Existing computer graphics tools simulate fluid simulation or geometric modeling.

	Parameter
Fluid simulation	Bridson (2015)
	Losasso et al. (2004)
	Enright et al. (2002)
Geometric modeling	Forward procedural modeling
	Vanegas et al. (2009)
	Müller et al. (2006)
	Inverse procedural modeling
	Demir et al. (2015)
	Vanegas et al. (2012)

The urban layout influences the distribution of water discharges between roads as well as the flow depths and velocities. In a sense, we explore urban geometric grammars that help reduce flooding: i.e. what urban design rules produce passive barrier against natural floods? Our methodology is concerned with accommodating the unavoidability of floods by pre-emptive modifications to urban design. Designing and evaluating different urban layouts in terms of flood damage requires considerable time and resources. Any effort to reduce the design time or required resources is a profitable investment.

In this study, we represent an urban area by dividing it into representative cells, typically 1×1 kilometers. For each cell, we define a parameterized procedural model that can generate a wide range of possible urban layout configurations which mimic actual real-world urban patterns. Thereafter, a porosity-based hydraulic model computes the water flow characteristics of a proposed urban layout cell.

6.1.2. Previous work

Our work builds on flood flow modeling within urban areas as well as forward and inverse procedural modeling. Three dimensional models have been employed for assessment and visualization of urban flood flow and characteristics. Mioc et al. (2012) used observed data to generate 3D city models and integrates it with an inundation model. This integrated model helps city managers determine unsafe buildings and infrastructure in case of flooding. Amirebrahimi et al. (2016) proposed an integrated framework to measure flood damage to buildings based on a detailed 3D building information model. More related to our work is the work proposed by Christensen (2016) who introduced a dynamic approach to understanding the effect that natural disaster emergencies can generate in urban areas, with a particular emphasis on flooding events in residential areas. This approach also enables the end-user to simulate multi-scenarios based on different flood or water levels and to evaluate the impact of policy or structural interventions on reducing flood damages using an interactive interface. However, the objective disregarded the impact of urban layout configurations on flood damage. Lin et al. (2016) and Vollmer et al. (2015) investigated the interactions between urbanization and inundation flow for the rehabilitation of

Ciliwung River in Jakarta, Indonesia. The inundation extent and water depths were compared between different rehabilitation scenarios to identify the most effective one to mitigate floods. Since the authors considered rehabilitation scenarios specific to their case study, their conclusions are difficult to generalize to other urban areas. Huang et al. (2014) studied the impact of built-up coverage on the increase of water depths for a rectangular flume with an array of aligned buildings obstructing the flow. They proposed a method to update the Manning's roughness coefficient according to the blockage effect of buildings but consider only one urban characteristic (i.e., coverage) of an idealized urban network.

Prior literature on geometric urban modeling for flood-sensitive urban areas has tended to focus on architectural design and general site layout recommendations (e.g. Lennon et al., 2014; Watson and Adams, 2010; White, 2008). The adaptation measures presented in this literature include usage of wet-proofing, construction based on elevated ground, building on stilts, using temporal flood defenses, increasing urban green areas and increasing the distance between buildings and water bodies (Mustafa et al., 2015b). Existing literature did not make a comprehensive analysis to identify the relationship between urban layout parameters and flood damage such as geometrical arrangement of road network, parcels, and buildings. Nonetheless, computational approaches such as ours can play a distinctive role in urban geometric design and flood damage assessment.

There are already existing models that enable urban designers to procedurally alter and explore urban configurations. An in-depth review of urban procedural modeling can be found in Smelik et al. (2014) and Vanegas et al. (2009). Parish and Müller (2001) introduced a system to model cities using a procedural approach based on L-systems. Aliaga et al. (2008) proposed an interactive example-based approach that synthesizes urban patterns based on procedural modeling and image-based modeling. Vanegas et al. (2009) tackled an interdisciplinary research problem which considers modelling of behavioral and geometrical aspects of cities interactively. Yang et al. (2013) applied an optimized hierarchical splitting method to design urban layout automatically and interactively. Vanegas et al. (2012) proposed an inverse procedural system that enables interactively editing urban procedural models.

Compared to previous work, we present a more systematic analysis to determine the respective influence of various urban planning characteristics on inundation water depths. We followed a three-step procedure. First, we used an urban procedural model to generate 2,000 quasi-realistic building layouts by varying randomly the values of 10 urban model parameters: average street length, street orientation, street curvature, major and minor street widths, parks coverage, mean parcel area and building setbacks (i.e. distance from a building to the parcel borders).

Second, we computed the inundation flow field for each building layout by considering the same hydraulic boundary conditions. To make the hydraulic computation tractable for the 2,000

synthetic urban configurations, we used sub-grid models which enable a reduction of the computational cost thanks to a coarsening of the computational grid while preserving the essence of the detailed topographic information. We opted for an anisotropic porosity model, in which fine scale topographic information are preserved at the coarse scale by means of porosity parameters involved in the governing equations (Sanders et al., 2008).

Finally, the influence of urban characteristics on the computed water depths were analyzed based on multiple linear regressions (MLR) and on Pearson correlation coefficients. Additionally, a conceptual model was developed to investigate the relationships between the inundation water depths and district-scale storage and conveyance porosity parameters, evaluated as a combination of the urban characteristics. The results show a good predictive capacity of the model based on just the two porosity parameters, with a prevailing influence of district-scale conveyance porosity. Hence, this model allows for quantifying to which extent flood-related impacts of an increase in the building coverage (i.e. new developments) can be mitigated by an appropriately chosen layout of the buildings.

In the present analysis, we decided to keep the terrain slope equal to zero and to consider just one steady flooding scenario so as to focus on the influence of the urban planning characteristics. Therefore, the conclusions do not apply for floodplains involving steep slopes; but are instead representative of floodplains of lowland rivers which are flooded gradually and with moderate flow velocity. The steady flow conditions considered here are a valid representation of long duration floods (e.g., in lowland rivers such as the Rhine or the Meuse); but not for short duration floods in steep rivers nor for flash flood events.

6.2. Method

As sketched in the flowchart of Figure 6.1, we setup a three-step methodology to analyze the influence of the building layout on inundation flow:

- first, procedural modelling was used to generate about 2,000 synthetic urban layouts considering ten input parameters, including typical street length, width and curvature, mean parcel area, setbacks … (section 6.2.1);
- second, by means of a porosity-based hydraulic model, the flow characteristics were computed for each urban layout, considering identical hydraulic boundary conditions (section 6.2.2); and
- finally, based on Pearson correlation coefficients and on multiple linear regression, we highlight the sensitivity of inundation flow to the input parameters (section 6.2.3).

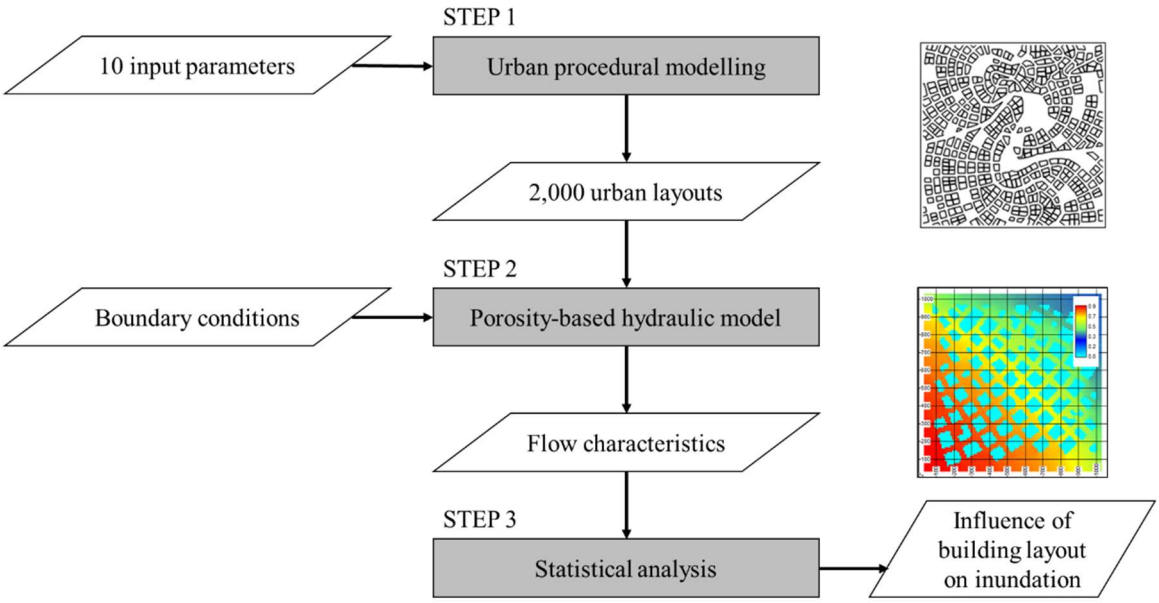

Figure 6.1: Methodology for the determination of the influence of building layout on inundation characteristics.

6.2.1 Parameterized urban model

We represent an urban layout using a parameterized procedural model. While cities can occupy hundreds of square kilometers (e.g, a typical European city is 180 km² in area (Eurostat, 2012)), we are only concerned with the part of a city near a river. Since the search space of all possible urban patterns is quite large, our procedural tool 1) divides the urban area into grid cells and provides design guidelines for each cell, and 2) reduces complexity by generating urban layouts based on a few number of rules and parameters (i.e., 12 parameters). Our system also enables users to import and export typical GIS data which facilitates migrating the system's outcomes into a wide range of GIS software.

Generation

Our procedural generation system is inspired by Parish and Müller (2001), Vanegas et al. (2009) and CityEngine (from ESRI). The system first generates roads, then parcels, and finally buildings. Roads are divided into a two-level hierarchy (i.e., major and local roads). While Chen et al. (2008) requires the user to manually draw some curves as constraints to determine the road network patterns, we use several parameters to automatically generate two orthogonal major roads outwards from an initial location. The initial radially-outward direction is called the h-direction and its perpendicular is called the v-direction. We adapt the tensor field approach Chen et al. (2008) as it supports a wide variety of road network patterns. The major roads are used as constraints to construct the tensor field. The next step is to take each area surrounded by roads, called a block,

and subdivide them into parcels, define parks, decide where to place buildings, and instantiate 3D building envelopes.

Parameters

Altogether, our procedural model is controlled by a 12 dimensional parameter vector. These parameters are selected according to a literature survey of common parameters involved in previous studies (e.g. Aliaga et al., 2013; Sarralde et al., 2015; Vanegas et al., 2012). In the following, we describe each parameter (Figure 6.2):

- average road length L_s-- the distance between two adjacent intersections,
- road orientation α-- orientation of the initial radially-outward road relative to lower-left corner,
- road curvature X-- rotation of a road segment when it passes through an intersection,
- major road width W, and
- minor roads width w.

Parcels are defined based on a recursive subdivision of oriented bounding boxes (OBB) fit around each city block, as in Vanegas et al. (2012). Parcels are controlled by the following parameters:

- average parcel area A_p, and
- percentage of parcels selected as parks P_c.

Buildings are generated with the following parameters:

- minimum number of floors F_{min},
- maximum number of floors F_{max} and
- front S_f, rear S_r, and side S_s building setbacks.

The variance of the input parameters representative of real-world locations are obtained by inspecting the cadastral data for a random sample of 500 sites of 1 km × 1 km of Wallonia (Belgium). Table 6.2 lists a summary of these findings.

By randomly selecting parameter values in their respective ranges of variation, we generated 2,000 urban layouts, covering each a square area of 1 km × 1 km. In Table 6.2, the minimum value of the side setback is 1 m. Therefore, configurations with a free space enclosed within a building (S_s = 0) are not considered. However, the findings of this study can be extended to these specific urban layouts by increasing the built-up coverage to reproduce the lack of access of the flow to the enclosed free-spaces.

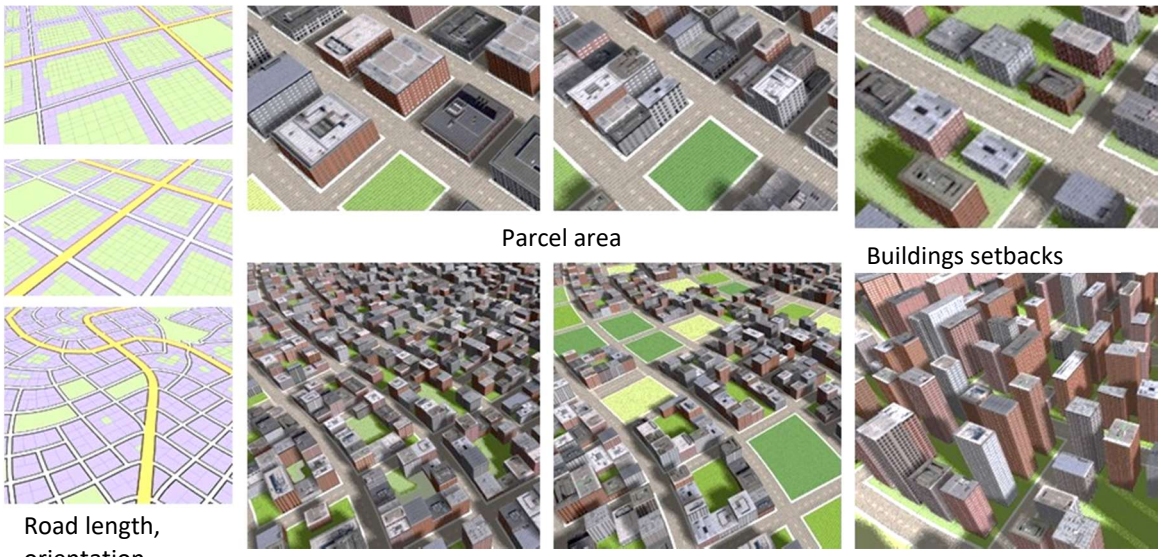

Figure 6.2: Urban Procedural Parameters

Table 6.2: Input parameters for the parameterized urban model engine.

	Parameter	Min Value	Max Value
L_s	Average street length	40 m	400 m
α	Road orientation	0°	180°
X	Road curvature	0 rad.	0.42 rad.
W	Major road width	16 m	34 m
w	Minor road width	8 m	16 m
P_c	Park coverage	5%	40%
A_p	Average parcel area	300 m^2	1,100 m^2
S_f	Building front setback	0 m	5 m
S_r	Building rear setback	0 m	5 m
S_s	Building side setback	0 m	5 m

Only the building footprints have an influence on the performed hydraulic computations. This enables merging some of the parameters listed in Table 6.2. For instance, parameters W (or w) and S_f should not be considered independently. Indeed, urban layouts characterized by distinct values of the street width W (or w) and front setback S_f, but with the same value of the sum $W + 2\,s_f$ (or $w + 2\,s_f$) would lead to the same distance between the buildings located on either sides of a street. This distance should be retained as the parameter which actually controls the flow conveyance through this street, instead of W (or w) and S_f independently. Therefore, although the parameters listed in Table 6.2 are the real inputs of the procedural system, we performed the statistical analysis of the results by considering a slightly modified set of variables (Table 6.3):

- Parameters W, w and S_f were replaced by just two variables: $x_4 = W + 2\,s_f$ and $x_5 = w + 2\,s_f$.
- To account for the periodicity in the street orientation resulting from the symmetry of the domain and boundary conditions, the orientation parameter α was replaced by variable $x_2 = \left|\sin\left(2\left(\alpha - 45°\right)\right)\right|$ (Figure 6.3).

- The park coverage P_c was not kept alone; but lumped into an overall *built-up coverage* ratio x_9, evaluated as the ratio between the total area of building footprints and the area of the whole district (1 km^2). Variable x_9 is a function of all input parameters.
- All other variables were each kept equal to one of the original input parameters listed in Table 6.2.

Table 6.3: Variables used for the statistical analysis of the modelling results.

Variable definition	Minimum	Maximum
$x_1 = L_s$	40 m	400 m
$x_2 = \left\|\sin\left(2\left(\alpha - 45°\right)\right)\right\|$	0	1
$x_3 = \chi$	0 km^{-1}	10 km^{-1}
$x_4 = W + 2\ s_f$	18 m	38 m
$x_5 = w + 2\ s_f$	10 m	21 m
$x_6 = A_p$	350 m^2	1,100 m^2
$x_7 = s_r$	1 m	5 m
$x_8 = s_s$	1 m	5 m
$x_9 = f(L_s, \alpha, \chi, W, w, P_c, A_p, s_r, s_f, s_s)$	0%	43%

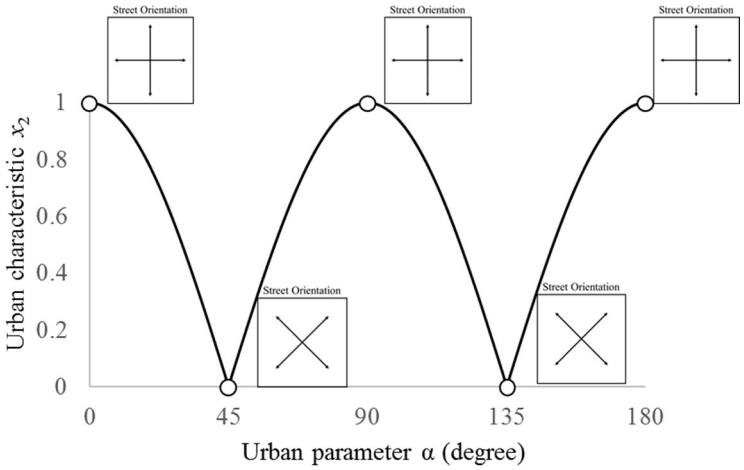

Figure 6.3: Relation between variable x_2 and street orientation parameter α.

6.2.2. Porosity-based hydraulic modelling

In the second step, we applied a hydraulic model to compute the flow characteristics for each of the 2,000 building layouts, under the same hydraulic boundary conditions. The terrain was assumed horizontal and infiltration in the soil was neglected because it has a limited influence on river flooding in urbanized floodplains.

Model description

Two-dimensional shallow-water hydraulic models are considered state-of-the-art for the simulation of inundation flow in urban areas (Abderrezzak et al., 2009; Ghostine et al., 2015). In such model, the buildings are idealized as impervious obstacles sufficiently high for not being overtopped by the flood. In general, three approaches can be considered to account for obstacles

in inundation modelling (Dottori et al., 2013; Schubert and Sanders, 2012): (*i*) increasing the roughness parameter, (*ii*) representing the obstacles as holes in the mesh or (*iii*) using a porosity-based model. The first one is particularly crude and requires calibration on a case-by-case basis. In the second one, each building needs to be explicitly resolved in the computational mesh, which makes this approach not suitable to investigate efficiently the 2,000 building layouts. In contrast, Schubert and Sanders (2012) showed that porosity-based models lead to the best balance between accuracy and run-time efficiency. They enable a coarsening of the mesh size by roughly one order of magnitude while preserving a good level of accuracy (Bruwier et al., 2017a; Kim et al., 2014, 2015; Özgen et al., 2016b; Schubert and Sanders, 2012). Therefore, we opted here for this third option.

The shallow-water model with porosity used here was described in section 5.2 of Arrault et al. (2016) as well as in Bruwier et al. (2017a) and a comprehensive validation is presented in Bruwier et al. (2017b). It involves two types of porosity parameters: a storage porosity, defined at the center of each cell, represents the void fraction in the cell while anisotropic conveyance porosities, defined at the edges of the computational cells, reproduce the blockage effect due to obstacles (Chen et al., 2012; Özgen et al., 2016a; Sanders et al., 2008). The values of these porosity parameters were determined geometrically from the building footprints.

The momentum equations involve the same drag loss term as in the formulation of Schubert and Sanders (2012). The drag coefficient c_D was set to the standard value $c_D = 3.0$. Bottom friction is modelled by Manning formula with a uniform roughness coefficient $n = 0.04$ sm$^{-1/3}$. This value of the roughness coefficient is comparable with the values suggested by Mignot et al. (2006) to account for the various sources of flow resistances in urban areas such as bottom friction and small scale obstacles (debris, cars, urban furniture, etc.).

The numerical discretization is based on a conservative finite volume scheme and a self-developed flux-vector splitting (Erpicum et al., 2010b). We used a Cartesian grid with a grid spacing of 10 m, which is comparable to the typical size of the buildings (>15 m) but the porosity parameters enable the fine-scale geometric features to be accounted for.

To enhance computational efficiency in the presence of low values of the storage porosity ϕ, we used a merging technique which consists in merging each cell having a low value of storage porosity ($\phi < \phi_{min} = 10\%$) with a neighboring cell (Bruwier et al. 2017a).

As detailed in Arrault et al. (2016) and Bruwier et al. (2017a, b), the model was successfully validated against fine scale computations and against experimental data for flow conditions similar to those prevailing here. The model is part of the academic code Wolf2D which was used in multiple flood risk studies (Beckers et al., 2013; Bruwier et al., 2015; Ernst et al., 2010).

6.2.3. Statistical analysis

The outcome of steps 1 and 2 of the methodology (Figure 6.1) consists in a set of 2,000 gridded flow characteristics data, representing the water depth and the two components of horizontal flow velocity in the 10,000 cells of the computational mesh. To make the subsequent analyses tractable, we synthetized the dataset by means of a single indicator *y* of flood severity for each of the 2,000 building layouts. We focused on the increase of the 90th percentile of the computed water depths along the upstream boundary of the domain (noted Δh_{90}) compared to a configuration without any buildings (h_{90} = 61 cm). This quantity is representative of the overall flow resistance (or loss of flow conveyance) induced by the layout of buildings and, hence, of the increase in flood levels that the presence of the buildings causes upstream of the considered area. If the buildings result from new development, indicator $y = \Delta h_{90}$ reflects the impact of this development on flood danger upstream.

We performed the statistical analysis of the results by considering standardized variables, noted $\overline{x_i}$ (*i* = 1 to 9) and $\overline{y}$, defined as:

$$\overline{x_i} = \frac{x_i - x_{i,\text{mean}}}{x_{i,\text{std}}} \quad \text{and} \quad \overline{y} = \frac{y - y_{\text{mean}}}{y_{\text{std}}} \tag{6.2}$$

with $x_{i,\text{mean}}$ and $x_{i,\text{std}}$ (resp. y_{mean} and y_{std}) the mean and standard deviation of the variable x_i (resp. *y*) over all the building layouts.

We introduce the matrix notations **X** and **Y** with $\overline{x_i}^N$ and $\overline{y}^n$ the values of $\overline{x_i}$ and $\overline{y}$ corresponding to the n^{th} building layout:

$$\mathbf{X} = \begin{bmatrix} \overline{x_1}^1 & \overline{x_2}^1 & \dots & \overline{x_9}^1 \\ \overline{x_1}^2 & \overline{x_2}^2 & \dots & \overline{x_9}^2 \\ \vdots & \vdots & \ddots & \vdots \\ \overline{x_1}^N & \overline{x_2}^N & \dots & \overline{x_9}^N \end{bmatrix} \quad \text{and} \quad \mathbf{Y} = \begin{bmatrix} \overline{y}^1 \\ \overline{y}^2 \\ \vdots \\ \overline{y}^N \end{bmatrix} \tag{6.3}$$

with *N* being the number of building layouts.

The influence of each of the nine variables x_i on the inundation indicator *y* was determined using a multiple linear regression (MLR). The outputs of the regression are the least square linear coefficients $\mathbf{A} = \left[a_1, a_2, ..., a_9\right]^T$, computed from Equation (6.4) and representing the sensitivity of *y* with respect to each variable x_i:

$$\mathbf{A} = \left(\mathbf{X}^{\mathrm{T}}\mathbf{X}\right)^{-1}\mathbf{X}^{\mathrm{T}}\mathbf{Y} \,. \tag{6.4}$$

We also used Pearson correlation coefficients ρ_i defined as:

$$\rho_i = \frac{\operatorname{cov}(x_i, y)}{x_{i,\text{std}}\ y_{\text{std}}} = \frac{1}{N-1}\sum_{k=1}^{N}\left(\frac{x_i^k - x_{i,\text{mean}}}{x_{i,\text{std}}}\right)\left(\frac{y^k - y_{\text{mean}}}{y_{\text{std}}}\right) = \frac{1}{N-1}\sum_{k=1}^{N}\overline{x}_i^k\,\overline{y}^k\ . \qquad (6.5)$$

6.3. Results

Although some urban layouts might not be represented accurately, our urban generation system supports a wide variety of typical urban layouts, which enables us to effectively find a desired layouts from an otherwise huge search space (Figure 6.4).

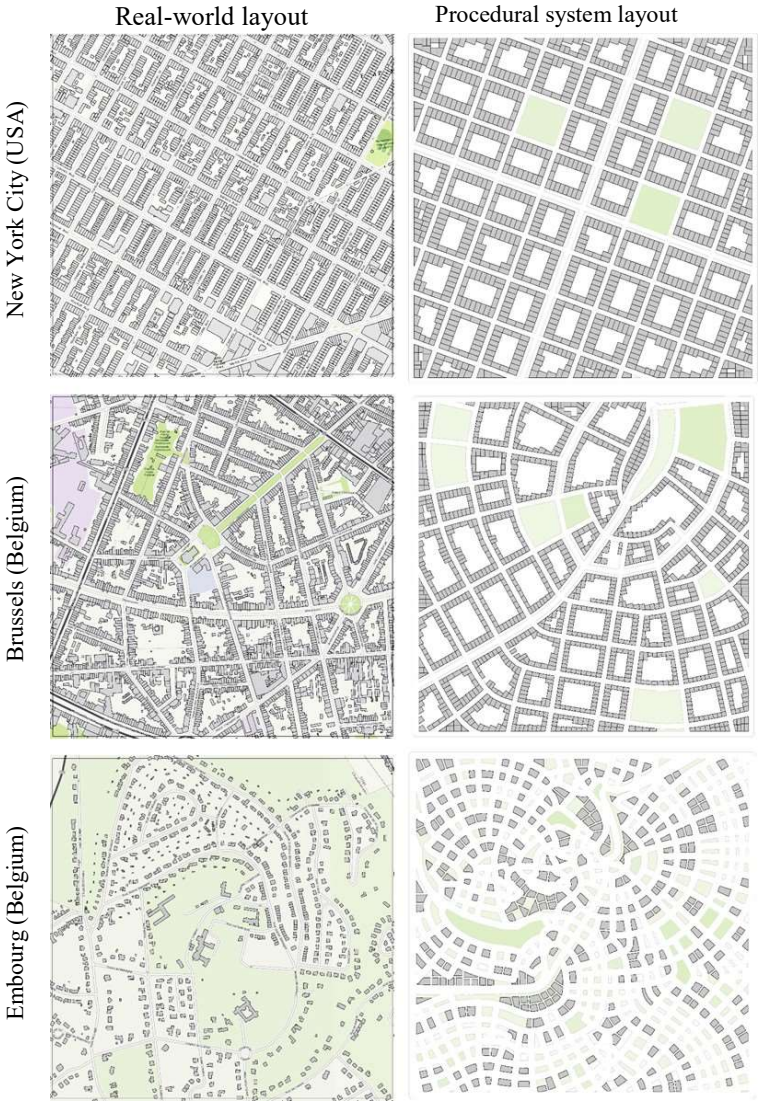

Figure 6.4 Real-world layouts versus procedural urban generator layouts.

Figure 6.5 illustrates six of the 2,000 generated urban layouts to enable the reader to appreciate the influence of the main input parameters (Tables 6.2 and 6.3). The variables x_1 to x_9 corresponding to the six layouts of Figure 6.5 are given in Table 6.4.

Layout (a) and (b) in Figure 6.5 correspond to the same input parameters, except for the average street length x_1 and street curvature x_3. In layout (a), the average street length is about 3.4 times

higher than in layout (b). This results in a more "fragmented" urban pattern in layout (b) compared to layout (a). Indeed, apart from the change in street curvature, layout (a) shows substantially larger building blocks than in layout (b). This observation also applies when layouts (c) and (d) are compared, as the average street length x_1 in layout (c) is almost three times higher than in layout (d). Layout (d) exemplifies an urban pattern characterized by a high value of the street curvature x_3. Comparing the urban layouts (c) with (d) also reveals that the mean parcel area x_6 has a significant influence on the size of the building footprints, as x_6 takes a value roughly three times larger in the case of layout (c) than for layout (d).

The street orientation (x_2) has a strong influence on the connectivity between the different faces. For instance, in layout (a) ($x_2 = 0$) the building alignment tends to guide the flow entering through the west (resp. south) upstream face towards the north (resp. east) downstream face. In contrast, layout (f) ($x_2 \approx 1$) seems to promote flow connection from the west (resp. south) upstream face towards the east (resp. north) downstream face.

The building rear setback x_7 is of little significance in our analysis as it mainly controls the distance between the back of the buildings and the limit of the corresponding plot of land. This distance has no direct influence on the flow computation. In contrast, the side setback x_8 plays a major part since it controls the distance in-between adjacent buildings and hence the possibility for water to penetrate inside a block of buildings. This is exemplified by building layouts (e) and (f). The side setback x_8 in the former layout is twice smaller than in the latter.

Table 6.4: Variables x_1 to x_9 (Table 6.3) characterizing the six building layouts displayed in Figure 6.5.

Conf.	x_1	x_2	x_3	x_4	x_5	x_6	x_7	x_8	x_9	h_{90}
a)	199 m	0	0.5 km^{-1}	28 m	18 m	500 m^2	3.0 m	3.0 m	13%	0.79 m
b)	59 m	0	1.7 km^{-1}	28 m	18 m	500 m^2	3.0 m	3.0 m	13%	0.74 m
c)	165 m	0.58	0.7 km^{-1}	35 m	15 m	1066 m^2	2.2 m	2.1 m	33%	1.02m
d)	57 m	0.15	3.9 km^{-1}	29 m	12 m	370 m^2	1.4 m	2.0 m	15%	0.75 m
e)	274 m	0.97	1.4 km^{-1}	28 m	11 m	880 m^2	2.5 m	2.3 m	26%	1.00 m
f)	293 m	0.97	0.5 km^{-1}	28 m	11 m	872 m^2	2.3 m	4.6 m	22%	0.86 m

6.3.1. Calibration and validation of the porosity-based model

The coarse model errors on the water depths are expected to be lower than 5% without any drag loss term while a reduction up to only 0.5% error can be obtained with an optimal calibration of the drag coefficient (Bruwier et al. 2017a). Based on very different urban layouts, it was shown that the range of variation of the optimal drag coefficient falls between 2.0 and 3.0 for the urban configurations considered in this study. Therefore, using a constant drag coefficient $c_{D,0}^{b} = 3.0$ for all computations, the coarse model error on the water depths should not exceed a few percent.

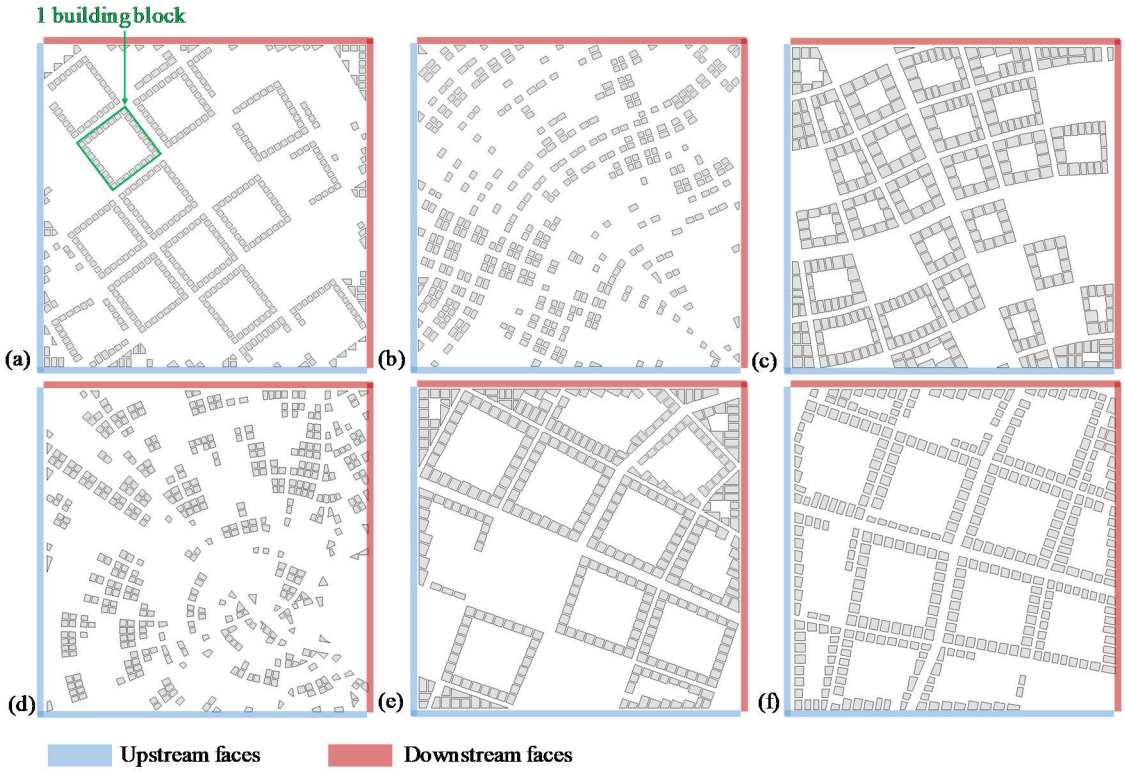

Figure 6.5: Building footprints for six out of the 2,000 layouts generated by procedural modelling.

Computed water depths and velocity fields

The results of the hydraulic simulations are 2D maps of computed water depths and velocity fields. Figure 6.6 shows examples of hydraulic modelling results for the building layouts (c), (d) and (f) defined in Figure 6.5. The white areas in the maps of Figure 6.6 correspond to holes in the computational domain, i.e. cells which are inactive because they are mostly included within a building and therefore excluded from the computation. For layouts (c) and (f), virtually all buildings are reproduced explicitly by holes in the computational domain and the porosity parameters enable to improve the geometric description of inclined boundaries. In contrast, much of the urban pattern of layout (d) is reflected only through the porosity parameters because in this case the buildings have a typical size comparable to the grid spacing. This results from the relatively low value of the mean parcel area x_6 in layout (d) (Table 6.4).

The computed water depths are minimum close to the downstream faces (north and east) and maximum along the upstream faces (west and south), due to the overall flow resistance induced by the buildings. The selected flood level indicator h_{90} along the upstream faces varies between 0.61 m and 1.14 m. Hence, for the tested configurations, varying the building layout may change the upstream flood level by a factor of almost two.

Overall, the flow remains relatively slow within the urban area, with a Froude number $F = ||\boldsymbol{v}|| / (g\,h)^{0.5}$ of the order of 0.1 ($||\boldsymbol{v}||$ represents the velocity magnitude). The maximum

value of F does not exceed 0.4. The velocity increases at local contractions. This is particularly visible in layout (f), which is characterized by a side setback x_8 more than twice larger than for layouts (c) and (d), enabling more intense flow exchanges between the streets and the void areas inside building blocks ("courtyards"). This is also remarkably shown by the higher flow velocity computed inside the building block in layout (f) (velocity magnitude ~ 0.20 m/s) compared to layout (c) (velocity magnitude ~ 0.1 m/s). This results also from the higher side setback value (x_8) in the former layout compared to the latter (Figure 6.5), making the void area within the building blocks more accessible to the flow in layout (f). The absolute velocities are high around the top-left and bottom-right corners where the flow avoids passing through the building area.

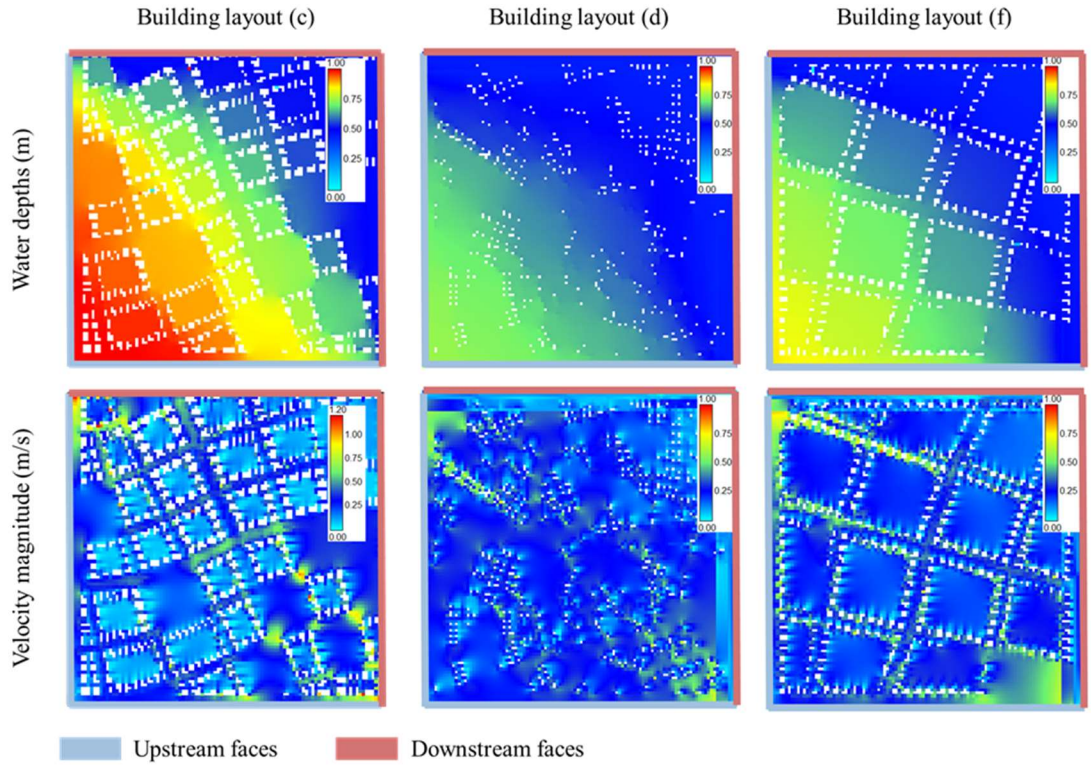

Figure 6.6: Representation of water depths and flow fields for some urban layouts.

6.3.2. Influence of urban characteristics on inundation water depths

Figure 6.7 shows the regression coefficients a_i computed with Equation (6.4) for an inundation indicator $y = \Delta h_{90}$ computed based on the 90th percentile of the computed water depths along the upstream boundaries of the domain. A positive value for a regression coefficient a_i indicates that an increase in the corresponding variable x_i leads to an increase in the water depths, and conversely for a negative value of the regression coefficient. Using the regression coefficients of Figure 6.7, the Δh_{90} values can be predicted with a mean absolute error and a root mean square error of, respectively, 2.3 cm and 2.9 cm. This represents less than 15% of the mean value of Δh_{90} (21.3 cm).

The results of the multiple linear regression (MLR) show that the built-up coverage (x_9) is by far the most influential urban layout design parameter. Besides the built-up coverage, the average street length (x_1) has also a substantial influence on the water depths, because it controls the size of the building blocks. As shown above, the lower the value of the average street length is, the more "fragmented" the urban layouts are. This contributes to avoid the creation of void areas surrounded by buildings, which are therefore not easily accessible to the flow. In a more fragmented urban pattern, a larger portion of void area contributes to the flow conveyance. Similarly, reducing of the building side setback (x_8) leads to higher water depths, due to the reduction of the conveyance capacity between adjacent buildings. This is consistent with the negative value obtained for coefficient a_8.

The increase in building size resulting from an increase in the mean parcel area (x_6) leads to higher water depths, as reflected by the positive value of a_6. The street orientation (x_2) and curvature (x_3) seem to have no significant influence on the water depths. This is certainly a result of the relatively low values of flow velocity in the considered urban area (F ~ 0.1), which are typical of lowland rivers. This finding is expected not to apply in the case of floodplains that are characterized by steeper topographic gradients, where the flow velocity would be higher and more dynamic effects would prevail.

The insignificant influence of the rear setback (x_7) can be explained by the weak influence of this variable on the flow conveyance since it mainly describes the void area within building blocks, which contribute anyway only very little to the overall flow conveyance through the urban area.

While the results of the MLR show no influence of the major street width (x_4) on the inundation water depths, a slight influence is shown for the minor street width (x_5). This should be explained by the high number of minor streets in the urban domain compared to only two major streets.

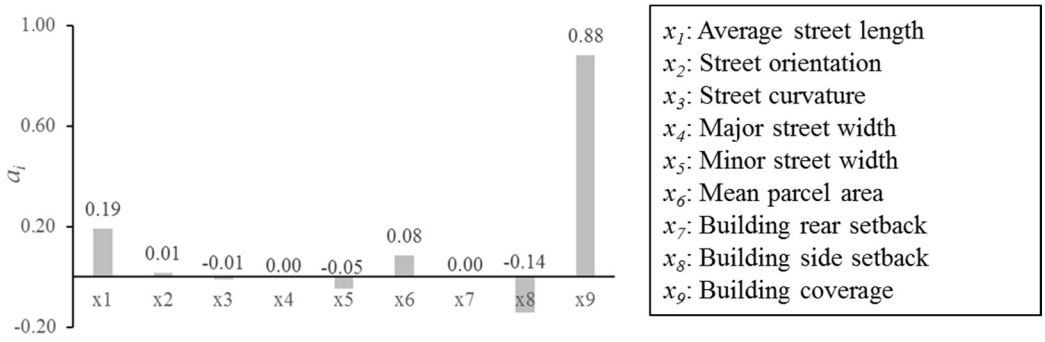

Figure 6.7: Regression coefficients α_i of the urban characteristics for Δh_{90}.

6.4. Discussion

The results are discussed here, based on a comprehensive sensitivity analysis (section 6.4.1) and by comparing them with those of a simple conceptual approach (section 6.4.2).

6.4.1. Sensitivity analysis

Indicator of inundation water depths

The performed analysis is based on the increase of the 90th percentile of the water depths computed along the upstream boundaries of the urban area: Δh_{90}. Here, we explore to which extent the conclusions of the analysis remain valid when another indicator of flood severity is chosen instead of Δh_{90}. In doing so, we repeated the analysis by considering percentiles from 50th to 90th with a constant step of 5th and these percentiles were evaluated either along the upstream boundaries of the domain, or throughout the whole domain.

In Figure 6.8-a, the sensitivity of the results of the MLR to the selection of the indicator of flood severity is shown through boxplots representing the variation of each coefficient a_i when all options described in section 6.3.2 are tested. This sensitivity remains low for all coefficients a_i. Coefficients a_1 and a_6 corresponding to the influence of the average street length (x_1) and the mean parcel area (x_6) show the highest sensitivity with values ranging respectively from 1.3×10^{-1} to 2.1×10^{-1} and from 1.0×10^{-2} to 8.3×10^{-2}. Nonetheless, the findings described in section 6.3.2 remain generally valid whatever the choice of the indicator of flood severity. Comparing Figure 6.8-b and Figure 6.8-c, the sensitivity of the results to the percentiles is higher when they are evaluated throughout the whole domain than along the upstream boundary.

Sample size

We investigated whether the sample size (2,000 building layouts) is large enough to produce robust and reliable results. For this purpose, we selected randomly 1,500, 1,000, 500 and 250 configurations out of the initial sample. For each sub-sample, the random selection was performed 10,000 times to assess the sensitivity of the results to the selected configurations.

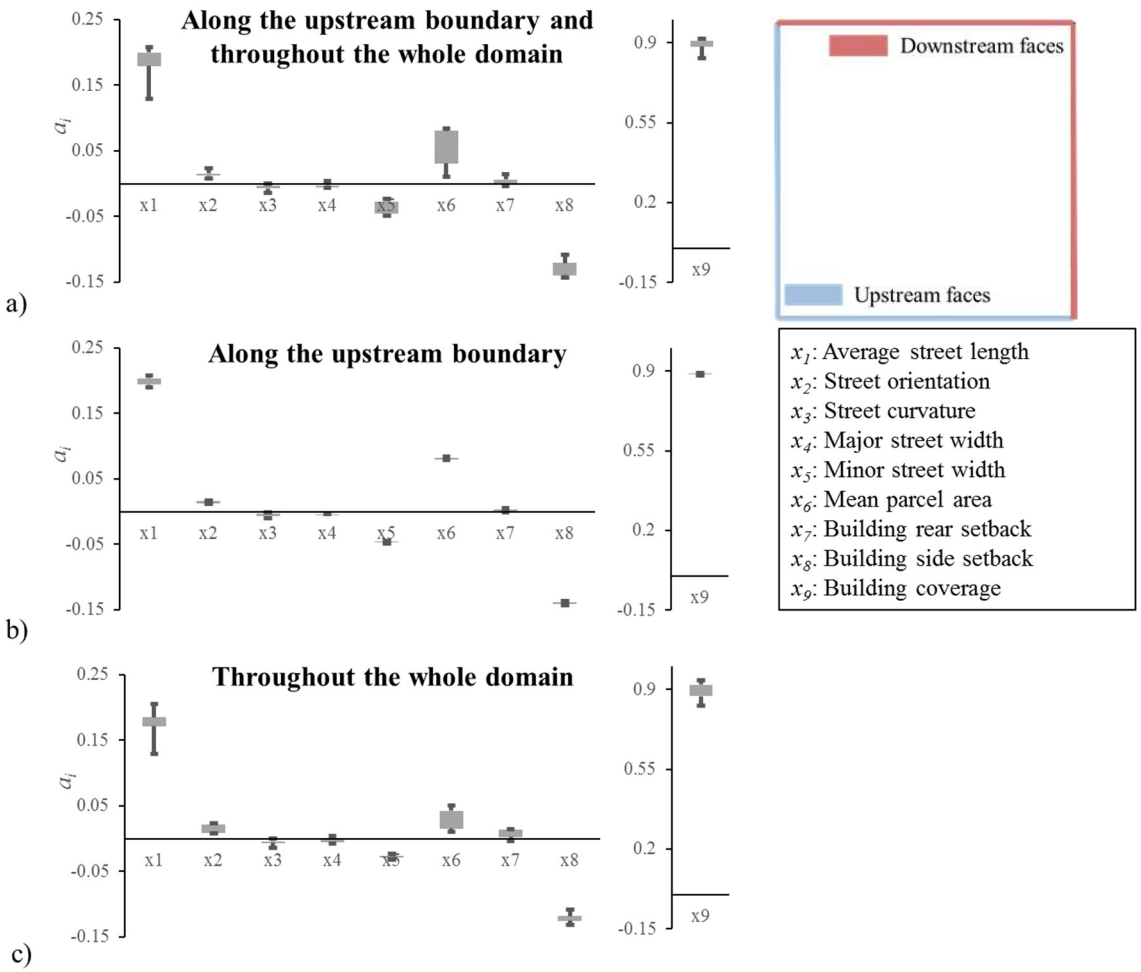

Figure 6.8: Sensitivity of the regression coefficients to choice of the indicator of flood severity by considering percentiles from 50th to 90th computed (a) either along the upstream boundaries of the domain, or throughout the whole domain and (b) along the upstream boundaries of the domain and (c) throughout the whole domain.

Similar to Figure 6.8, we display the results in the form of boxplots obtained from the sets of regression coefficients corresponding to the 10,000 different sub-samplings (Figure 6.9). Again, the findings of section 6.3.2 are hardly affected by a reduction of the sample size, at least when the subsample size remains above 1,000. In all cases, the most influencing urban characteristic remains the built-up coverage (x_9) and only variables x_1, x_5, x_6, x_8 and x_9 show a significant influence on the computed water depths. Even for a sample size lower than 1,000, most of the results remain consistent with the findings of section 6.3.2, and only few coefficients show substantial variations. Hence, the sample size of 2,000 different urban layouts is deemed sufficient.

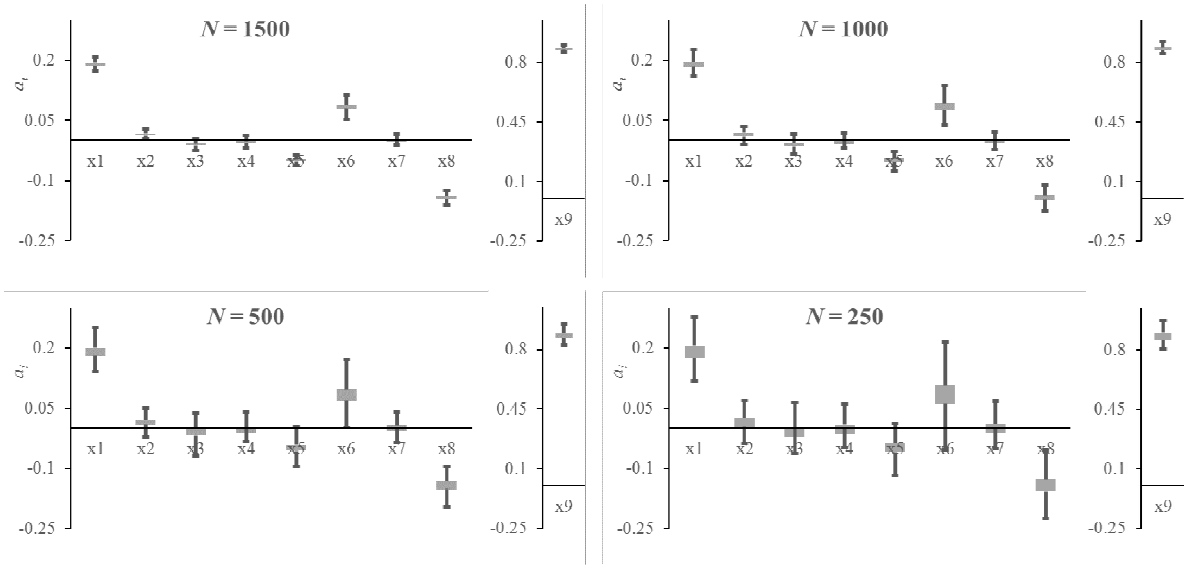

Figure 6.9: Sensitivity of the absolute values of the regression coefficients of the urban characteristics for Δh_{90} to the sample size (N).

Number of urban characteristics used in the regression analysis

The respective influence of each of the nine selected urban characteristics on the computed water depths was shown to be very different, suggesting that some of the urban characteristics could be neglected in the regression analysis. Here, we compare the predictive capacity of regressions based either on all urban characteristics (variables x_1 to x_9) or just on the most influential ones. The predictive capacity of each regression is assessed through the resulting root mean square error. Using only the built-up coverage (x_9) for the linear regression leads to a root mean square error roughly 37% higher than with the MLR based on all variables (Table 6.5). The prediction of Δh_{90} based on the five most influential variables (x_1, x_5, x_6, x_8 and x_9) gives an accuracy similar to the one obtained with all nine variables.

Table 6.5: Root mean square errors on the estimation of Δh_{90} for sets of urban characteristics used in the MLR.

Considered variables	x_9	x_1, x_5, x_6, x_8 and x_9	x_1 to x_9
Root mean square error (cm)	4.01	2.93	2.93

Model choice

In all analyses above, a linear relationship was assumed between the rise in water depth $y = \Delta h_{90}$ and variables x_1 to x_9:

$$\overline{y} = a_0 + \sum_{i=1}^{9} a_i \overline{x}_i \tag{6.6}$$

Here, we check whether our findings are affected by the choice of another model. For this purpose, we tested two approaches:

- First, we used an alternate model, assuming that Δh_{90} can be predicted by means of a power law involving all parameters x_1 to x_9:

$$\frac{y}{y_{\text{mean}}} = b_0 \prod_{i=1}^{9} \left(\frac{x_i}{x_{i,\text{mean}}} \right)^{b_i} , \tag{6.7}$$

  in which b_0 to b_9 are coefficients to be calibrated. Coefficients b_i certainly do not take the same values as parameters a_i; but still their relative values provide an indication on which of the variables x_i have more influence on the determination of Δh_{90}.

- Second, we computed *Pearson correlation coefficients* ρ_i, which also reflect the link between variables, but it does so independently of the choice of a particular model.

In practice, the estimation of coefficients b_i in Equation (6.7) is performed by means of a MLR, after applying a logarithmic transformation to variables x_i and y:

$$\ln\left(\frac{y}{y_{\text{mean}}} \right) = \ln b_0 + \sum_{i=1}^{9} b_i \ln\left(\frac{x_i}{x_{i,\text{mean}}} \right). \tag{6.8}$$

The configurations involving a street orientation (x_2) equal to zero were disregarded; but they represent only 2.5 % of all building layouts in the sample.

Coefficients a_i, b_i and ρ_i are compared in Figure 6.10. Each set of coefficients has been scaled so that the sum of the nine absolute values is one. The following observations can be made.

- In all three approaches, variables x_9 is shown to have a substantial influence on, or be strongly correlated with, the flood severity indicator Δh_{90}. The prevailing influence of the built-up coverage is therefore a robust outcome of the analysis.

- A major difference between different approaches is the mean parcel area, x_6. On the one hand, the Pearson correlation approach indicates the same importance level for both x_6 and x_9, mean parcel area and built-up coverage. On the other hand, x_6 shows much lower magnitude than x_9 in both standard MLR and MLR with logarithmic transform. This difference may result from the existing positive correlation between x_6 and x_9, as revealed in Figure 6.11. Given this correlation, the lower weight assigned to x_9 by the Pearson correlation compared to the standard MLR is simply compensated by a higher weight assigned to x_6.

- In all approaches, the coefficients assigned to the minor street width (x_5) and the building side setback (x_8) are consistently negative and of substantial magnitude. This confirms that considering variables x_5 and x_8 as strongly controlling the flow through the urban area is a robust outcome of the analysis.

- Likewise, the coefficients associated with the major street width (x_4) and the building rear setback (x_7) take consistently negative values of small magnitude, while those related to

x_2 (street orientation) are also consistently small but positive. Therefore, these variables may safely be disregarded, as shown also in Table 6.4.

- The regression coefficients related to the average street length (x_1) and the street curvature (x_3) (a_1, a_3 and b_1, b_3) have an opposite sign compared to the corresponding Pearson correlation coefficients (ρ_1 and ρ_3). This is a result of the significant negative correlation between x_1 and x_3, as revealed in Figure 6.11. Although this correlation makes sense from an urban planning point of view, as a stronger street curvature implies more short streets in the inner area of the curved streets, it somehow hampers drawing truly robust conclusions on the relation between the street length and the upstream flood severity.

- Another interesting finding obtained from the Pearson regression coefficients is that several variables have a similar importance to x_9, while according to the standard MLR and the MLR with logarithmic transform, only x_9 seemed to be of prevailing influence. This result is consistent with those presented in the next section, which indicate that the built-up coverage is of lower importance than another composite indicator of flow *conveyance* at the scale of the urban area (district-scale), while x_9 is *stricto sensu* a proxy for the *storage* capacity (and not the conveyance capacity) in the urban area.

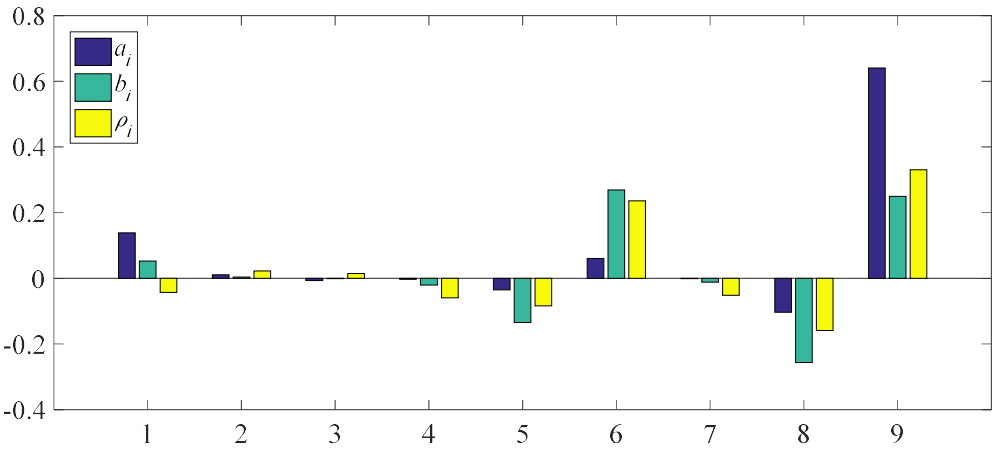

Figure 6.10: Comparison of regression coefficients α_i and b_i obtained from multiple linear regression, without and with logarithmic transform, and with Pearson correlation coefficients ρ_i. Each set of coefficients has been scaled so that the sum of the nine absolute values is one.

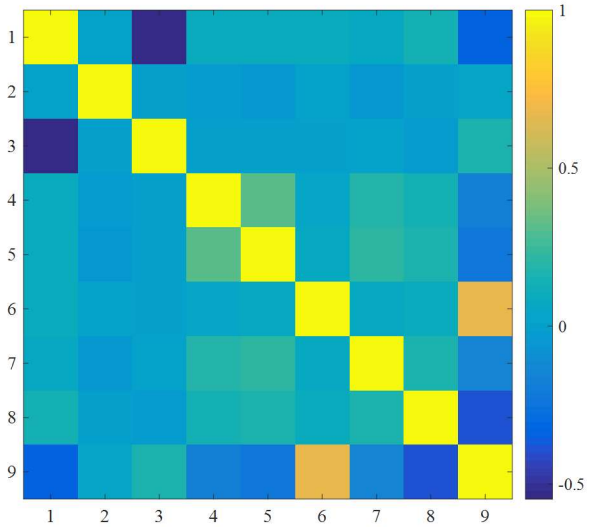

Figure 6.11: Pearson correlation coefficients between all variables x_1 to x_9.

6.4.2. Conceptual approach

The set of input variables x_1 … x_9 were selected for their significance in terms of urban planning. However, as such, they are neither optimal for statistical analysis (Figure 6.10) nor of direct relevance for hydraulic analysis. Therefore, we present here a simple conceptual model which relates these urban planning parameters to just two parameters of direct relevance for hydraulic analysis: a district-scale storage porosity Φ_D, and a district-scale conveyance porosity Ψ_D.

The district-scale storage porosity is straightforward to evaluate from the built-up coverage $(\Phi_D = 1 - x_9)$, while the district-scale conveyance porosity was estimated based on an idealization of the geometry of the considered urban layouts. Despite a number of simplifying assumptions, we show that these two district-scale porosity parameters well explain the results obtained in section 6.3 for the whole set of 2,000 quasi-realistic urban layouts.

Conceptualization

First, we aim to derive an expression relating the district-scale conveyance porosity Ψ_D to the input parameters of relevance for urban planning. To do so, we introduce the following simplifying assumptions, which enable obtaining analytical expression for Ψ_D (Figure 6.12):

- the street orientation and curvature are neglected ($\alpha = \chi = 0$), so that all streets are straight and aligned either along the west-east direction or the north-south direction;
- these streets are separated by building-blocks of identical size;
- the size of a building-block is given by the average street length L_s;
- all minor (resp. major) streets have the same width equal to w (resp. W);
- each building-block is split into several identical square parcels of length equal to the square root of the mean parcel area A_p;

- the size of a building is determined from the parcel area and the three setbacks s_f, s_r and s_s;
- we estimate the conveyance porosity as the minimum void fraction in a section normal to the west-east direction (as if the flow as aligned with this direction).

Consistently with our procedural modelling, the idealized urban layouts considered here also comply with the following rules:

- one single major street is introduced in each direction;
- only the external parcels of the building-blocks are urbanized while the others remain undeveloped.

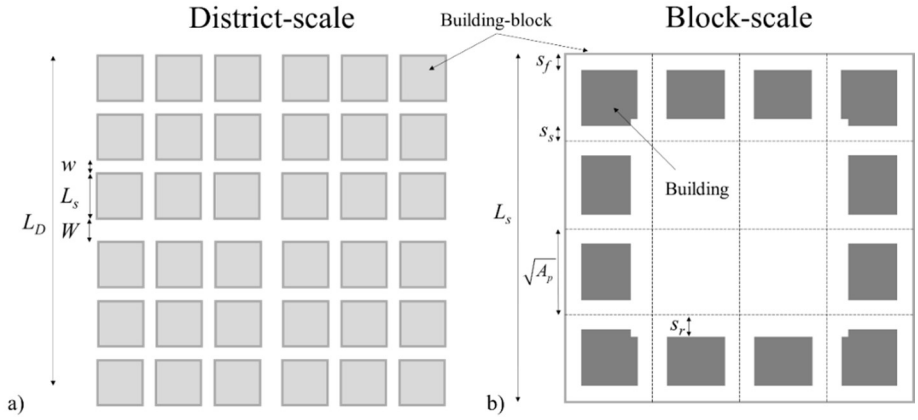

Figure 6.12: Idealized urban pattern at the district-scale (a) and block-scale (b).

Under these simplified assumptions, the number n of building-blocks over the length L_D of the urban area can be derived from the urban parameters by:

$$L_D = (n-2)(L_s + w) + 2\left(L_s + \frac{w+W}{2}\right) \quad \Rightarrow \quad n = \frac{L_D - (W - w)}{L_s + w} \quad . \tag{6.9}$$

The number n_b of buildings (or parcels) over the length L_s of a building-block is simply equal: $L_s / \sqrt{A_p}$.

The block-scale conveyance porosity Ψ_B is estimated as the ratio between the minimum free length along the north-south or east-west direction and the total length of the building-block L_s:

$$\Psi_B = \left(\frac{L_s}{\sqrt{A_p}} - 2\right)\frac{2s_s}{L_s} + 2\frac{s_s + s_f}{L_s} \Rightarrow \Psi_B = 2\left(\frac{s_s}{\sqrt{A_p}} + \frac{s_f - s_s}{L_s}\right). \tag{6.10}$$

Similarly, the district-scale conveyance porosity Ψ_D is computed as:

$$\Psi_D = (n-2)\frac{\Psi_b L_s + w}{L_D} + 2\frac{\Psi_b L_s + \frac{W+w}{2}}{L_D} \quad (6.11)$$
$$\Rightarrow \Psi_D = \frac{\Psi_b L_s + w}{L_s + w} + \frac{w}{L_D}\left(\frac{W}{w} - 1\right)\left(1 - \frac{\Psi_b L_s + w}{L_s + w}\right)$$

Results

Based on the district-scale storage and conveyance porosities, Φ_D and Ψ_D, a regression analysis was performed as follows:

$$\Delta h_{90} = a\,(1-\Phi_D)^b\,(1-\Psi_D)^c \quad (6.12)$$

Since $\Delta h_{90} = 0$ for $\Phi_D = \Psi_D = 1$, Δh_{90} in Equation (6.12) is logically expressed as a function of $1 - \Phi_D$ and $1 - \Psi_D$. The values of parameters *a*, *b* and *c* were determined by minimizing the root mean square error between Δh_{90} derived from Equation (6.12) and the corresponding values extracted from the hydraulic simulations of the 2,000 building layouts.

Figure 6.13 shows the remarkable correlation obtained between Equation (6.12), with calibrated coefficients *a* = 1.63, *b* = 0.75 and *c*= 2.24, and the reference values. The mean absolute and root mean square errors on the prediction of Δh_{90} from Equation (6.12) over the 2,000 computed urban patterns are respectively equal to 2.0 cm and 2.6 cm.

Considering only the district-scale storage porosity in the regression analysis (*c* = 0) gives optimal coefficient *a* = 1.00 and exponent *b* = 0.91. The mean absolute and root mean square errors increase by respectively 47% and 57% when neglecting the district-scale conveyance porosity in the regression analysis. Neglecting the district-scale storage porosity (*b* = 0), the errors increase dramatically by more than a factor of 3.

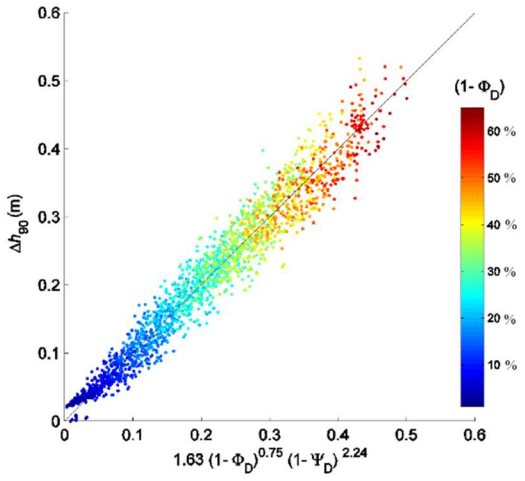

Figure 6.13: Relationships between the optimal regression analysis of the district-scale porosities Φ_D and Ψ_D and the inundation indicator Δh_{90} for the 2,000 computed urban patterns.

Interpretation

Although the conceptual model is based on an idealization of the urban layouts and on relatively crude assumptions, the results obtained with this simple model are promising. While the minimum value of the root mean square error computed with a regression analysis based on the nine urban characteristics is 2.9 cm (section 6.3.2), this error is found here to drop to 2.6 cm when only the two district-scale porosity parameters are used.

The standard MLR analysis indicates that the storage porosity (i.e. the built-up coverage) is by far the urban characteristic influencing most the water depths (section 6.3.2). This is somehow misleading since we find here, based on parameters of direct hydraulically significance, that the conveyance porosity has actually an even stronger influence (exponent c = 2.24 ~ 3 × exponent b), which, in turn, implies a nonlinear relationship between the dependent and independent variables. This aspect was already suggested in section 6.4.1, which highlighted that other parameters than the built-up coverage (x_9) seem to have a similar importance when a logarithmic transformation was applied to all variables, as well as based on Pearson regression coefficients.

However, the storage porosity is a key parameter to capture the influence of urban layout characteristics on inundation water depths. While the accuracy of the conceptual model decreases by around 50% when neglecting the conveyance porosity, it drops by a factor 3 when the storage porosity is not considered.

Implication for urban planning

Figure 6.14 provides two examples of urban layouts leading to similar water depths upstream, although they are characterized by significantly different building coverage ratios, i.e. different values of the district-scale storage porosity (Φ_D ~ 0.6 vs. Φ_D ~ 0.8). In both cases, the higher value of the built-up coverage is compensated by a higher value of the district-scale conveyance porosity.

These results are fully consistent with Equation (6.12), which highlights that potential detrimental effect of reduction of the storage porosity (i.e. new developments increasing the built-up coverage) can be mitigated by means of a suitable layout of the buildings which increases the conveyance porosity. This finding is of high relevance to guide more flood-resilient urban developments.

Equations (6.10) and (6.11) reveal that the district-scale conveyance porosity can be increased mainly in two ways:

- at the district-scale, increasing the fragmentation of the urban pattern (i.e. increasing the value of n) by reducing the average street length L_s or by favoring a high number of narrow streets to a low number of large ones;

- at the building-block scale, increasing the building side setback s_s or reducing the building size (i.e. reducing the mean parcel area $\sqrt{A_p}$).

The findings described above were obtained based on fixed hydraulic boundary conditions. Nonetheless, the overall conclusions would certainly remain unchanged if, for instance, the inflow magnitude was varied. Indeed, we expect that increasing (resp. decreasing) the inflow discharge would mainly magnify (resp. shrink) the water level differences between the upstream and downstream faces of the urban area for all configurations, without changing substantially the flow distribution within the street network. This effect was shown by Arrault et al. (2016) based on a laboratory model of an urban district, in which the inflow discharge was varied systematically over one order of magnitude. Consequently, varying the inflow discharge is unlikely to substantially modify the ranking of the various urban layouts in terms of flood-resilience. Similarly, Arrault et al. (2016) demonstrated that varying the inflow partition between the upstream faces has a limited influence on the flow within the urban area. In contrast, introducing a bottom slope would promote higher flow velocity so that parameters which play a little part in the configuration considered here (flat bottom) would become far more important (e.g., street orientation and curvature).

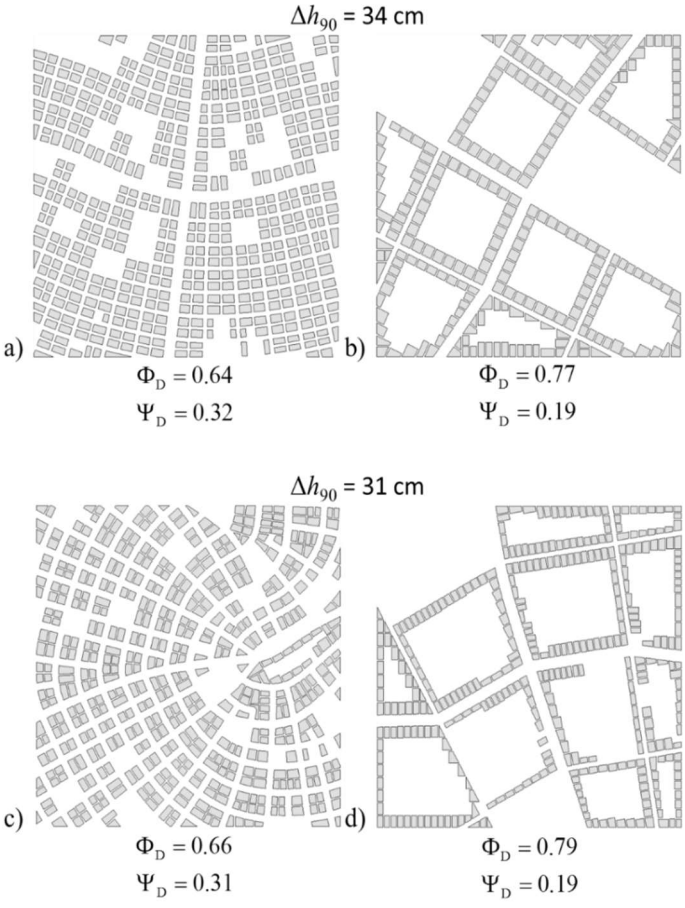

Figure 6.14: Urban layouts with different district-scale porosity values leading to similar upstream water depths.

6.5. Conclusions

This research presents a novel systematic study of inundation flow in quasi-realistic urbanized areas, which links hydraulic modelling results to parameters of direct significance for urban planning. Based on porosity-based hydraulic computations of inundation flow for a set of 2,000 different urban layouts, the relative influence of nine urban characteristics (average street length, street orientation and curvature, major and minor street widths, mean parcel area, rear and side building setbacks and built-up coverage) on inundation water depths were assessed. We focused on the water depth upstream of the considered urban area, as it reflects the impact of the developed area on the severity of flooding upstream. The terrain slope was neglected, so that the analysis results apply mostly to floodplains of typical lowland rivers.

The most influential parameters were found to be the built-up coverage, the mean parcel area (controlling directly the building size), the building side-setbacks, and to a lesser extent, the length and width of the streets. For the tested configurations, the more fragmented the urban pattern is (relatively small parcel sizes and street length), the lower the upstream water depths. This aspect is related to urban design at the district and building-block scales. Additionally, increasing the voids in-between the buildings (i.e. larger side setbacks) was shown to also contribute to a decrease in the upstream water depth. This aspect relates to urban planning at the local level of a single parcel. This goes against usual urban planning guidance that recommends increasing compactness and density especially in areas with good accessibility.

We also proposed a simple conceptual model based on storage and conveyance porosity parameters determined at the district-scale. Although particularly simple, the model was shown to provide surprisingly accurate predictions of the influence of the building layout on upstream water depths. The model parameters reveal that an increase in built-up coverage in an urban area (i.e. new developments, leading to a decrease in the district-scale storage porosity) can be compensated by a suitable location of the buildings so that the district-scale conveyance capacity increases.

This study paves the way for more quantitative approaches in water-sensitive urban design, based on process-oriented modelling of the interactions between complex urban systems and flooding mechanisms, enabling more flood-resilient urban developments.

Further research is needed to reach a deeper understanding of the influence of environmental parameters, such as the terrain slope and imperviousness, man-made structures (sewage system, underground structures …) and obstacles (cars, trees …) as well as varying hydraulic conditions (unsteady flood waves, pluvial flooding …).

6.6. Key contributions

- Built-up coverage has a strong contribution to flood damage. In addition, the mean parcel area and the building side-setbacks show moderate contribution to the flood damage.
- General guidelines to design more flood-resilient urban layouts are:
  increasing the distance between the buildings (i.e. larger side setbacks), and
  increasing the fragmentation of the urban pattern, by reducing the average street length or by favoring a high number of narrow streets to a low number of large ones.
- Since 1000 samples are sufficient for discriminating variables, we can adopt a different approach for the simulation. It could be exclusively based on observed samples from the territory instead of synthetic urban layouts.
- The h_{90} indicator is robust to test the relation between urban layout parameters and flood risk.
- Less number of urban layout variables, 5 in our case, are enough to predict the water depth at 100% accuracy compared to the model with full layout variables.
- The results reveal a nonlinear relationship between the model variable.

Chapter 7: General Conclusions

I will conclude this thesis by revisiting the research questions and providing recommendations for future research. Beside climate change, urbanization is widely acknowledged to be one of the major causes of a substantial increase in the frequency and magnitude of urban flooding across the globe. Thus, there is a need to monitor urban development to support efficient planning policies. This thesis sought to understand and mitigate the potential impact of future urbanization on flood risks up to 2100. In doing so, four scientific challenges considered as research questions in this thesis. Wallonia (Belgium) was selected as a case study. Wallonia represents two major challenges in terms of urbanization modeling: urban sprawl, and low development rates. Many regions, especially in USA and Europe, are characterized by sprawl expansion. Having low rate of development means having less information to calibrate any model.

7.1. Revisiting research questions

The main research questions addressed in the thesis were:

Q1. What is the potential of analyzing and modeling multiple urban densities in a highly fragmented built-up landscape?

Q2. Which urban expansion model structure is the most appropriate?

Q3. What is the relative impact of future urbanization on the flood damage across Wallonia?

Q4. What is the relation between urban layout design and flood damage?

In what follows, each of this questions will be answered and the key findings will be summarized.

Q1. What is the potential of analyzing and modeling multiple urban densities in a highly fragmented built-up landscape?

Many studies assumed a binary process of expansion, i.e., urban vs non-urban. Chapter one showed that the assumption of a binary approach led to inaccurate conclusions as the relative importance of the controlling factors typically varies with density, for both expansion and densification processes. Chapter one also demonstrated the importance of analyzing both development processes, expansion and densification. Urban sprawl is acknowledged as a significant environmental, economic, and social challenge in both the USA and Europe, policies

have been developed to curb this phenomenon by promoting densification. This thesis provided a deep analysis of the densification spatial drivers. Chapter one concluded that densification processes are mainly driven by self-organization dynamics whereas the expansion processes are strongly controlled by the zoning plan (policy).

Q2. Which urban expansion model structure is the most appropriate?

This question was answered by examining different modeling approaches and considering uncertainty in the future forecasting. All models were calibrated using 1990-2000 Belgian Cadastral data in a raster format. The calibration results were then used to validate the models' performances against the actual map of 2010. It is worth noting that the validation is only possible for historic patterns and cannot provide a full assessment of the model performance for future. However, the validation in this research meant provided information about the quality of models against each other. Several performance measurements were used to evaluate the models' abilities to locate new developments. In regard to calibration, all models are calibrated with statistical models (logistic regression) and/or an advanced genetic algorithm (GAs). Therefore, the thesis explored the potential of GAs for land-use planning tools.

In chapter two, a coupled multinomial logistic regression and cellular automata model (MNL-CA) was proposed to simulate urbanization. Whereas, chapter three proposed a coupled CA and agent-based model (CA-AB). The performance of both models was measured and compared. The main finding was that CA-AB model outperformed MNL-CA model and furthermore the calibration results of CA-AB were more stable than MNL-CA in terms of future simulations.

Simulating urban development for up to 2100 was the main aim of this research. Forecasting land-use change over such time frames entails very significant uncertainties. As a result, this study paid much attention to uncertainty modeling. Chapter four proposed a novel approach for tuning uncertainty over time. This approach was referred to as Time Monte-Carlo (TMC) technique. The analysis revealed that the TMC produces results comparable with well-known methods to modeling uncertainty over the short-term validation period (2000-2010). Furthermore, it is capable of tuning uncertainty on longer-term time horizons, which is essential feature of our method as the far future involves more uncertainty. It has been demonstrated that introducing uncertainty always improved the performance of the model when compared to pure deterministic approaches.

Q3. What is the relative impact of future urbanization on the flood damage across Wallonia?

In chapter five, a set of 24 urbanization scenarios for 2030, 2050, 2070, and 2100 for the entire Wallonia were produced, with a spatial resolution of 100 m, considering two modules: (i) a non-spatial module that was applied to predict the quantity of new urban development, and (ii) a spatially-explicit allocation module that allocated new development. This research extrapolated three development rates (1990-2000, 2000-2010, and 1990-2010/2) to assume the future quantity of new development. The CA-AB model was used to allocate new development. Again, the research considered both expansion and densification processes. By means of sensitivity analysis, we showed the added-value of having land-use maps containing sub-grid information about the built-up density, and not just a binary information (urban/non-urban).

The proposed scenarios differed in development rate (high, medium, and low), spatial policies (business-as-usual vs. densification) and flood management policies (ban on new development with flood-prone zones). The results revealed that without considering any flood management policies, the increase in total flood risk varied by a factor of approximately two at the end of the century depending on the urbanization scenario. More importantly, the sensitivity of the computed flood risk to the spatial policy was shown to be higher than the development rate. This highlighted that spatial policy, especially densification, may have a substantial influence on future flood risk.

Q4. What is the relation between urban layout and flood damage?

One of the main conclusions of chapter five was that floodplain development may continue apace, regardless of potential planning policies to control this development. Chapter six concerned with accommodating the unavoidability of floods through modifications to urban layout design. This chapter answered Q4 by systematically exploring the inundation flow in quasi-realistic urbanized areas, which links hydraulic modeling results with parameters of direct significance for urban planning. Based on porosity-based hydraulic computations of inundation flow for a set of 2,000 different urban layouts, the relative influence of nine urban characteristics (average street length, street orientation and curvature, major and minor street widths, mean parcel area, rear and side building setbacks and building coverage) on inundation water depths were assessed. The research found that the most influential urban layout parameters was the built-up coverage, the mean parcel area (controlling directly the building size), the building side-setbacks, and to a lesser extent, the length and width of the streets. In a sense, chapter six provided guidelines for urban geometric grammars that help passively reduce flood damage.

7.2. Recommendations for future research

Several considerations and recommendation can be drawn from the thesis. In this extensive research, I dealt with huge amounts of data and with different scientific domains. As I progressed through this thesis, many further research directions were raised.

1. The spatial data used in this research exhibited spatial autocorrelation, which biases the results of the analysis. Following previous studies, the regression analysis was calibrated based on a data sampling approach. A number of scholar proposed alternative solution which is the auto-logistic regression model. However, some authors (e.g. Dormann, 2007) have reported that the logistic regression model tends to outperform the auto-logistic model in terms of estimation of model parameters. Future research could be oriented towards handling autocorrelation in spatial land-use models.

2. This research underlay competitive advantage of using several urban densities, however, it did not capture the variety of very local responses to each urbanization driver. This offers urban planners and modelers the potential for analyzing of urbanization process at the urban micro-level. Many studies employed geographically weighted regression model to analyze the behavior of drivers at a local level. I used the genetic algorithm (GA) to calibrate the land-use models presented in this thesis. Due to their use of a population, GAs can find multiple optima, as opposed to a single calibration solution. This may enable researchers to explore each single solution in terms of spatial variation by incorporating an advanced GA in land-use models.

3. Two land-use change models were proposed in this research, MNL-CA and CA-AB. I found that the performance of CA-AB is slightly better than MNL-CA. However, I assumed that this improvement might be related to the interactions between different agents. Nonetheless, this could also related to the fact that MNL-CA was calibrated using both logistic regression and GA whereas CA-AB was solely calibrated using GA. Further research can examine the performance of GA against logistic regression.

4. I found that the effect of accessibility indicators outpaced many other drivers behind urban development. According to many studies (e.g. Cammerer et al., 2013; Poelmans and Van Rompaey, 2010), I used the distance to roads and cities as the measurement of accessibility. Although this spatial measurement is easy to interpret and communicate to planners, but it does not take into account the temporal and individual components and therefore it does not reveal the full potential of the accessibility impacts. Land Use and Transport Integrated models (LUTIs) is promising research direction as it can provide advanced accessibility measures based on weighting the opportunities located in an area

and/or an individual's ability to reach opportunities given the person's daily activity pattern and spatiotemporal constraints.

5. Addressing allocation uncertainty by the TMC technique, chapter four, I assumed that the future land-use patterns exposed to the same source of allocation uncertainty. More research on how to quantify several allocation uncertainty sources such as uncertainties related to the model structure, model simplification, and model parameter estimates need to be conducted.

6. This research considered only damages related to buildings and it did not pay attention to damages related to other land-uses like infrastructure, agriculture, and forest. Furthermore, it was assumed that flow characteristics do not change with the future urban development. Further research should, therefore, explore these two limitations when coupling urban development scenarios and inundation models.

7. It was found that the most influential parameters of urban layout configuration were the built-up coverage, and far less, the mean parcel area, the building side-setbacks, and to a lesser extent, the length and width of the streets. Offering further analysis of the relationship between urban layout parameters and inundation, considering several fixed built-up coverages will also provide more understanding of how urban geometrical configurations affect flood.

8. The results revealed that about 1000 samples were enough to discover the relationship between inundation water depth and a number of urban layout design parameters. Therefore, future research can exclusively use real samples from the territory, which would easily allow integrating other aspects, not included in this research, such as slopes at the micro-level, drainage systems, building typologies etc.

9. The proposed land-use change models and the procedural generation systems are generic and can be applied to other case studies. Still, an explicit investigation of the transferability of the model by proposed to other regional/context, characterized by different urbanization processes, is an important direction for future research.

References

Abderrezzak, K.E.K., Paquier, A., Mignot, E., 2009. Modelling flash flood propagation in urban areas using a two-dimensional numerical model. Nat. Hazards 50, 433–460. https://doi.org/10.1007/s11069-008-9300-0

Aburas, M.M., Ho, Y.M., Ramli, M.F., Ash'aari, Z.H., 2016. The simulation and prediction of spatio-temporal urban growth trends using cellular automata models: A review. Int. J. Appl. Earth Obs. Geoinformation 52, 380–389. https://doi.org/10.1016/j.jag.2016.07.007

Achmad, A., Hasyim, S., Dahlan, B., Aulia, D.N., 2015. Modeling of urban growth in tsunami-prone city using logistic regression: Analysis of Banda Aceh, Indonesia. Appl. Geogr. 62, 237–246. https://doi.org/10.1016/j.apgeog.2015.05.001

Aguayo, M., Wiegand, T., Azócar, G., Wiegand, K., Vega, C., 2007. Revealing the Driving Forces of Mid-Cities Urban Growth Patterns Using Spatial Modeling: a Case Study of Los Ángeles, Chile. Ecol. Soc. 12. https://doi.org/10.5751/ES-01970-120113

Ahmed, B., Ahmed, R., Zhu, X., 2013. Evaluation of Model Validation Techniques in Land Cover Dynamics. ISPRS Int. J. Geo-Inf. 2, 577–597. https://doi.org/10.3390/ijgi2030577

Al-Ahmadi, K., See, L., Heppenstall, A., Hogg, J., 2009. Calibration of a fuzzy cellular automata model of urban dynamics in Saudi Arabia. Ecol. Complex. 6, 80–101. https://doi.org/10.1016/j.ecocom.2008.09.004

Aliaga, D.G., Vanegas, C., Lei, M., Niyogi, D., 2013. Visualization-Based Decision Tool for Urban Meteorological Modeling. Environ. Plan. B Plan. Des. 40, 271–288. https://doi.org/10.1068/b38084

Aliaga, D.G., Vanegas, C.A., Benes, B., 2008. Interactive Example-based Urban Layout Synthesis, in: ACM SIGGRAPH Asia 2008 Papers, SIGGRAPH Asia '08. ACM, New York, NY, USA, p. 160:1–160:10. https://doi.org/10.1145/1457515.1409113

Amirebrahimi, S., Rajabifard, A., Mendis, P., Ngo, T., 2016. A framework for a microscale flood damage assessment and visualization for a building using BIM–GIS integration. Int. J. Digit. Earth 9, 363–386. https://doi.org/10.1080/17538947.2015.1034201

Arlinghaus, S.L., Kerski, J.J., 2013. Spatial Mathematics: Theory and Practice through Mapping. CRC Press.

Arrault, A., Finaud-Guyot, P., Archambeau, P., Bruwier, M., Erpicum, S., Pirotton, M., Dewals, B., 2016. Hydrodynamics of long-duration urban floods: experiments and numerical modelling. Nat Hazards Earth Syst Sci 16, 1413–1429. https://doi.org/10.5194/nhess-16-1413-2016

Ban, H., Ahlqvist, O., 2009. Representing and negotiating uncertain geospatial concepts – Where are the exurban areas? Comput. Environ. Urban Syst. 33, 233–246. https://doi.org/10.1016/j.compenvurbsys.2008.10.001

Batisani, N., Yarnal, B., 2009. Urban expansion in Centre County, Pennsylvania: Spatial dynamics and landscape transformations. Appl. Geogr. 29, 235–249. https://doi.org/10.1016/j.apgeog.2008.08.007

Batty, M., 2008. The Size, Scale, and Shape of Cities. Science 319, 769–771. https://doi.org/10.1126/science.1151419

Batty, M., 2007. Cities and Complexity: Understanding Cities with Cellular Automata, Agent-based Models, and Fractals. MIT Press.

Beckers, A., Dewals, B., Erpicum, S., Dujardin, S., Detrembleur, S., Teller, J., Pirotton, M., Archambeau, P., 2013. Contribution of land use changes to future flood damage along the river Meuse in the Walloon region. Nat Hazards Earth Syst Sci 13, 2301–2318. https://doi.org/10.5194/nhess-13-2301-2013

Belgian Federal Government, 2013. Statistics Belgium [WWW Document]. Stat. Belg. URL http://statbel.fgov.be/fr/statistiques/chiffres/ (accessed 4.29.14).

Berberoğlu, S., Akın, A., Clarke, K.C., 2016. Cellular automata modeling approaches to forecast urban growth for adana, Turkey: A comparative approach. Landsc. Urban Plan. 153, 11–27. https://doi.org/10.1016/j.landurbplan.2016.04.017

Braimoh, A.K., Onishi, T., 2007. Spatial determinants of urban land use change in Lagos, Nigeria. Land Use Policy 24, 502–515. https://doi.org/10.1016/j.landusepol.2006.09.001

Bridson, R., 2015. Fluid Simulation for Computer Graphics, Second Edition. CRC Press.

Brown, D.G.B.C., Page, S., Riolo, R., Zellner, M., Rand, W., 2005. Path dependence and the validation of agent-based spatial models of land use. Int. J. Geogr. Inf. Sci. 19, 153–174. https://doi.org/10.1080/13658810410001713399
Bruwier, M., Archambeau, P., Erpicum, S., Pirotton, M., Dewals, B., 2017a. Shallow-water models with anisotropic porosity and merging for flood modelling on Cartesian grids. J. Hydrol. 554, 693–709. https://doi.org/10.1016/j.jhydrol.2017.09.051
Bruwier, M., Erpicum, S., Archambeau, P., Pirotton, M., Dewals, B., 2017b. Computing flooding of crossroads with obstacles using a 2D numerical model. J. Hydraul. Res. 55, 737–741. https://doi.org/10.1080/00221686.2017.1326406
Bruwier, M., Erpicum, S., Pirotton, M., Archambeau, P., Dewals, B.J., 2015. Assessing the operation rules of a reservoir system based on a detailed modelling chain. Nat Hazards Earth Syst Sci 15, 365–379. https://doi.org/10.5194/nhess-15-365-2015
Burchell, R.W., Listokin, D., Galley, C.C., 2000. Smart growth: More than a ghost of urban policy past, less than a bold new horizon. Hous. Policy Debate 11, 821–879. https://doi.org/10.1080/10511482.2000.9521390
Cammerer, H., Thieken, A.H., Verburg, P.H., 2013. Spatio-temporal dynamics in the flood exposure due to land use changes in the Alpine Lech Valley in Tyrol (Austria). Nat. Hazards 68, 1243–1270. https://doi.org/10.1007/s11069-012-0280-8
Chen, A.S., Evans, B., Djordjević, S., Savić, D.A., 2012. A coarse-grid approach to representing building blockage effects in 2D urban flood modelling. J. Hydrol. 426–427, 1–16. https://doi.org/10.1016/j.jhydrol.2012.01.007
Chen, G., Esch, G., Wonka, P., Müller, P., Zhang, E., 2008. Interactive procedural street modeling, in: ACM Transactions on Graphics (TOG). ACM, p. 103.
Chen, Y., Li, X., Liu, X., Ai, B., 2014. Modeling urban land-use dynamics in a fast developing city using the modified logistic cellular automaton with a patch-based simulation strategy. Int. J. Geogr. Inf. Sci. 28, 234–255. https://doi.org/10.1080/13658816.2013.831868
Christensen, P.H., 2016. Understanding the potential of 4D geospatial modeling to enhance flood mitigation planning in residential areas. Invent. House Case-Specif. Stud. Hous. Innov. 6.
Christiansen, P., Loftsgarden, T., 2011. Drivers behind urban sprawl in Europe. TOI Rep. 1136, 2011.
Clark, W.A.V., Hosking, P.L., 1986. Statistical Methods for Geographers, 1 edition. ed. Wiley, New York.
Clarke, K.C., Gaydos, L.J., 1998. Loose-coupling a cellular automaton model and GIS: long-term urban growth prediction for San Francisco and Washington/Baltimore. Int. J. Geogr. Inf. Sci. 12, 699–714. https://doi.org/10.1080/136588198241617
Clarke, K.C., Hoppen, S., Gaydos, L., 1997. A Self-Modifying Cellular Automaton Model of Historical Urbanization in the San Francisco Bay Area. Environ. Plan. B Plan. Des. 24, 247–261. https://doi.org/10.1068/b240247
Crols, T., White, R., Uljee, I., Engelen, G., Poelmans, L., Canters, F., 2015. A travel time-based variable grid approach for an activity-based cellular automata model. Int. J. Geogr. Inf. Sci. 29, 1757–1781. https://doi.org/10.1080/13658816.2015.1047838
Danielsen, K.A., Lang, R.E., Fulton, W., 1999. Retracting suburbia: Smart growth and the future of housing. Hous. Policy Debate 10, 513–540. https://doi.org/10.1080/10511482.1999.9521341
De Decker, P., 2008. Facets of housing and housing policies in Belgium. J. Hous. Built Environ. 23, 155–171. https://doi.org/10.1007/s10901-008-9110-4
De Smet, F., Teller, J., 2016. Characterising the Morphology of Suburban Settlements: A Method Based on a Semi-automatic Classification of Building Clusters. Landsc. Res. 41, 113–130. https://doi.org/10.1080/01426397.2015.1045464
Deb, K., 2001. Multi-Objective Optimization Using Evolutionary Algorithms. John Wiley & Sons.
Demir, \.Ilke, Aliaga, D.G., Benes, B., 2015. Coupled Segmentation and Similarity Detection for Architectural Models. ACM Trans Graph 34, 104:1–104:11. https://doi.org/10.1145/2766923
DGO3/SPW, 2015a. District hydrographique international de l'Escaut : Projet de Plan de Gestion des Risques d'Inondation en Wallonie. Ministère de la Région Wallone.
DGO3/SPW, 2015b. Rapport d'incidences environnementales du Plan de Gestion des Risques d'Inondation en Wallonie (PGRI) du district hydrographique international de la Meuse. Ministère de la Région Wallone.
Dieleman, F., Wegener, M., 2004. Compact City and Urban Sprawl. Built Environ. 1978- 30, 308–323.
Dormann, C.F., 2007. Assessing the validity of autologistic regression. Ecol. Model. 207, 234–242. https://doi.org/10.1016/j.ecolmodel.2007.05.002

Dottori, F., Di Baldassarre, G., Todini, E., 2013. Detailed data is welcome, but with a pinch of salt: Accuracy, precision, and uncertainty in flood inundation modeling. Water Resour. Res. 49, 6079–6085. https://doi.org/10.1002/wrcr.20406

Downs, A., 2001. What does smart growth really mean. Planning 67, 20–25.

Dubovyk, O., Sliuzas, R., Flacke, J., 2011. Spatio-temporal modelling of informal settlement development in Sancaktepe district, Istanbul, Turkey. ISPRS J. Photogramm. Remote Sens., Quality, Scale and Analysis Aspects of Urban City Models 66, 235–246. https://doi.org/10.1016/j.isprsjprs.2010.10.002

Dujardin, S., Marique, A.-F., Teller, J., 2014. Spatial planning as a driver of change in mobility and residential energy consumption. Energy Build. 68, 779–785. https://doi.org/10.1016/j.enbuild.2012.10.059

Dujardin, S., Pirart, F., Brévers, F., Marique, A.-F., Teller, J., 2012. Home-to-work commuting, urban form and potential energy savings: A local scale approach to regional statistics. Transp. Res. Part Policy Pract. 46, 1054–1065. https://doi.org/10.1016/j.tra.2012.04.010

EEA, 2011a. Landscape fragmentation in Europe (Publication). European Environment Agency.

EEA, 2011b. Mapping the impacts of natural hazards and technological accidents in Europe (Publication No. 13/2010). European Environment Agency.

EEA, 2006. Urban sprawl in Europe - The ignored challenge [WWW Document]. URL http://www.eea.europa.eu/publications/eea_report_2006_10 (accessed 8.28.15).

EEA, 1994. CORINE Land cover (Publication). European Environment Agency.

Enright, D., Marschner, S., Fedkiw, R., 2002. Animation and Rendering of Complex Water Surfaces, in: Proceedings of the 29th Annual Conference on Computer Graphics and Interactive Techniques, SIGGRAPH '02. ACM, New York, NY, USA, pp. 736–744. https://doi.org/10.1145/566570.566645

Ernst, J., Dewals, B.J., Detrembleur, S., Archambeau, P., Erpicum, S., Pirotton, M., 2010. Micro-scale flood risk analysis based on detailed 2D hydraulic modelling and high resolution geographic data. Nat. Hazards 55, 181–209. https://doi.org/10.1007/s11069-010-9520-y

Erpicum, S., Dewals, B., Archambeau, P., Detrembleur, S., Pirotton, M., 2010a. Detailed Inundation Modelling Using High Resolution DEMs. Eng. Appl. Comput. Fluid Mech. 4, 196–208. https://doi.org/10.1080/19942060.2010.11015310

Erpicum, S., Dewals, B.J., Archambeau, P., Pirotton, M., 2010b. Dam break flow computation based on an efficient flux vector splitting. J. Comput. Appl. Math., Fourth International Conference on Advanced COmputational Methods in ENgineering (ACOMEN 2008) 234, 2143–2151. https://doi.org/10.1016/j.cam.2009.08.110

ESPON, 2005. Governance of territorial and urban policies (No. 2nd Interim Report), ESPON Project 2.3.2. European spatial planning observation network.

European Union, 1997. The EU compendium of spatial planning systems and policies.

Eurostat, 2012. European cities [WWW Document]. URL http://ec.europa.eu/eurostat/web/cities/spatial-units (accessed 5.16.17).

Feng, T., Yu, L.-F., Yeung, S.-K., Yin, K., Zhou, K., 2016. Crowd-driven Mid-scale Layout Design. ACM Trans Graph 35, 132:1–132:14. https://doi.org/10.1145/2897824.2925894

Feng, Y., 2017. Modeling dynamic urban land-use change with geographical cellular automata and generalized pattern search-optimized rules. Int. J. Geogr. Inf. Sci. 31, 1198–1219. https://doi.org/10.1080/13658816.2017.1287368

Feng, Y., Liu, Y., Tong, X., Liu, M., Deng, S., 2011. Modeling dynamic urban growth using cellular automata and particle swarm optimization rules. Landsc. Urban Plan. 102, 188–196. https://doi.org/10.1016/j.landurbplan.2011.04.004

Fokkens, B., 2006. THE DUTCH STRATEGY FOR SAFETY AND RIVER FLOOD PREVENTION, in: Extreme Hydrological Events: New Concepts for Security. Springer, Dordrecht, pp. 337–352. https://doi.org/10.1007/978-1-4020-5741-0_23

Fraile, A., Larrodé, E., Alberto Magreñán, Á., Sicilia, J.A., 2016. Decision model for siting transport and logistic facilities in urban environments: A methodological approach. J. Comput. Appl. Math., Mathematical Modeling and Computational Methods 291, 478–487. https://doi.org/10.1016/j.cam.2014.12.012

García, A.M., Santé, I., Boullón, M., Crecente, R., 2013. Calibration of an urban cellular automaton model by using statistical techniques and a genetic algorithm. Application to a small urban settlement of NW Spain. Int. J. Geogr. Inf. Sci. 27, 1593–1611. https://doi.org/10.1080/13658816.2012.762454

García, A.M., Santé, I., Crecente, R., Miranda, D., 2011. An analysis of the effect of the stochastic component of urban cellular automata models. Comput. Environ. Urban Syst. 35, 289–296. https://doi.org/10.1016/j.compenvurbsys.2010.11.001
Garcia-Dorado, I., Aliaga, D.G., Bhalachandran, S., Schmid, P., Niyogi, D., 2017. Fast Weather Simulation for Inverse Procedural Design of 3D Urban Models. ACM Trans Graph 36, 21:1–21:19. https://doi.org/10.1145/2999534
Garcia-Dorado, I., G. Aliaga, D., V. Ukkusuri, S., 2014. Designing Large-scale Interactive Traffic Animations for Urban Modeling. Comput Graph Forum 33, 411–420. https://doi.org/10.1111/cgf.12329
Ghostine, R., Hoteit, I., Vazquez, J., Terfous, A., Ghenaim, A., Mose, R., 2015. Comparison between a coupled 1D-2D model and a fully 2D model for supercritical flow simulation in crossroads. J. Hydraul. Res. 53, 274–281. https://doi.org/10.1080/00221686.2014.974081
Grant, J.L., 2009. Theory and Practice in Planning the Suburbs: Challenges to Implementing New Urbanism, Smart Growth, and Sustainability Principles. Plan. Theory Pract. 10, 11–33. https://doi.org/10.1080/14649350802661683
Guzy, M., Smith, C., Bolte, J., Hulse, D., Gregory, S., 2008. Policy Research Using Agent-Based Modeling to Assess Future Impacts of Urban Expansion into Farmlands and Forests. Ecol. Soc. 13. https://doi.org/10.5751/ES-02388-130137
Hagen, A., 2003. Fuzzy set approach to assessing similarity of categorical maps. Int. J. Geogr. Inf. Sci. 17, 235–249. https://doi.org/10.1080/13658810210157822
Hagen-Zanker, A., Martens, P., 2008. Map Comparison Methods for Comprehensive Assessment of Geosimulation Models, in: Computational Science and Its Applications – ICCSA 2008, Lecture Notes in Computer Science. Presented at the International Conference on Computational Science and Its Applications, Springer, Berlin, Heidelberg, pp. 194–209. https://doi.org/10.1007/978-3-540-69839-5_15
Haggert, B.A., 1995. Review of Land Use and the Causes of Global Warming. Trans. Inst. Br. Geogr. 20, 518–520. https://doi.org/10.2307/622983
Han, J., Hayashi, Y., Cao, X., Imura, H., 2009. Application of an integrated system dynamics and cellular automata model for urban growth assessment: A case study of Shanghai, China. Landsc. Urban Plan. 91, 133–141. https://doi.org/10.1016/j.landurbplan.2008.12.002
Han, Y., Jia, H., 2016. Simulating the spatial dynamics of urban growth with an integrated modeling approach: A case study of Foshan, China. Ecol. Model. https://doi.org/10.1016/j.ecolmodel.2016.04.005
Hansheng, L., Lishan, K., 1999. Balance between exploration and exploitation in genetic search. Wuhan Univ. J. Nat. Sci. 4, 28–32. https://doi.org/10.1007/BF02827615
Hao, P., Hooimeijer, P., Sliuzas, R., Geertman, S., 2013. What Drives the Spatial Development of Urban Villages in China? Urban Stud. 50, 3394–3411. https://doi.org/10.1177/0042098013484534
Hennig, E.I., Schwick, C., Soukup, T., Orlitová, E., Kienast, F., Jaeger, J.A.G., 2015. Multi-scale analysis of urban sprawl in Europe: Towards a European de-sprawling strategy. Land Use Policy 49, 483–498. https://doi.org/10.1016/j.landusepol.2015.08.001
Herbert, D.T., Thomas, C.J., 1982. Urban Geography: A First Approach. Wiley.
Holland, J.H., 1975. Adaptation in natural and artificial systems. U Michigan Press, Oxford, England.
Hosseinali, F., Alesheikh, A.A., Nourian, F., 2013. Agent-based modeling of urban land-use development, case study: Simulating future scenarios of Qazvin city. Cities 31, 105–113. https://doi.org/10.1016/j.cities.2012.09.002
Hu, Z., Lo, C.P., 2007. Modeling urban growth in Atlanta using logistic regression. Comput. Environ. Urban Syst. 31, 667–688. https://doi.org/10.1016/j.compenvurbsys.2006.11.001
Huang, B., Xie, C., Tay, R., 2010. Support vector machines for urban growth modeling. GeoInformatica 14, 83–99. https://doi.org/10.1007/s10707-009-0077-4
Huang, C.-J., Hsu, M.-H., Teng, W.-H., Wang, Y.-H., 2014. The Impact of Building Coverage in the Metropolitan Area on the Flow Calculation. Water 6, 2449–2466. https://doi.org/10.3390/w6082449
Huong, H.T.L., Pathirana, A., 2013. Urbanization and climate change impacts on future urban flooding in Can Tho city, Vietnam. Hydrol Earth Syst Sci 17, 379–394. https://doi.org/10.5194/hess-17-379-2013
Jantz, C.A., Goetz, S.J., Shelley, M.K., 2003. Using the Sleuth Urban Growth Model to Simulate the Impacts of Future Policy Scenarios on Urban Land Use in the Baltimore-Washington Metropolitan Area. Environ. Plan. B Plan. Des. 31, 251–271. https://doi.org/10.1068/b2983

Jehling, M., Hecht, R., Herold, H., 2016. Assessing urban containment policies within a suburban context—An approach to enable a regional perspective. Land Use Policy. https://doi.org/10.1016/j.landusepol.2016.10.031
Jelinski, D.E., Wu, J., 1996. The modifiable areal unit problem and implications for landscape ecology. Landsc. Ecol. 11, 129–140. https://doi.org/10.1007/BF02447512
Jenks, G.F., Caspall, F.C., 1971. Error on Choroplethic Maps: Definition, Measurement, Reduction. Ann. Assoc. Am. Geogr. 61, 217–244. https://doi.org/10.1111/j.1467-8306.1971.tb00779.x
Jiang, F., Liu, S., Yuan, H., Zhang, Q., 2007. Measuring urban sprawl in Beijing with geo-spatial indices. J. Geogr. Sci. 17, 469–478. https://doi.org/10.1007/s11442-007-0469-z
Jr, D.W.H., Lemeshow, S., 2004. Applied Logistic Regression. John Wiley & Sons.
Kim, B., Sanders, B.F., Famiglietti, J.S., Guinot, V., 2015. Urban flood modeling with porous shallow-water equations: A case study of model errors in the presence of anisotropic porosity. J. Hydrol. 523, 680–692. https://doi.org/10.1016/j.jhydrol.2015.01.059
Kim, B., Sanders, B.F., Schubert, J.E., Famiglietti, J.S., 2014. Mesh type tradeoffs in 2D hydrodynamic modeling of flooding with a Godunov-based flow solver. Adv. Water Resour. 68, 42–61. https://doi.org/10.1016/j.advwatres.2014.02.013
Kreibich, H., Seifert, I., Merz, B., Thieken, A.H., 2010. Development of FLEMOcs – a new model for the estimation of flood losses in the commercial sector. Hydrol. Sci. J. 55, 1302–1314. https://doi.org/10.1080/02626667.2010.529815
Kumar, A., Pandey, A.C., Jeyaseelan, A.T., 2012. Built-up and vegetation extraction and density mapping using WorldView-II. Geocarto Int. 27, 557–568. https://doi.org/10.1080/10106049.2012.657695
Landuyt, D., Broekx, S., Engelen, G., Uljee, I., Van der Meulen, M., Goethals, P.L.M., 2016. The importance of uncertainties in scenario analyses – A study on future ecosystem service delivery in Flanders. Sci. Total Environ. 553, 504–518. https://doi.org/10.1016/j.scitotenv.2016.02.098
Lennon, M., Scott, M., O'Neill, E., 2014. Urban Design and Adapting to Flood Risk: The Role of Green Infrastructure. J. Urban Des. 19, 745–758. https://doi.org/10.1080/13574809.2014.944113
Li, X., Liu, X., 2006. An extended cellular automaton using case-based reasoning for simulating urban development in a large complex region. Int. J. Geogr. Inf. Sci. 20, 1109–1136. https://doi.org/10.1080/13658810600816870
Li, X., Zhou, W., Ouyang, Z., 2013. Forty years of urban expansion in Beijing: What is the relative importance of physical, socioeconomic, and neighborhood factors? Appl. Geogr. 38, 1–10. https://doi.org/10.1016/j.apgeog.2012.11.004
Liao, J., Tang, L., Shao, G., Qiu, Q., Wang, C., Zheng, S., Su, X., 2014. A neighbor decay cellular automata approach for simulating urban expansion based on particle swarm intelligence. Int. J. Geogr. Inf. Sci. 28, 720–738. https://doi.org/10.1080/13658816.2013.869820
Lin, E., Shaad, K., Girot, C., 2016. Developing river rehabilitation scenarios by integrating landscape and hydrodynamic modeling for the Ciliwung River in Jakarta, Indonesia. Sustain. Cities Soc. 20, 180–198. https://doi.org/10.1016/j.scs.2015.09.011
Lin, Y.-P., Chu, H.-J., Wu, C.-F., Verburg, P.H., 2011. Predictive ability of logistic regression, auto-logistic regression and neural network models in empirical land-use change modeling – a case study. Int. J. Geogr. Inf. Sci. 25, 65–87. https://doi.org/10.1080/13658811003752332
Litman, T., 2016. Evaluating Transportation Land Use Impacts: Considering the Impacts, Benefits and Costs of Different Land Use Development Patterns.
Liu, C., Ma, X., 2011. Analysis to driving forces of land use change in Lu'an mining area. Trans. Nonferrous Met. Soc. China 21, Supplement 3, s727–s732. https://doi.org/10.1016/S1003-6326(12)61670-7
Liu, X., Li, X., Liu, L., He, J., Ai, B., 2008a. A bottom-up approach to discover transition rules of cellular automata using ant intelligence. Int. J. Geogr. Inf. Sci. 22, 1247–1269. https://doi.org/10.1080/13658810701757510
Liu, X., Li, X., Shi, X., Wu, S., Liu, T., 2008b. Simulating complex urban development using kernel-based non-linear cellular automata. Ecol. Model. 211, 169–181. https://doi.org/10.1016/j.ecolmodel.2007.08.024
Liu, X., Ma, L., Li, X., Ai, B., Li, S., He, Z., 2014. Simulating urban growth by integrating landscape expansion index (LEI) and cellular automata. Int. J. Geogr. Inf. Sci. 28, 148–163. https://doi.org/10.1080/13658816.2013.831097
Liu, Y., He, Q., Tan, R., Liu, Y., Yin, C., 2016. Modeling different urban growth patterns based on the evolution of urban form: A case study from Huangpi, Central China. Appl. Geogr. 66, 109–118. https://doi.org/10.1016/j.apgeog.2015.11.012

Loibl, W., Toetzer, T., 2003. Modeling growth and densification processes in suburban regions—simulation of landscape transition with spatial agents. Environ. Model. Softw., Applying Computer Research to Environmental Problems 18, 553–563. https://doi.org/10.1016/S1364-8152(03)00030-6

Loibl, W., Tötzer, T., Köstl, M., Steinnocher, K., 2007. Simulation of Polycentric Urban Growth Dynamics Through Agents, in: Koomen, E., Stillwell, J., Bakema, A., Scholten, H.J. (Eds.), Modelling Land-Use Change, The GeoJournal Library. Springer Netherlands, pp. 219–236. https://doi.org/10.1007/978-1-4020-5648-2_13

Long, Y., Han, H., Lai, S.-K., Mao, Q., 2013. Urban growth boundaries of the Beijing Metropolitan Area: Comparison of simulation and artwork. Cities 31, 337–348. https://doi.org/10.1016/j.cities.2012.10.013

Loo, B.P.Y., Cheng, A.H.T., Nichols, S.L., 2017. Transit-oriented development on greenfield versus infill sites: Some lessons from Hong Kong. Landsc. Urban Plan. 167, 37–48. https://doi.org/10.1016/j.landurbplan.2017.05.013

Losasso, F., Gibou, F., Fedkiw, R., 2004. Simulating Water and Smoke with an Octree Data Structure, in: ACM SIGGRAPH 2004 Papers, SIGGRAPH '04. ACM, New York, NY, USA, pp. 457–462. https://doi.org/10.1145/1186562.1015745

Marique, A.-F., Dujardin, S., Teller, J., Reiter, S., 2013. Urban sprawl, commuting and travel energy consumption. Proc. Inst. Civ. Eng. Energy 166. https://doi.org/10.1680/ener.12.00002

McConnell, V., Wiley, K., 2011. Infill Development: Perspectives and Evidence from Economics and Planning. Resour. Future 1–34. https://doi.org/10.1093/oxfordhb/9780195380620.013.0022

Merz, B., Thieken, A.H., Gocht, M., 2007. Flood Risk Mapping At The Local Scale: Concepts and Challenges, in: Flood Risk Management in Europe, Advances in Natural and Technological Hazards Research. Springer, Dordrecht, pp. 231–251. https://doi.org/10.1007/978-1-4020-4200-3_13

Mignot, E., Paquier, A., Haider, S., 2006. Modeling floods in a dense urban area using 2D shallow water equations. J. Hydrol. 327, 186–199. https://doi.org/10.1016/j.jhydrol.2005.11.026

Mioc, D., Anton, F., Nickerson, B., Santos, M., Adda, P., Tienaah, T., Ahmad, A., Mezouaghi, M., MacGillivray, E., Morton, A., Tang, P., 2012. Flood Progression Modelling and Impact Analysis, in: Efficient Decision Support Systems - Practice and Challenges in Multidisciplinary Domains. InTech, pp. 227–246.

Mitsova, D., Shuster, W., Wang, X., 2011. A cellular automata model of land cover change to integrate urban growth with open space conservation. Landsc. Urban Plan. 99, 141–153. https://doi.org/10.1016/j.landurbplan.2010.10.001

Moel, H. de, Aerts, J.C.J.H., 2010. Effect of uncertainty in land use, damage models and inundation depth on flood damage estimates. Nat. Hazards 58, 407–425. https://doi.org/10.1007/s11069-010-9675-6

Montgomery, D.C., Runger, G.C., 2003. Applied Statistics and Probability for Engineers, Fourth. ed. John Wiley & Sons, New York.

Müller, P., Wonka, P., Haegler, S., Ulmer, A., Van Gool, L., 2006. Procedural Modeling of Buildings, in: ACM SIGGRAPH 2006 Papers, SIGGRAPH '06. ACM, New York, NY, USA, pp. 614–623. https://doi.org/10.1145/1179352.1141931

Muller, W., 2000. ATKIS® data base revision and generation of digital topographic base maps. Int. Arch. Photogramm. Remote Sens. 33, 710–717.

Munshi, T., Zuidgeest, M., Brussel, M., van Maarseveen, M., 2014. Logistic regression and cellular automata-based modelling of retail, commercial and residential development in the city of Ahmedabad, India. Cities 39, 68–86. https://doi.org/10.1016/j.cities.2014.02.007

Mustafa, A., Bruwier, M., Teller, J., Archambeau, P., Erpicum, S., Pirotton, M., Dewals, B., 2016. Impacts of urban expansion on future flood damage: A case study in the River Meuse basin, Belgium, in: Sustainable Hydraulics in the Era of Global Change. Taylor & Francis Group, pp. 856–862.

Mustafa, A., Cools, M., Saadi, I., Teller, J., 2017a. Coupling agent-based, cellular automata and logistic regression into a hybrid urban expansion model (HUEM). Land Use Policy 69C, 529–540. https://doi.org/10.1016/j.landusepol.2017.10.009

Mustafa, A., Cools, M., Saadi, I., Teller, J., 2015a. Urban Development as a Continuum: A Multinomial Logistic Regression Approach, in: Gervasi, O., Murgante, B., Misra, S., Gavrilova, M.L., Rocha, A.M.A.C., Torre, C., Taniar, D., Apduhan, B.O. (Eds.), Computational Science and Its Applications -- ICCSA 2015, Lecture Notes in Computer Science. Springer International Publishing, pp. 729–744.

Mustafa, A., Dewals, B., Archambeau, P., Pirotton, M., Teller, J., 2015b. Sustainable integrated land-use plan and flood risk management: A review.

Mustafa, A., Heppenstall, A., Omrani, H., Saadi, I., Cools, M., Teller, J., 2018. Modelling built-up expansion and densification with multinomial logistic regression, cellular automata and genetic algorithm. Comput. Environ. Urban Syst. 67, 147–156. https://doi.org/10.1016/j.compenvurbsys.2017.09.009
Mustafa, A., Saadi, I., Cools, M., Teller, J., 2014. Measuring the Effect of Stochastic Perturbation Component in Cellular Automata Urban Growth Model. Procedia Environ. Sci., 12th International Conference on Design and Decision Support Systems in Architecture and Urban Planning, DDSS 2014 22, 156–168. https://doi.org/10.1016/j.proenv.2014.11.016
Mustafa, A., Van Rompaey, A., Cools, M., Saadi, I., Teller, J., 2017b. Addressing the determinants of built-up expansion and densification processes at the regional scale. Urban Stud. 1–19. https://doi.org/10.1177/0042098017749176
Nabielek, K., 2012. The Compact City: Planning strategies, recent developments and future prospects in the Netherlands - PBL Netherlands Environmental Assessment Agency, in: Proceedings of the AESOP 26th Annual Congress. Presented at the AESOP 26th Annual Congress, Ankara.
Nechyba, T.J., Walsh, R.P., 2004. Urban Sprawl. J. Econ. Perspect. 18, 177–200. https://doi.org/10.1257/0895330042632681
Nong, Y., Du, Q., 2011. Urban growth pattern modeling using logistic regression. Geo-Spat. Inf. Sci. 14, 62–67. https://doi.org/10.1007/s11806-011-0427-x
Omrani, H., Abdallah, F., Charif, O., Longford, N.T., 2015. Multi-label class assignment in land-use modelling. Int. J. Geogr. Inf. Sci. 29, 1023–1041. https://doi.org/10.1080/13658816.2015.1008004
O'Neill, E., 2013. Neighbourhood Design Considerations in Flood Risk Management. Plan. Theory Pract. 14, 129–134. https://doi.org/14649357.2012.761904
Ooi, J.T.L., Le, T.T.T., 2013. The spillover effects of infill developments on local housing prices. Reg. Sci. Urban Econ. 43, 850–861. https://doi.org/10.1016/j.regsciurbeco.2013.08.002
Openshaw, S., 1984. The modifiable areal unit problem. Presented at the CATMOG 38, Geo Abstracts University of East Anglia.
Openshaw, S., Taylor, P.J., 1979. A million or so correlation coefficients: three experiments on the modifiable areal unit problem. Stat. Appl. Spat. Sci. 21, 127–144.
Ortúzar, J. de D., Willumsen, L.G., 1994. Modelling Transport, Second. ed. Wiley.
Oueslati, W., Alvanides, S., Garrod, G., 2015. Determinants of urban sprawl in European cities. Urban Stud. 0042098015577773. https://doi.org/10.1177/0042098015577773
Overmars, K.P., de Koning, G.H.J., Veldkamp, A., 2003. Spatial autocorrelation in multi-scale land use models. Ecol. Model. 164, 257–270. https://doi.org/10.1016/S0304-3800(03)00070-X
Özgen, I., Liang, D., Hinkelmann, R., 2016a. Shallow water equations with depth-dependent anisotropic porosity for subgrid-scale topography. Appl. Math. Model. 40, 7447–7473. https://doi.org/10.1016/j.apm.2015.12.012
Özgen, I., Zhao, J., Liang, D., Hinkelmann, R., 2016b. Urban flood modeling using shallow water equations with depth-dependent anisotropic porosity. J. Hydrol. 541, 1165–1184. https://doi.org/10.1016/j.jhydrol.2016.08.025
Parish, Y.I.H., Müller, P., 2001. Procedural Modeling of Cities, in: Proceedings of the 28th Annual Conference on Computer Graphics and Interactive Techniques, SIGGRAPH '01. ACM, New York, NY, USA, pp. 301–308. https://doi.org/10.1145/383259.383292
Pfister, L., Kwadijk, J., Musy, A., Bronstert, A., Hoffmann, L., 2004. Climate change, land use change and runoff prediction in the Rhine–Meuse basins. River Res. Appl. 20, 229–241. https://doi.org/10.1002/rra.775
Poelmans, L., 2010. Modelling urban expansion and its hydrological impacts (Unpublished PhD dissertation). Katholieke Universiteit Leuven, Leuven.
Poelmans, L., Rompaey, A.V., Ntegeka, V., Willems, P., 2011. The relative impact of climate change and urban expansion on peak flows: a case study in central Belgium. Hydrol. Process. 25, 2846–2858. https://doi.org/10.1002/hyp.8047
Poelmans, L., Van Rompaey, A., 2010. Complexity and performance of urban expansion models. Comput. Environ. Urban Syst. 34, 17–27. https://doi.org/10.1016/j.compenvurbsys.2009.06.001
Poelmans, L., Van Rompaey, A., 2009. Detecting and modelling spatial patterns of urban sprawl in highly fragmented areas: A case study in the Flanders–Brussels region. Landsc. Urban Plan. 93, 10–19. https://doi.org/10.1016/j.landurbplan.2009.05.018
Poelmans, L., Van Rompaey, A., Batelaan, O., 2010. Coupling urban expansion models and hydrological models: How important are spatial patterns? Land Use Policy 27, 965–975. https://doi.org/10.1016/j.landusepol.2009.12.010

Pontius Jr., R.G., Schneider, L.C., 2001. Land-cover change model validation by an ROC method for the Ipswich watershed, Massachusetts, USA. Agric. Ecosyst. Environ. 85, 239–248. https://doi.org/10.1016/S0167-8809(01)00187-6

Pontius, R.G., Huffaker, D., Denman, K., 2004. Useful techniques of validation for spatially explicit land-change models. Ecol. Model. 179, 445–461. https://doi.org/10.1016/j.ecolmodel.2004.05.010

Prokop, G., Jobstmann, H., Schönbauer, A., 2011. Best practices for limiting soil sealing and mitigating its effects (Technical Report No. 2011-050). European Commission – DG Environment.

Puertas, O.L., Henríquez, C., Meza, F.J., 2014. Assessing spatial dynamics of urban growth using an integrated land use model. Application in Santiago Metropolitan Area, 2010–2045. Land Use Policy 38, 415–425. https://doi.org/10.1016/j.landusepol.2013.11.024

Rand, W., Brown, D., Riolo, R., Robinson, D., 2005. Toward a Graphical ABM Toolkit with GIS Integration. Presented at the Proceedings of the Agent 2005 Conference on Generative Social Processes, Models and Mechanisms, pp. 27–41.

Rienow, A., Goetzke, R., 2015. Supporting SLEUTH – Enhancing a cellular automaton with support vector machines for urban growth modeling. Comput. Environ. Urban Syst. 49, 66–81. https://doi.org/10.1016/j.compenvurbsys.2014.05.001

Robinson, D.T., Murray-Rust, D., Rieser, V., Milicic, V., Rounsevell, M., 2012. Modelling the impacts of land system dynamics on human well-being: Using an agent-based approach to cope with data limitations in Koper, Slovenia. Comput. Environ. Urban Syst., Special Issue: Geoinformatics 2010 36, 164–176. https://doi.org/10.1016/j.compenvurbsys.2011.10.002

Roy Chowdhury, P.K., Maithani, S., 2014. Modelling urban growth in the Indo-Gangetic plain using nighttime OLS data and cellular automata. Int. J. Appl. Earth Obs. Geoinformation 33, 155–165. https://doi.org/10.1016/j.jag.2014.04.009

Rui, Y., Ban, Y., 2010. Multi-agent Simulation for Modeling Urban Sprawl In the Greater Toronto Area, in: 13th AGILE. Presented at the 13th International Conference on Geographic Information Science 2010, Portugal.

Sanders, B.F., Schubert, J.E., Gallegos, H.A., 2008. Integral formulation of shallow-water equations with anisotropic porosity for urban flood modeling. J. Hydrol. 362, 19–38. https://doi.org/10.1016/j.jhydrol.2008.08.009

Santé, I., García, A.M., Miranda, D., Crecente, R., 2010. Cellular automata models for the simulation of real-world urban processes: A review and analysis. Landsc. Urban Plan. 96, 108–122. https://doi.org/10.1016/j.landurbplan.2010.03.001

Sarralde, J.J., Quinn, D.J., Wiesmann, D., Steemers, K., 2015. Solar energy and urban morphology: Scenarios for increasing the renewable energy potential of neighbourhoods in London. Renew. Energy, Sustainable Development in Building and Environment (SuDBE) 2013 73, 10–17. https://doi.org/10.1016/j.renene.2014.06.028

Satterthwaite, D., 2007. Adapting to Climate Change in Urban Areas: The Possibilities and Constraints in Low- and Middle-income Nations. IIED.

Schubert, J.E., Sanders, B.F., 2012. Building treatments for urban flood inundation models and implications for predictive skill and modeling efficiency. Adv. Water Resour. 41, 49–64. https://doi.org/10.1016/j.advwatres.2012.02.012

Sewall, J., Wilkie, D., Lin, M.C., 2011. Interactive Hybrid Simulation of Large-scale Traffic, in: Proceedings of the 2011 SIGGRAPH Asia Conference, SA '11. ACM, New York, NY, USA, p. 135:1–135:12. https://doi.org/10.1145/2024156.2024169

Shafizadeh-Moghadam, H., Helbich, M., 2015. Spatiotemporal variability of urban growth factors: A global and local perspective on the megacity of Mumbai. Int. J. Appl. Earth Obs. Geoinformation 35, Part B, 187–198. https://doi.org/10.1016/j.jag.2014.08.013

Shan, J., Alkheder, S., Wang, J., 2008. Genetic Algorithms for the Calibration of Cellular Automata Urban Growth Modeling. Photogramm. Eng. Remote Sens. 74, 1267–1277. https://doi.org/10.14358/PERS.74.10.1267

Shu, B., Zhang, H., Li, Y., Qu, Y., Chen, L., 2014. Spatiotemporal variation analysis of driving forces of urban land spatial expansion using logistic regression: A case study of port towns in Taicang City, China. Habitat Int. 43, 181–190. https://doi.org/10.1016/j.habitatint.2014.02.004

Smelik, R.M., Tutenel, T., Bidarra, R., Benes, B., 2014. A Survey on Procedural Modelling for Virtual Worlds. Comput. Graph. Forum 33, 31–50. https://doi.org/10.1111/cgf.12276

Song, Y., Zenou, Y., 2006. Property tax and urban sprawl: Theory and implications for US cities. J. Urban Econ. 60, 519–534. https://doi.org/10.1016/j.jue.2006.05.001

SPW, 2008. Carte d'Occupation du Sol de Wallonie (COSW) - Version 1_05 [WWW Document]. URL http://geoportail.wallonie.be/catalogue/7539bf98-4d80-459f-8274-312563c2bab4.html (accessed 7.15.16).
Sunde, M.G., He, H.S., Zhou, B., Hubbart, J.A., Spicci, A., 2014. Imperviousness Change Analysis Tool (I-CAT) for simulating pixel-level urban growth. Landsc. Urban Plan. 124, 104–108. https://doi.org/10.1016/j.landurbplan.2014.01.007
Tachieva, G., 2010. Sprawl Repair Manual, 2 edition. ed. Island Press, Washington.
Tannier, C., Thomas, I., 2013. Defining and characterizing urban boundaries: A fractal analysis of theoretical cities and Belgian cities. Comput. Environ. Urban Syst. 41, 234–248. https://doi.org/10.1016/j.compenvurbsys.2013.07.003
Tayyebi, A.H., Tayyebi, A., Khanna, N., 2014. Assessing uncertainty dimensions in land-use change models: using swap and multiplicative error models for injecting attribute and positional errors in spatial data. Int. J. Remote Sens. 35, 149–170. https://doi.org/10.1080/01431161.2013.866293
Thomas, I., Frankhauser, P., Biernacki, C., 2008. The morphology of built-up landscapes in Wallonia (Belgium): A classification using fractal indices. Landsc. Urban Plan. 84, 99–115. https://doi.org/10.1016/j.landurbplan.2007.07.002
Tian, G., Ma, B., Xu, X., Liu, X., Xu, L., Liu, X., Xiao, L., Kong, L., 2016. Simulation of urban expansion and encroachment using cellular automata and multi-agent system model—A case study of Tianjin metropolitan region, China. Ecol. Indic., Navigating Urban Complexity: Advancing Understanding of Urban Social – Ecological Systems for Transformation and Resilience 70, 439–450. https://doi.org/10.1016/j.ecolind.2016.06.021
Traore, A., Watanabe, T., 2017. Modeling Determinants of Urban Growth in Conakry, Guinea: A Spatial Logistic Approach. Urban Sci. 1, 12. https://doi.org/10.3390/urbansci1020012
UNISDR, 2009. 2009 UNISDR terminology on disaster risk reduction.
Valbuena, D., Verburg, P.H., Bregt, A.K., 2008. A method to define a typology for agent-based analysis in regional land-use research. Agric. Ecosyst. Environ. 128, 27–36. https://doi.org/10.1016/j.agee.2008.04.015
van Vliet, J., Bregt, A.K., Brown, D.G., van Delden, H., Heckbert, S., Verburg, P.H., 2016. A review of current calibration and validation practices in land-change modeling. Environ. Model. Softw. 82, 174–182. https://doi.org/10.1016/j.envsoft.2016.04.017
Vanegas, C.A., Aliaga, D.G., Benes, B., Waddell, P.A., 2009. Interactive Design of Urban Spaces Using Geometrical and Behavioral Modeling, in: ACM SIGGRAPH Asia 2009 Papers, SIGGRAPH Asia '09. ACM, New York, NY, USA, p. 111:1–111:10. https://doi.org/10.1145/1661412.1618457
Vanegas, C.A., Garcia-Dorado, I., Aliaga, D.G., Benes, B., Waddell, P., 2012. Inverse Design of Urban Procedural Models. ACM Trans Graph 31, 168:1–168:11. https://doi.org/10.1145/2366145.2366187
Veldkamp, A., Lambin, E.F., 2001. Predicting land-use change. Agric. Ecosyst. Environ., Predicting Land-Use Change 85, 1–6. https://doi.org/10.1016/S0167-8809(01)00199-2
Verburg, P.H., van Eck, J.R.R., de Nijs, T.C.M., Dijst, M.J., Schot, P., 2004. Determinants of Land-Use Change Patterns in the Netherlands. Environ. Plan. B Plan. Des. 31, 125–150. https://doi.org/10.1068/b307
Vermeiren, K., Van Rompaey, A., Loopmans, M., Serwajja, E., Mukwaya, P., 2012. Urban growth of Kampala, Uganda: Pattern analysis and scenario development. Landsc. Urban Plan. 106, 199–206. https://doi.org/10.1016/j.landurbplan.2012.03.006
Vollmer, D., Costa, D., Lin, E.S., Ninsalam, Y., Shaad, K., Prescott, M.F., Gurusamy, S., Remondi, F., Padawangi, R., Burlando, P., Girot, C., Grêt-Regamey, A., Rekittke, J., 2015. Changing the Course of Rivers in an Asian City: Linking Landscapes to Human Benefits through Iterative Modeling and Design. JAWRA J. Am. Water Resour. Assoc. 51, 672–688. https://doi.org/10.1111/1752-1688.12316
Wang, H., He, S., Liu, X., Dai, L., Pan, P., Hong, S., Zhang, W., 2013. Simulating urban expansion using a cloud-based cellular automata model: A case study of Jiangxia, Wuhan, China. Landsc. Urban Plan. 110, 99–112. https://doi.org/10.1016/j.landurbplan.2012.10.016
Ward, D.P., Murray, A.T., Phinn, S.R., 2000. A stochastically constrained cellular model of urban growth. Comput. Environ. Urban Syst. 24, 539–558. https://doi.org/10.1016/S0198-9715(00)00008-9
Watson, D., Adams, M., 2010. Design for Flooding: Architecture, Landscape, and Urban Design for Resilience to Climate Change. John Wiley & Sons.
Weber, B., Müller, P., Wonka, P., Gross, M., 2009. Interactive Geometric Simulation of 4D Cities. Comput. Graph. Forum 28, 481–492. https://doi.org/10.1111/j.1467-8659.2009.01387.x
White, I., 2008. The absorbent city: urban form and flood risk management. Proc. Inst. Civ. Eng. - Urban Des. Plan. 161, 151–161. https://doi.org/10.1680/udap.2008.161.4.151

White, R., Engelen, G., 2000. High-resolution integrated modelling of the spatial dynamics of urban and regional systems. Comput. Environ. Urban Syst. 24, 383–400. https://doi.org/10.1016/S0198-9715(00)00012-0
White, R., Engelen, G., 1997. Cellular Automata as the Basis of Integrated Dynamic Regional Modelling. Environ. Plan. B Plan. Des. 24, 235–246. https://doi.org/10.1068/b240235
White, R., Engelen, G., 1993. Cellular Automata and Fractal Urban Form: A Cellular Modelling Approach to the Evolution of Urban Land-Use Patterns. Environ. Plan. A 25, 1175–1199. https://doi.org/10.1068/a251175
White, R., Engelen, G., Uljee, I., 2015. The Cellular Automaton Eats the Regions: Unified Modeling of Activities and Land Use in a Variable Grid Cellular Automaton, in: Modeling Cities and Regions As Complex Systems: From Theory to Planning Applications. The MIT Press, Cambridge , Massachusetts.
White, R., Uljee, I., Engelen, G., 2012. Integrated modelling of population, employment and land-use change with a multiple activity-based variable grid cellular automaton. Int. J. Geogr. Inf. Sci. 26, 1251–1280. https://doi.org/10.1080/13658816.2011.635146
Wind, H.G., Nierop, T.M., de Blois, C.J., de Kok, J.L., 1999. Analysis of flood damages from the 1993 and 1995 Meuse Floods. Water Resour. Res. 35, 3459–3465. https://doi.org/10.1029/1999WR900192
Wu, F., 2002. Calibration of stochastic cellular automata: the application to rural-urban land conversions. Int. J. Geogr. Inf. Sci. 16, 795–818. https://doi.org/10.1080/13658810210157769
Xian, G., Crane, M., 2005. Assessments of urban growth in the Tampa Bay watershed using remote sensing data. Remote Sens. Environ. 97, 203–215. https://doi.org/10.1016/j.rse.2005.04.017
Yang, Q., Li, X., Shi, X., 2008. Cellular automata for simulating land use changes based on support vector machines. Comput. Geosci. 34, 592–602. https://doi.org/10.1016/j.cageo.2007.08.003
Yang, X., 2010. Integration of Remote Sensing with GIS for Urban Growth Characterization, in: Jiang, B., Yao, X. (Eds.), Geospatial Analysis and Modelling of Urban Structure and Dynamics, GeoJournal Library. Springer Netherlands, pp. 223–250. https://doi.org/10.1007/978-90-481-8572-6_12
Yang, Y.-L., Wang, J., Vouga, E., Wonka, P., 2013. Urban Pattern: Layout Design by Hierarchical Domain Splitting. ACM Trans Graph 32, 181:1–181:12. https://doi.org/10.1145/2508363.2508405
Yijie, S., Gongzhang, S., 2008. Improved NSGA-II Multi-objective Genetic Algorithm Based on Hybridization-encouraged Mechanism. Chin. J. Aeronaut. 21, 540–549. https://doi.org/10.1016/S1000-9361(08)60172-7
Zhang, H., Zeng, Y., Bian, L., Yu, X., 2010. Modelling urban expansion using a multi agent-based model in the city of Changsha. J. Geogr. Sci. 20, 540–556. https://doi.org/10.1007/s11442-010-0540-z
Zhang, Q., Ban, Y., Liu, J., Hu, Y., 2011. Simulation and analysis of urban growth scenarios for the Greater Shanghai Area, China. Comput. Environ. Urban Syst., Geospatial Analysis and Modeling 35, 126–139. https://doi.org/10.1016/j.compenvurbsys.2010.12.002
Zhang, Z., Su, S., Xiao, R., Jiang, D., Wu, J., 2013. Identifying determinants of urban growth from a multi-scale perspective: A case study of the urban agglomeration around Hangzhou Bay, China. Appl. Geogr. 45, 193–202. https://doi.org/10.1016/j.apgeog.2013.09.013